LICENTIATE THESIS

Behaviour of Pretensioned Bolts in Friction Connections

Towards the Use of Higher Strength Steels in Wind Towers

Christine Heistermann

LULEÅ UNIVERSITY OF TECHNOLOGY

LULEÅ UNIVERSITY OF TECHNOLOGY

LICENTIATE THESIS 2011

BEHAVIOUR OF PRETENSIONED BOLTS IN FRICTION CONNECTIONS

TOWARDS THE USE OF HIGHER STRENGTH STEELS IN WIND TOWERS

Christine Heistermann

Luleå, June 2011

Division of Structural and Construction Engineering – Steel Structures
Department of Civil, Environmental and Natural Resources Engineering
Luleå University of Technology
SE - 971 87 LULEÅ
www.ltu.se

Printed by Universitetstryckeriet, Luleå 2011

ISSN: 1402-1757
ISBN 978-91-7439-267-8

Luleå 2011

www.ltu.se

Abstract

During recent years wind energy has established as an alternative to common energy sources. To advance its competitiveness, the costs for the construction of a wind tower have to be reduced. One possible option is the use of friction grip joints instead of flange connections to join various tower segments in a tubular steel tower. Additionally, the time necessary for installation and maintenance of the bolts in these connections can be decreased, not only for implementation in tubular towers but also in lattice towers.

Four different bolt types have been investigated with respect to the ease of installation and maintenance on the one hand and structural applicability on the other hand. The latter one is mainly defined by the behaviour of the pretension force in the bolts. Various influences on the reduction of clamping force are experimentally checked, such as the type and thickness of coating, the thickness of the clamping package and external loading.

The slip factor, which plays an important role in friction connections, is experimentally achieved in a test on a double shear lap joint. The experiment is thoroughly examined by a finite element analysis, which models the interaction between bolts and plates.

In various numerical analyses the influence of steel grade and possible assembling tolerances on the resistance of a friction joint is investigated both for single and double shear lap joints.

Shortages of EN 1993 parts 1-8 and 1-12 for the use of slip critical joints are identified.

Abstract in Swedish

På senare år har vindenergi blivit ett allt vanligare alternativ till de mer traditionella energikällorna. För att ytterligare stärka konkurrenskraften behöver installationskostnaden för vindkraftverken minskas. Ett sätt att göra detta är att använda friktionsförband istället för att sammanfoga flänsarna hos de olika segmenten i vindkraftverk uppbyggda av stålrör. Man kan dessutom minska den erforderliga tiden för att montera och underhålla skruvarna i dessa förband, vilket inte bara gäller för rörkonstruktioner utan även för vindkraftverk av fackverkstyp.

Fyra olika sorters skruvar har undersökts, å ena sidan avseende hur enkla de är att montera och underhålla, å andra sidan avseende den strukturella tillämpligheten. Den senare beror huvudsakligen på beteendet hos förspänningskraften i skruvarna. Olika sorters påverkan på fastspänningskraften har undersökts experimentellt, exempelvis ytskiktens tjocklek, klämlängden samt den påförda yttre lasten.

Friktionskoefficienten vid glidning, som har en viktig roll i friktionsförband, har erhållits experimentellt genom försök med ett tvåskärigt skjuvförband. Försöken har utvärderats noga med FE-analyser, där interaktionen mellan skruvar och plattor har modellerats.

Inverkan av vald stålsort samt utförandetoleranser har undersökts genom numeriska analyser för både enskäriga och tvåskäriga skjuvförband.

Brister i EN-1993 del 1-8 och 1-12 har identifierats vid användning av förband som är känsliga för glidning.

Contents

Preface

The research presented in this thesis was carried out at the Department of Civil, Environmental and Natural Resources Engineering at Luleå University of Technology (LTU), in the Research Group of Steel Structures at the Division of Structural and Construction Engineering. It was firstly initiated as part of the work for the European project HISTWIN, which targeted the improvement of tower structures for wind energy converters. One of the main ideas of this project was to substitute flange connections of tower segments by friction connections. By time it turned out that the behaviour of bolts in friction connections was not only interesting for the partners of this particular project but also for other financers. Thereby, the focus of my research broadened from friction connections with long open slotted holes to friction connections with normal clearance holes, from one type of bolt to a number of types, from one specific steel grade to various ones. Now, the findings are not only of value for the use in wind towers but also for friction connections in any type of structure.

For financial support thanks are given to RFSR-CT-2006-00031 and RFSR-CT-2010-00031, the European Research Fund of Coal and Steel, Rautaruukki Oyj, Finland, and as main sponsor of this work the Centre for High-performance Steel (CHS) at Luleå University of Technology, Sweden.

The supply of Huck BobTail lockbolts and the according installation wrenches by Alcoa Inc. is gratefully acknowledged.

For giving me the opportunity to work on this topic I would like to thank my supervisor Prof. Milan Veljkovic. His supervision made it possible to realize this thesis. For valuable discussions my gratitude goes to my colleagues Marouene Limam and Tim Heistermann, who also took over some of my work

load while I was writing the following chapters. Furthermore, my other colleagues deserve thanks for support, distraction and amusement.

I am thankful for the assistance of the staff of Complab, laboratory at Luleå University of Technology, in developing test methods, modifying specimens and performing the actual experimental work.

Many thanks are due to Prof. Carlos Rebelo from the University of Coimbra, Portugal, for accepting to be the faculty examiner of my work.

Last but not least, I thank my husband Tim for his love, support, encouragement and always being there.

Luleå, June 2011

Christine Heistermann

Abbreviations

Latin capital letters

A	Area	[mm^2]
A_{net}	Area of net cross section	[mm^2]
A_s	Bolt stress area	[mm^2]
D_d	Accumulated damage	[-]
$F_{b,R}$	Characteristic bearing resistance	[kN]
F_{max}	Maximum load	[kN]
F_p	Initial preload	[kN]
$F_{p,actual}$	Actual preload at a certain time	[kN]
$F_{p,initial}$	Initial preload	[kN]
$F_{p,C}$	Characteristic pretension	[kN]
$F_{p,Cd}$	Design preload	[kN]
$F_{p,C,lt}$	Remaining pretension force	[kN]
$F_{p,C,xx}$	Remaining pretension force for either bolts with or without extension sleeves	[kN]

F_{max}	Actual slip resistance in the static test of specimen RuH-S_4	[kN]
$F_{s,R}$	Characteristic static resistance	[kN]
$F_{s,Rd}$	Static design resistance	[kN]
L_x	External tension load	[kN]
$N_{net,R}$	Characteristic plastic resistance of the net cross section	[kN]
N_{Ri}	Endurance	[-]
V_x	Coefficient of variation	[-]

Latin small letters

d_0	Hole diameter	[mm]
d_a	External diameter	[mm]
e_1	End distance from the centre of a fastener hole to the adjacent end of any part, measured in the direction of load transfer	[mm]
f_{ub}	Bolt ultimate strength	[N/mm^2]
f_y	Plate yield strength	[N/mm^2]
f_{yb}	Bolt yield strength	[N/mm^2]
k_n	Fractile factor	[-]
k_s	Correction factor or reduction factor	[-]
m	Slope of S-N curve	[-]
m_x	Mean value	[-]

n	Number of bolts, load introduction factor, number of tests, number of friction surfaces	[-]
n_{Ei}	Number of cylces	[-]
p_1	Spacing between centres of fasteners in a line in the direction of load transfer	[mm]
s_x	Standard deviation	[-]
t	Time	[s], [a]
t	Plate thickness	[mm]
w	Plate width	[mm]

Greek capital letters

ΔF_B	Bolt force variation	[kN]
ΔF_J	Joint force variation	[kN]
ΔL	Bolt elongation before application of external load	[mm]
$\Delta L'$	Bolt elongation after application of external load	[mm]
ΔT	Compression of joint members before application of external load	[mm]
$\Delta T'$	Compression of joint members after application of external load	[mm]
$\Delta\sigma_C$	Fatigue detail category or reference fatigue strength	[N/mm^2]
σ_{gross}	Stress in the gross cross section area	[N/mm^2]
$\sigma_{max,hole}$	Maximum stress at the bolt hole	[N/mm^2]

σ_{net}	Stress in the net cross section area	[N/mm^2]

Greek small letters

γ_{Ff}	Partial safety factor for equivalent constant amplitude stress ranges	[-]
γ_{M3}	Partial safety factor for joints, taking the slip resistance at ultimate limit state (Category C) into account	[-]
γ_{M7}	Partial safety factor for joints, taking the preload of high strength bolts into account	[-]
γ_{Mf}	Partial safety factor for fatigue strength $\Delta\sigma_C$, $\Delta\tau_C$	[-]
ε_{nom}	Nominal strains	[-]
ε_{true}	True strains	[-]
μ	Slip factor	[-]
$\mu_{friction}$	Apparent friction coefficient	[-]
μ_{slip}	Apparent slip factor	[-]
σ_{nom}	Nominal stress	[N/mm^2]
σ_{true}	True stress	[N/mm^2]

Test specimens

LT	Longterm test, single lap joint coated with Temasil 90 on all surfaces Loaded for 15 weeks by a constant load resembling 60 % or 80 % of the expected static resistance
R0	Pure relaxation test, none of the surfaces of the main plate painted with Temasil 90
R1	Pure relaxation test, one of the surfaces of the main plate painted with Temasil 90
R2	Pure relaxation test, both of the surfaces of the main plate painted with Temasil 90
RuH_0	Pure relaxation test on a symmetric lap joint connection, none of the plate surfaces hot dip galvanized, Huck BobTail lockbolts 1”/M25,4
RuH_2	Pure relaxation test on a symmetric lap joint connection, four of the plate surfaces hot dip galvanized, Huck BobTail lockbolts 1”/M25,4
RuH_4	At first pure relaxation test on a symmetric lap joint connection, all of the plate surfaces hot dip galvanized, Huck BobTail lockbolts 1”/M25,4 This specimen is also used for a test with cyclic loading.
RuH-S_0	Pure relaxation test on a symmetric lap joint connection, none of the plate surfaces hot dip galvanized, Huck BobTail lockbolts 1”/M25,4 plus additional extension sleeve
RuH-S_2	Pure relaxation test on a symmetric lap joint connection, four of the plate surfaces hot dip galvanized, Huck BobTail lockbolts 1”/M25,4 plus additional extension sleeve
RuH-S_4	At first pure relaxation test on a symmetric lap joint connection, all of the plate surfaces hot dip galvanized, Huck BobTail lockbolts 1”/M25,4 plus additional extension sleeve This specimen is also used for a test with static loading.

Bolts

F	Friedberg HV Rändel, M20
H	Huck BobTail lockbolt, M20 and 1”/M25,4
N	Standard structural bolt with NordLock washers, M30
T	Tension control bolt (TCB), M30

1 INTRODUCTION

The demand in use of electrical energy generated from renewable sources is constantly increasing and it is foreseen that this trend will remain even in future. One of the resources that nowadays is of great importance for development and creation of new jobs in Norrbotten, the northernmost Swedish province, is the use of wind power. During the last decades wind farms have been built all over the world, especially in Europe and in recent years the interest is grown in Sweden. The goal of Swedish wind power industry is to reach 20 TWh of electrical energy generated on-shore by 2020 [1].

To advance the competitiveness of wind-energy, costs have to be reduced. According to Sahin [2] the capital cost for constructing a power plant and coupling it into the grid accounts for 75-90 % of the total costs. Within this amount of costs for the construction expenses of about 15-20 % arise for the tower itself [3].

A reduction of costs per kilowatt-hour electrical energy can be realized by improving the relationship between the generated electric energy and the costs per converter. One possible solution is to construct higher towers to reach zones of higher and more constant wind speeds, which is associated with increase of construction costs on the one hand and a rise of generated energy on the other hand. In the following chapters two types of steel towers are taken into account while trying to find improvements.

1.1 Towers for wind turbines

Each wind energy plant consists of rotor, nacelle, tower, foundation and transformer. The turbines rest on various kinds of towers: concrete-, steel-,

hybrid- or timber-towers. The most common solution for onshore wind farms are steel tubular towers, as they combine aesthetical, economical and safety reasons. But also another type of steel tower, the lattice tower has recently increased its competitiveness. Also other types of towers exist, such as, for example, concrete or hybrid towers. However, here, the focus is turned on steel towers. The biggest part of the costs for a wind power plant is allocated to the turbines and therefore the size of the turbine and its productivity are the most determining factors. Due to the increasing construction costs for higher towers the construction work becomes increasingly important. The new trend to built higher and larger turbines is justified by the wind speed which rises dramatically with height above ground, see Figure 1.1-1.

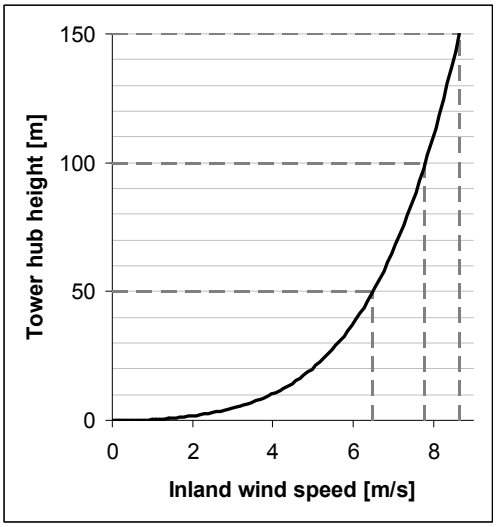

Figure 1.1-1: Inland wind speed increasing with hub height [4]

The competitiveness of steel towers in comparison with other types of structures for wind towers has been proofed in the "Elforsk"-report [5]. Here, alternative solutions, such as concrete or hybrid concrete-steel towers, are investigated and it is found that for the particular case of a wind tower of 125 m hub height with a turbine capacity of 3 MW the lattice tower is about 20 % cheaper than the hybrid solution.

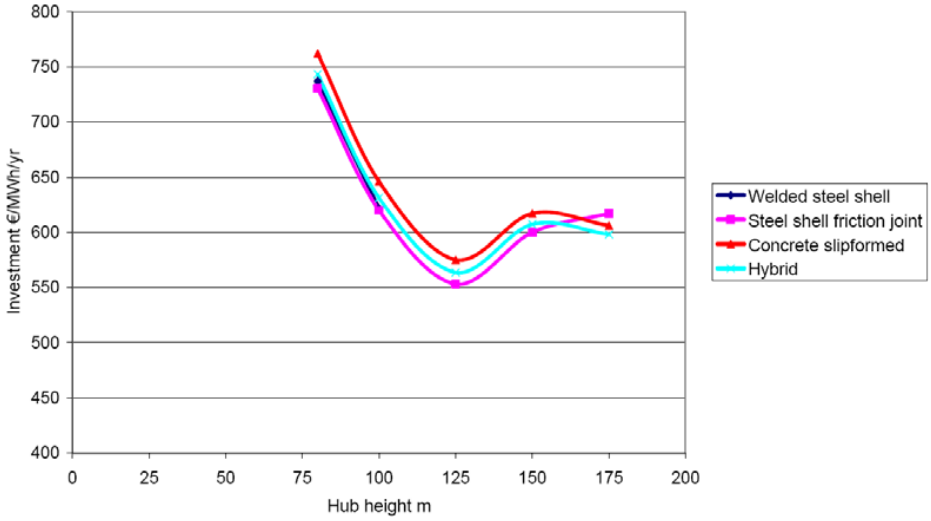

Figure 1.1-2: Costs per type of tower for a 5 MW turbine depending on hub height [5]

1.1.1 Tubular steel towers

Right now steel tubular towers, as shown in Figure 1.1-3, can only be built up to a height of 80-100 m. The fatigue resistance of the flange connections, which joint the individual tower sections, limits the structure. Furthermore, the maximum diameter of the tower base is confined by transportation matters.

These problems try to be overcome in a recently finished European project called HISTWIN [6]. Herein the attention is turned to the optimization of the tower geometry and innovative solutions for the assembly joints. One of the details which the project targets at is the flange connection of the individual tower sections. Investigations have demonstrated that the flange connection can be replaced by a friction connection with long open slotted holes. The advantages of this are big cost savings related to production and assembling of the tower. In addition to this, friction connections are less sensitive to fatigue.

As one of the main advantages of steel tubular towers the closed geometry has to be mentioned. The tubular tower offers protection for the construction workers during installation and maintenance, protection of the bolts against weather influences and also against vandalism.

Figure 1.1-3: 80 m high tubular steel tower from Martifer, Portugal

Bolted ring flange connections

Currently the sections of tubular steel towers are assembled with bolted ring flange connections. Steel rings are welded to both tube ends and connected by high strength bolts, cp. Figure 1.1-4.

Flanges can be fabricated by welding or rolling. To fulfil the requirements for maximum imperfections further treatment is necessary, which increase the production costs.

Due to various disadvantages of this type of connection, as for example low fatigue resistance, a laborious and cost intensive fabrication process, which is accompanied by a long delivery time, as well as complex design, this traditional method is suggested to be replaced by an alternative option: The use of single overlapping friction connections with long open slotted holes.

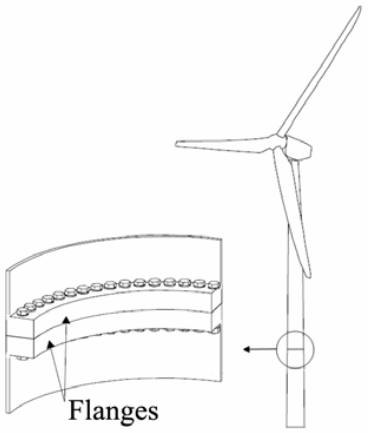

Figure 1.1-4: Bolted L-flange connection [7]

High strength friction grip connections

The innovative solution for the assembling joints is the use of high strength friction grip connections (herein after referred to as friction connection) with long open slotted holes [6]. Compared to the common flange connections their design process is much easier and can be processed a lot faster, as described in chapter 2.2.

In a friction connection the long open slotted holes are cut into the lower tower segment, so that the upper segment with standard holes, in which the bolts are already preassembled, can easily be slid on top of the lower one, cp. Figure 1.1-5. Thereby, bolts can be preinstalled. This facilitates the alignment of the segment towards the open slotted holes and the actual installation process of tightening the bolts is accelerated. A group of bolts per long open slotted hole is held together by a cover plate, which is used instead of single washers per bolt to uniformly spread the stresses inserted into the plates due to bolt pretension.

The main objective of the described experiments is to assess an optimal fastener for this type of connection, having in mind structural performance, initial costs and maintenance costs. The loss of pretension over time of a possible type of bolt is presented in chapters 3 and 4.

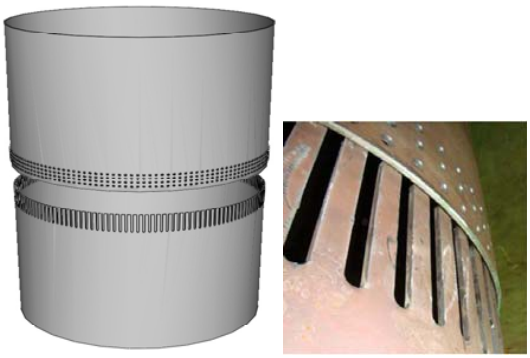

Figure 1.1-5: High strength friction grip connection [6]

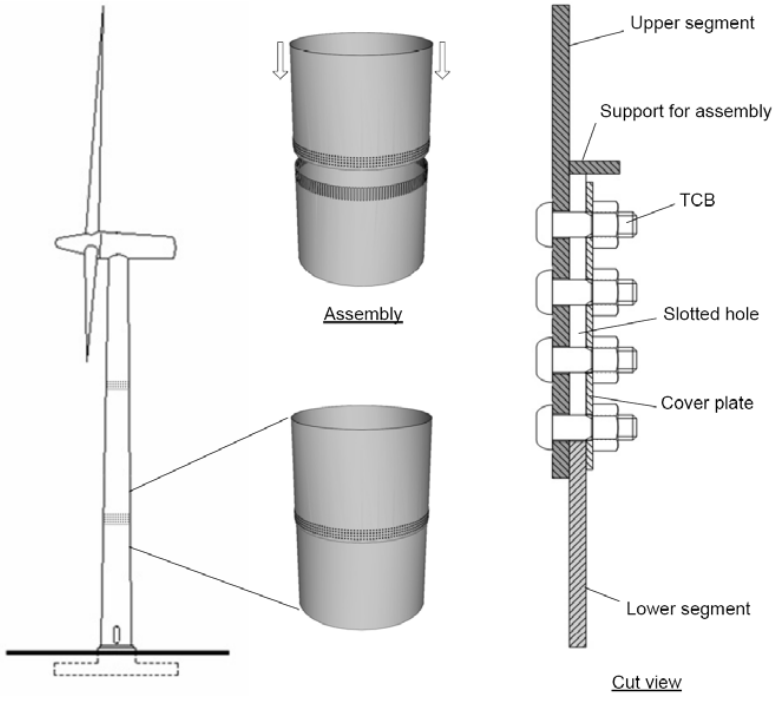

Figure 1.1-6: Proposed friction connection [8]

1.1.2 Lattice towers

Lattice towers, as Figure 1.1-7 shows, are not as often seen for onshore wind energy plants as steel tubular towers. Due to their big needs of ground area they are not applicable in all kinds of environments. Besides, their outward appearance is often regarded as unpleasant. But seen from a distance the truss-construction of a lattice tower turns into an advantage as it becomes indistinct. Other factors to vote for the construction of a lattice tower are the big hub heights, the ease of transportation, its low self weight, that it can be assembled on the ground and, where required, disassembled again.

For construction of a lattice tower friction connections are used. But in contrast to the new idea of the HISTWIN-project the common solution is the use of normal holes.

Figure 1.1-7: 160 m high lattice tower from SeeBA [9]

Also for lattice towers a new concept is developed by a Rautaruukki Oyj, a Finnish steel manufacturer. The idea is to use new profiles, which are cold formed and piece them together, so that they compose one column of the tower

with a hexagonal cross section. All joints of the cross section are connected with bolts and work via friction. A picture of such a cold formed plate modelled with finite element analysis can be seen in Figure 1.1-8.

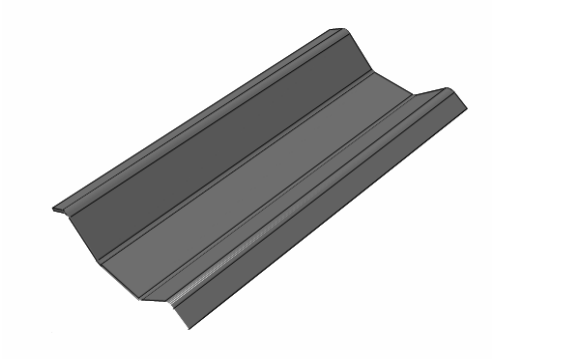

Figure 1.1-8: Cold formed-plate for lattice towers [10]

1.2 Bolts

Bolts play the most important role in a friction connection: They ensure whether the connection withstands an applied load or not. Thus it is very important that the bolts constantly keep the pretension force that they are designed for.

A well known problem of bolted connections is that they open by themselves. This self loosening effect leads to the necessity of regular control and maintenance of bolted connections, which raises the question if there are bolts available on the market, that do not untighten by themselves. Therefore this study investigates four different types of bolts, which are foreseen as potentially competitive solutions. These bolts are the Tension Control Bolt (described in chapter 1.2.1), the Huck BobTail lockbolt (see chapter 1.2.2), a standard bolt in combination with pairs of NordLock washers (cp. chapter 1.2.3) and the Friedberg HV Rändel (read chapter 1.2.4). Pictures of the bolts are shown in *Figure 1.2-1*.

Figure 1.2-1:TCB, Huck, standard bolt with Nordlock and Friedberg HV Rändel

Another problem with bolts is that they loose some of their pretension over time. Hence this survey deals with the reduction of pretension force over time due to certain parameters, as there are variation of surface finishing of the connected plates and external loading.

All measurements of bolt forces are done with the help of BTM-6C strain gauges [11], which are inserted into the bolts' shanks, as shown in Figure 1.2-2. For this, a hole of 2 mm diameter is drilled from the head of the bolt into the shank. Then the strain gauge is glued into the hole. From strain gauge calibration which is carried out in advance, the forces in the bolts can be calculated.

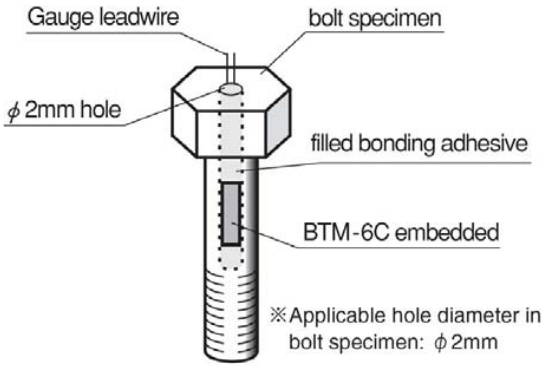

Figure 1.2-2: Position of strain gauges in the bolts [11]

Although the hole in the shank reduces the cross-section area of the bolt and therefore also the tensile and bending resistance minimally, this can be neglected [12].

1.2.1 Tension Control Bolts

Tension Control Bolts (TCBs) are a special type of high strength fastener with tightening carried out entirely at the nut end by the use of a special electric wrench. They are available on the market in metric sizes up to M30. The mechanical properties are equivalent to those of High Strength Bolts: grade S10T can be considered as bolt grade 10.9 [13], [14]. As tightening is performed at the nut end only, no torsion is introduced in the shank [15]. This property is believed to reduce the risk of self loosening and the amount of torsional relaxation.

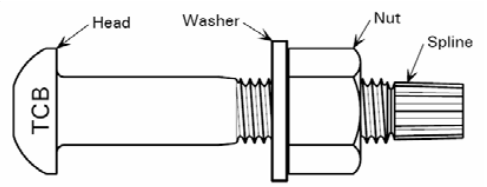

Figure 1.2-3: Tension Control Bolt [14]

1.2.2 Huck BobTail Lockbolts

The Huck BobTail lockbolt is a special type of high strength fastener; a lockbolt produced by Alcoa Fasting Systems in Great Britain, see *Figure 1.2-4*. The tightening of the bolt can be performed from the nut end only and has to be carried out with the help of a certain installation tool. The noticeable property is a threadless nut, which gets swaged to the shank of the bolt. To open the bolt again, the same machine as for the installation plus a special cutting device is necessary. By this swaging-technique Alcoa Fastening Systems claims the bolt to be vibration-proof. Due to this the bolt is chosen for the performed experiments, as well as for its simple and fast way of installation.

The Huck bobtail lockbolts used in the tests of this paper are classified as steel grade 8 according to the SAE-system. This equals class 10.9 of the ISO

standards. Dimensions can be found in Annex E, as well as a description of tensile tests on the 1”/M25,4 Huck BobTail lockbolts. These have been carried out to achieve more knowledge about the material properties and behaviour of the bolts.

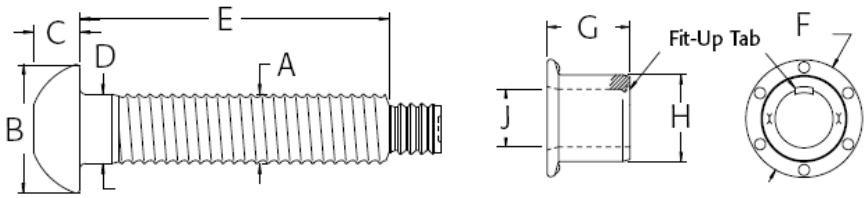

Figure 1.2-4: Huck BobTail lockbolt [16]

The six circular spots, which can be seen in view F of *Figure 1.2-4*, function as marks for the installation process to show whether the bolt is completely tightened: If at least three of them are imprinted, the bolt is engaged successfully.

1.2.3 Standard Bolts with NordLock-Washers

The NordLock security system is a unique wedge locking system of washers, which has to be used in combination with standard structural steel bolts, here of grade 10.9. They are always used in pairs, and work by the use of tension instead of friction. This means that while tightening the bolt the washer-pair is pressed together. As soon as the bolt starts to open, the washer pair does the same. But due to different angles in the washer and the bolt thread, see Figure 1.2-5, the bolt keeps pretensioned, since the pair of washers will always open a little more than the pitch of the thread.

Figure 1.2-5: NordLock Washers [17]

1.2.4 Friedberg HV Rändel

Friedberg HV Rändel is a press-fitted bolt produced by August Friedberg GmbH in Germany [18]. It is a high strength bolt, which has a knurl at the shank below the bolt head. This bolt has been chosen for testing for two reasons: On the one hand the knurl fixes the bolt in the hole, so that the position of the bolt can always be ensured. On the other hand the bolt can be tightened from one side only by use of conventional tools [12].

These bolts are tested in down-scale test in HISTWIN and because they are not in regular production only few bolts were available at LTU for testing. In Annex E the inspection certificate for these newly developed bolts can be found.

It should be noted that due to the fact that Friedberg HV Rändel are press-fitted bolts, they are not completely comparable to the other bolts tested and described in this survey. Press-fitted bolts transfer one part of their clamping force by pressure on the clamping package, as also TCB, Huck BobTail lockbolts and standard structural bolts do, but the other part is transferred by friction of the fitted bolt shank.

1.3 General

The licentiate thesis is conceived in effort to search and propose improvements of assembling joints for steel towers. The two tower types described above are recognized as competitive structural solutions. The existing tubular towers are limited in diameter, which is expected to be resolved in the ongoing RFCS-project “HISTWIN2” [19].

For lattice towers there are, at least theoretically, no limits concerning height or diameter.

Understanding of friction type joints, such as a single shear lap joint instead of flange connections in tubular towers and double shear lap joint in lattice towers, are important issues for the optimization of construction costs.

Friction connections, often denoted as slip critical joints, are joints that have low probability of slip during the life time of a structure. Traditionally, for normal clearance holes, the resistance of a friction connection has to be designed to prevent slip in the joint at the serviceability load level. However, in a case of open slotted holes, as used in the single shear lap joints of tubular towers, a slip of more than 0,15 mm should not be reached at the ultimate limit load [20].

Two factors are crucial for the optimal design of the friction joint: the slip factor and the level of pretension force in the bolt.

Experimental and numerical investigation of these two variables is the main objective in this thesis. The purpose of the investigation is to establish prerequisites for the use of higher strength steel grades leading to improvements of steel tower competitiveness.

The following questions are studied:

- What is the remaining resistance of the friction joint after a certain period of time and at the end of the life time of a tower?

- What is influence of assembling tolerances on the behaviour of a friction joint?

- Is it justified to use higher strength steel grades in friction joints of a tower for wind turbines?

- Is it possible to design a joint of a tower for a wind turbine that does not need inspection during the life time?

- Is it necessary to make any changes in existing European Standards, in particular in SS-EN-1993-1-8?

1.4 Outline

This thesis started with a general introduction to the topic “wind towers” in chapter 1. Here, various types of towers for wind turbines are described, as well as drawbacks, which might arise during their construction and life time. An idea how to solve these problems, which mainly affect connections of various steel members, plus possibly usable bolts are presented.

This is followed by information about the actual state of the art on connections and the reduction of clamping force in pretensioned bolts in chapter 2.

In chapters 3 to 5 the tests carried out at Luleå University of Technology are explained, results are shown and the behaviour of pretensioned bolts is analyzed and interpreted.

For further understanding of load transfer a description of a finite element analysis of one of the performed experiments is given in chapter 6 on the one hand and a finite element analysis of single lap joints is described in chapter 7 on the other hand. For both calculations various steel grades and assembling tolerances are modelled, comparing their influence on the stiffness of the structure. The slip behaviour of the two types of joints is investigated.

Finally, the thesis is completed with conclusions in chapter 8 to give recommendations for the use of various bolt types in friction connections and a final outlook on future work in chapter 9 giving some suggestions for further research.

2 STATE OF THE ART

The focus of this thesis is brought on connections of steel structures as they are used in steel tubular towers and lattice towers. Here, the common way is joining various segments with flange connections, which in tubular steel towers shall be replaced by friction connections. In the following paragraphs for both types of joints the basic background for the design is explained, as it is carried out nowadays. The most important factors for load transfer in a friction grip connection are the force in the bolt and the surface conditions of the clamping package, given by a friction coefficient μ. On each of the factors research has been done during recent years. Some of this is introduced in this chapter.

2.1 Design of flange connections

Various models for the design of flange connections have been developed during the last decades. The most common way is to use the model of Petersen [21], which was later on modified by Seidel [22]. Here, the design of flange connections is done segment wise, which means that the resistance is calculated for a segment of a width that equals the distance between two bolts, see Figure 2.1-1. This one bolt section has to fulfil the requirements of the ultimate limit state, fatigue strength, as well as serviceability limit state. The latter one is not described any further, since it is not regarded as authoritative for the design of a tubular tower.

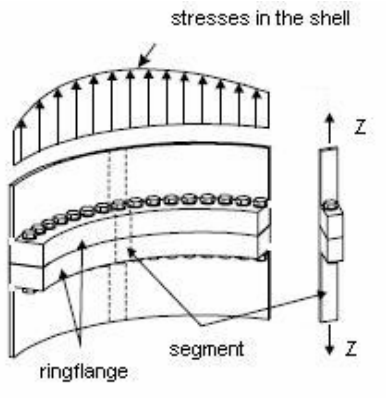

Figure 2.1-1: Segment wise design approach [22]

The failure at the ultimate limit state can either appear by exceeding the resistance in the bolt, in the flange or both at the same time, which are called failure modes A – C by Petersen. Seidel then differentiates between failure in the flange at the axis of the bolt or below the washer and called these failure modes D and E instead of C.

For fatigue the damage of the bolt is the resistance controlling problem. However, this cannot exclusively be the limit for the design. As Figure 2.1-2 shows, the relationship between the forces in the bolt and the applied tension in the tower shells is non linear and can be divided into four ranges. Usually, the existing service and fatigue loads occur in ranges one to three.

Due to the non linearity the system of damage equivalent loads (DEL) for design cannot be used and stress ranges have rather be determined by the help of a Rainflow matrix and use of Wöhler curves. Then the resistance of the structure can be shown according to Eurocode 3, part 1-9 [23].

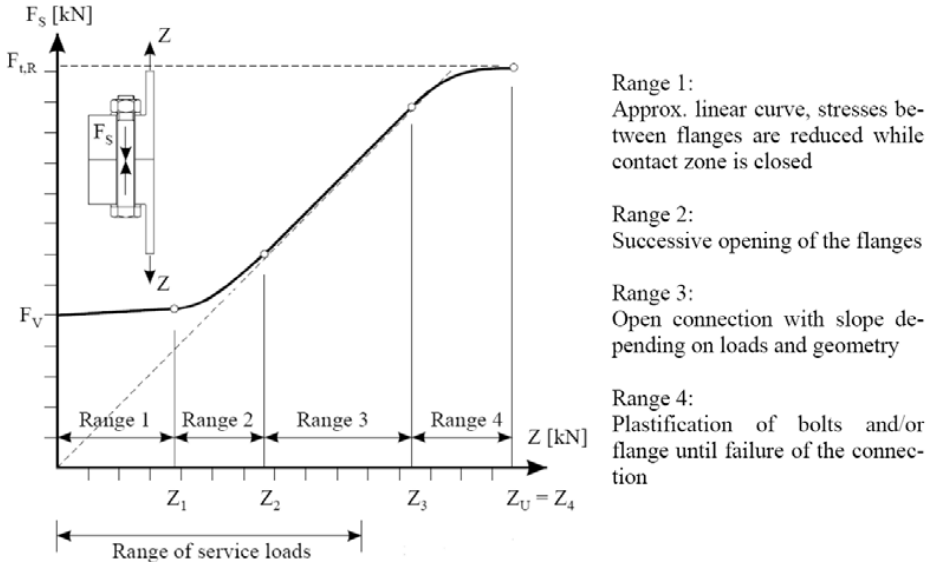

Figure 2.1-2:Non linear relationship between bolt force and applied load in the shell of tubular towers with flange connections [7]

2.2 Design of high strength friction grip connections

High strength friction grip connections, or simply friction connections, work by clamping together the plates of the joint by the help of high strength friction grip bolts. These bolts are usually of grade 10.9 or even higher. Load applied on the plates is lead across the connection by friction.

For design of a friction connection the general rules of for example Eurocode 3 part 1-8 [24] can be followed. Then the slip resistance of the connection can be regarded as ultimate limit state. Of course, fatigue of the connection has to be checked as well. The friction connection in steel tubular towers can be regarded as detail category 90 and should withstand a number of 10^8 load cycles [25].

The design for a friction connection can be carried out segment wise, so that not the complete cross-section of the tubular tower has to be taken into account but only a segment, which corresponds to the distance between two rows of bolts. It is important that although the lap joint becomes unsymmetrical by this

simplification, it can still be regarded as constraint in three dimensions by the complete tower cross-section.

It is self evident, that also the serviceability limit state needs to be checked, but it is not regarded as authoritative for the design of a tubular tower.

2.3 Flange connection versus friction connection

A comparison of the design of a flange and a friction connection using tension control bolts is carried out by Husson [7], [8]. In these studies the resistances for both types of connections are calculated for a typical wind tower of 80 m height, which corresponds to two tower segment connections of different cross-sections. Actual tower dimensions as well as static and fatigue loads are provided by the turbine producer.

Table 2-1: Connections based on static resistance at ULS [8]

	Component	Unit price [€]	Amount	Total price [€]
Bolted ring flange connections				
Section 1	Flange (d_a=3917mm)	6762.00	2	13524
	Bolt (M42x245 10.9)	20.32	124	2520
			Total :	16044
Section 2	Flange (d_a=3448mm)	4395.00	2	8790
	Bolt (M36x205 10.9)	11.40	116	1322
			Total :	10112
Friction connections				
Section 1	Bolt (M30x110 S10T)	5.45	588	3205
Section 2	Bolt (M30x110 S10T)	5.45	351	1913

The results, which are based on material prices from 2007, given in Table 2-1 obviously show that, although costs for fabrication and installation of the tower are not included, material costs for one tower can be reduced by about 20000 € by the use of friction connections instead of flange connections.

Furthermore the competitiveness of friction connections in comparison to flange connections and types of towers other than steel tubular towers is proven by feasibility tests carried out in Portugal [6], [31].

2.4 Loss of pretension

The force that is needed to assemble a friction joint is in literature often referred to as clamping force, bolt pretension or preload. The reduction of this force in a connection is a well known phenomenon, which occurs not only in structural engineering but even more in mechanical engineering. It can be divided into three sections: First, the initial loss of pretension, which mainly depends on the tightening process. Second, the short term relaxation, which occurs within the first twelve hours after joint assembly. And third, long term relaxation, which has been observed to continue asymptotically. As an example, the development of the measured strains of one of the tested bolts is shown in Figure 2.4-1. From the measured strains the forces can be calculated by the help of calibration data. Here, only phase one and the beginning of the second phase are visible. However, it gives an idea, how the development of the pretension force in a bolt looks like.

The first drop in pretension force happens within the first ten seconds after the bolt is tightened. The bigger the maximum or initial pretension force is, the bigger is the initial loss. It increases even more if the bolt has been pulled beyond its yield limit. For faster tightening processes the reduction in clamping force has been observed to increase [26].

If groups of bolts are tightened, they usually influence each other, meaning, that the bolt tightened firstly will show a loss in pretension force at the moment the second bolt is pretensioned. For example, for the case of TCB this is extensively examined and described by Husson [8].

Short term relaxation occurs after the initial loss of pretension has happened. In consequence of loading past their yield point, the members of the joint may creep and thereby evoke a reduction of elongation in the bolt, which leads to a loss of clamping force [26]. However, the most common reason for short term relaxation is embedment, if mistakes in installation and design of the bolts as well as changes in temperature can be excluded.

In general, as mentioned by Sedlacek and Kammel [29], loss of pretension or insufficient pretension forces can appear due to self loosening, relaxation in the connection, insufficient pretension force at installation (e.g. because of poor execution), material creep, use of unsuitable coatings and plastification of the bolt in the threaded part of the engaged shaft. If external loads are applied, loss of pretension can also be a result of plate thinning due to in-plane plate tensile stresses.

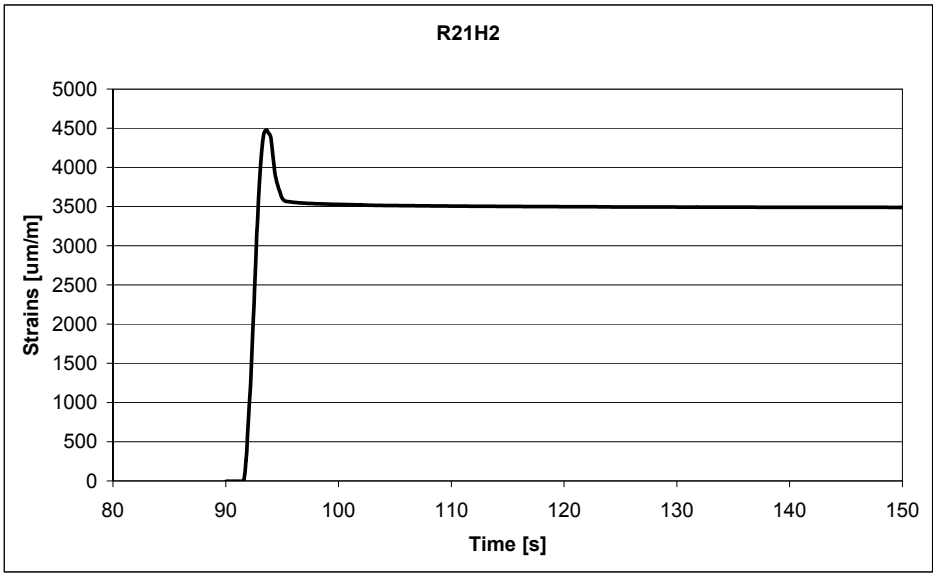

Figure 2.4-1: Strain development in a pretensioned bolt during the first minute after tightening (here for a Huck BobTail lockbolt M20 with a grip length of 40 mm as an example)

Within the first 12 hours after tightening, short term relaxation is said to be terminated. The remaining force in the bolts is often called for residual preload.

The problem of loss of pretension force has been examined various times with respect to the type of coating [27], [28], [29]. But it is not known for the silica rich primer Temasil 90, which is a common corrosion protection paint for structures, in combination with the types of bolts described in chapter 1.2. For common hexagonal high strength bolts even a guideline exists to calculate the resilience of bolts [30].

The clamping force of course also depends on the stiffness of a joint, which is based on the stiffness of the single members. Usually, the bolt has a higher strength than the material of the clamping package. Then the loss of pretension and the actual bolt force in case of tensile loading, as for example in a flange connection (see Figure 2.1-1), can be visualized by a bolted joint diagram as shown in Figure 2.4-2. Here, the bolt elongates due to pretensioning plus the additionally applied tensile force on the connection. But at the same time, the

clamping package reduces in thickness because of the compression force acting on it.

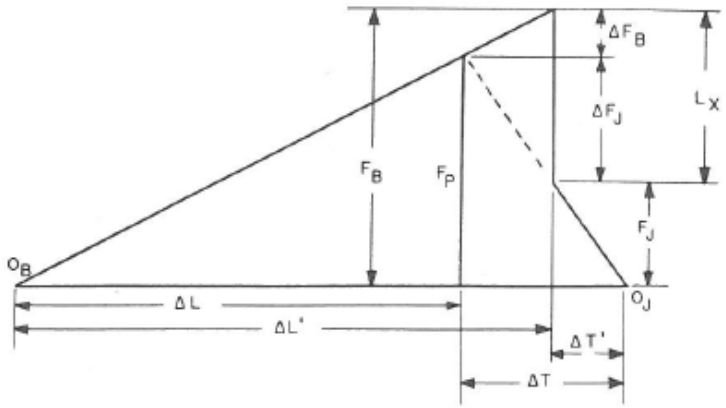

Figure 2.4-2: Bolted joint diagram [26]

Where

F_p	is the initial preload,
L_x	is the external tension load,
ΔF_B	is the change in load in bolt,
ΔF_J	is the change in load in joint,
ΔL, $\Delta L'$	is the elongation of bolt before and after application of external load,
ΔT, $\Delta T'$	is the compression of joint members before and after application of the external load.

In a friction joint the bolt is loaded in shear. Until failure occurs, more precisely until the connection starts to slip, the bolt is loaded by pure axial

tension only. This originates completely from tightening of the bolt. Therefore, the bolted joint diagram for a friction connection can be described by ΔL plus ΔT only, see Figure 2.4-2, since no external force is acting on the bolt in that very moment.

2.5 Slip factor

For the design of a friction connection the friction on the surfaces of the clamped package are of great importance. It is taken into account by a so called slip factor or by the friction coefficient. These factors vary depending on the type of surface finishing as well as the steel grade of the clamped plates in a friction connection.

While the slip factor is defined as the slip load divided by the clamping force in the beginning of the tests, the friction coefficient is identified as the slip load over the actual clamping force. As slip load in the Eurocodes, the load is designated, which occurs at the maximum permitted slip of 0,15 mm [20].

Establishment of the slip factor is setup dependent. Therefore, certain tests have to be carried out in accordance with EN 1090, part 2 [20], which prescribes the specific specimen and the necessary procedure.

Within the earlier mentioned HISTWIN project a number of slip factors has been determined for various kinds of steels and surface finishings [6], see Table 2-2 and Table 2-3, at the Faculty of Science and Technology in Coimbra, Portugal.

Table 2-2: Slip factors for various surface finishings of S275 [6]

	Type A	Type B	Type C	Type D	Type E	Type F
Surface blasted	with shot grit, degree Sa 2½	with shot steel, degree Sa 2½	with shot steel, degree Sa 3	chemistry	with shot steel, degree Sa 2½	with shot steel, degree Sa 2½
Surface treatment	without treatment	without treatment	spray metalized with zinc 75 µm	galvanization by hot immersion with zinc 160 µm	painted with zinc ethyl-silicate (one layer) with 70µm	painted with zinc epoxy (one layer) with 70µm (current product in Portugal)
Surface appearance	 0,47	 0,50	 0,40	 0,40	 0,40	 0,30

Table 2-3: Slip factors for various surface finishings of S690 and S355 [6]

	High strength steel S 690			Cor-Ten steel S 355		
	Type B	**Type C**	**Type F**	**Type BI**	**Type BE**	**Type BEE**
Surface blasted	with shot steel, degree Sa 2½	with shot steel, degree Sa 3	with shot steel, degree Sa 2½	with shot steel, degree Sa 2½	with shot steel, degree Sa 2½	with shot steel, degree Sa 2½
Surface treatment	without treatment	spray metalized with zinc 75 µm nominal (75 µm real)	painted with zinc epoxy (one layer) with 70µm nominal (135 mm real) (current product in Portugal)	without treatment exposed to the environment in the Interior of the Laboratory - 10 days	without treatment exposed to the environment in the Interior of the Laboratory - 15 days + Exposed to the outside environment - 20 days	without treatment exposed to the environment in the Interior of the Laboratory - 15 days + Exposed to the outside environment - 80 days
Surface appearance	 0,50	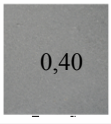 0,40	 0,20	 0,50	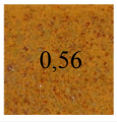 0,56	 0,30

3 REMAINING PRETENSION FORCE IN A FRICTION CONNECTION

Two types of tests are performed to quantify the contribution of tension control bolts (TCB) and a plate coating on the loss of pretension in a lap joint. In these tests two main variables are considered in the experimental program: the load on the lap joint (long term tests) and the thickness of the primer in the connection (relaxation tests).

The influence of a tensile load on the joint is experimentally established in long-term tests, where the specimens are left under a stress which is 80 % and 60 % of the static resistance for a period of four months. Ethyl silicate zinc rich paint is a commonly used primer in wind towers and its influence is investigated in so called relaxation tests, the second type of test.

3.1 Introduction

As already mentioned before is the main objective of the performed experiments to assess an optimal fastener for a friction connection in this type of application, having in mind structural performance, initial costs and maintenance costs. The loss of pretension over time of a possible type of bolt is presented in this chapter.

Within previous experimental work carried out at Luleå University of Technology (LTU) a loss of pretension in bolts of friction connections was monitored. To achieve a better understanding of the influences on this loss of pretension, two types of tests are performed. First, so called long-term tests are done to examine the behaviour of one segment of a tubular tower high strength friction grip connection under a static load [8]. Then, a number of relaxation

tests is carried out to check the influence of the steel plate coating on the loss of pretension.

3.2 Experimental setup and conditions

In both specimens the same type of tension control bolt (TCB, see chapter 1.2.1) with a diameter of 30 mm is tested. It has grade S10T, which corresponds to mechanical properties of high strength bolts and can be regarded as class 10.9. The advantage of this type of bolt is that it can be tightened from the nut-side only. No significant torsion is introduced into the bolt shank and a well controlled pretension force is achieved [4].

The two types of tests are performed in a constant indoor environment, which means that no influence of corrosion is taken into account. Besides, possible influences on the loss of pretension due to temperature changes can be neglected. In both tests a cover plate replaces the single washers per bolt, which simplifies and accelerates the installation process in the field and spreads the bolt forces equally in the main plates. The cover plates are fabricated of grit blasted Raex400, whereas the actual plates are made of S355, which are grit blasted or coated with a zinc rich primer, respectively.

The used zinc rich primer is called TEMASIL 90, produced by Tikkurila Coatings and contains a zinc content of 70 – 90 % according to the producer. A product information can be found in the Annex F. The producer also claims that the paint has good resistance against abrasion and can either be used singly or as a primer in combination with other surface coatings.

All of the specimens are first grit blasted with a steel grit size of G70 until a quality of Sa 2 ½ is reached. Then, the respective painted surfaces are coated with the zinc rich primer up to a nominal coating thickness of 50 – 80 μm.

3.2.1 Long-term tests

The long term behaviour of friction connections has been examined by Husson [8]. A single segment of the joint is tested instead of a tubular section, arguments for this can be found in chapter 2.2. The lap joint consists of a group of three bolts connecting two steel plates - one of them with normal clearance holes and one with a long open slotted hole, cp. Figure 3.2-1. The specimens are first tightened, starting with the bolt in the middle and then proceeding from inside the connection to the outer ends, as demanded in the standards. Then the specimen is kept without any additional loading for 12 hours to

monitor the loss of pretension in the bolts. Afterwards the specimens are placed into a test rig and a tensile load is applied to the plates. The external axial loading on the plates corresponds to 80 % and 60 % respectively of the characteristic static resistance of the joint.

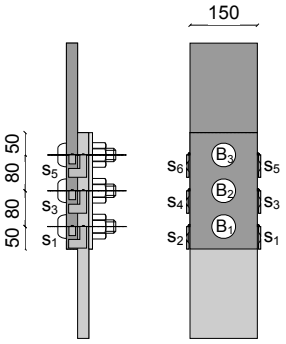

Figure 3.2-1: Specimen for long-term tests [8]

The three normal holes in the specimen are of diameter 33 mm in a 25 mm thick plate. The second plate, which is coloured in a lighter grey in Figure 3.2-1, has the same thickness but a long open slotted hole instead of three with normal clearances. This cut out is of a width of 33 mm and a length of 235 mm. Instead of three single washers a cover plate with 8mm thickness is used. The dimensions are chosen in agreement with the measures in an actual wind tower.

3.2.2 Relaxation tests

The other type of test, the relaxation test, consists of a so called main plate (plate no. 2) and a cover plate (plate no. 1), which is used to replace washers. The two plates are jointed by three bolts, cp. Figure 3.2-2.

The main attention is to estimate the influence of the primer, ethyl silicate zinc rich paint, on the loss of pretension. For this reason the actual two plates of the long term tests are here replaced by only one plate, the main plate, which is exactly as thick as the sum of plates in the long term tests before. By this, the influence of the shear planes on the loss of pretension shall be excluded.

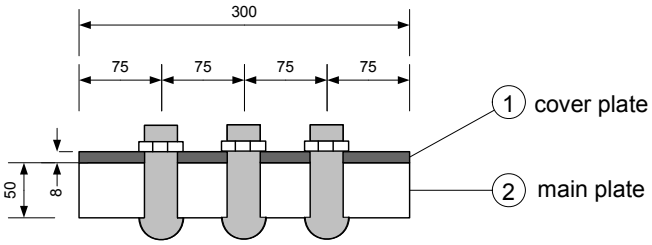

Figure 3.2-2: Specimen for relaxation tests

Three alternatives of the main plate coating are considered: no primer, primer on the top surface and primer on top and bottom surface of the main plate, with an average primer thickness of 80 µm. The plates are of dimension 300 mm x 100 mm with 3 holes of diameter 33 mm and a thickness of 50 mm for the main plate and 8 mm for the cover plate. No additional force is applied on the plates.

3.3 Remaining pretension force

The pretension in the bolts is measured constantly over time. The results given in the paragraphs below are the average of the measured values per type of test specimen, from which a general design value of the remaining pretension force $F_{p,C,lt}$ during a period of time should be evaluated, using a general formula acc. to EN 1990 [27] and the initial pretension force $F_{p,C}$ acc. to EN 1993-1-8 [34].

$$F_{p,C,lt} = F_{p,C} - m_x \cdot (1 + k_n \cdot \frac{s_X}{m_X}) \tag{3-1}$$

Where

$F_{p,C,lt}$ is the remaining pretension force after a certain time

$F_{p,C,lt}$ it the initial pretension force as calculated acc. to EC 3 [34]

m_x is the mean loss of pretension force in bolts,

$k_n = 1{,}64$ is the factor given for the 5% characteristic value,

$V_x = s_x/m_x$ is the coefficient of variation of the pretension losses.

3.3.1 Long-term tests

Performing the long-term tests (herein after referred to as LT) starts with tightening the bolts. Irrespective of the position in the bolts this gives an average loss of pretension per bolt, which is shown in Table 3-1: The time in seconds refers to the time which has passed after the bolt is completely tightened, which means that the maximum pretension is reached. The loss of pretension in % also refers to this maximum bolt force.

Table 3-1: Average loss of pretension [%]

Time after Max.	**Loss of pretension [%]**
10 s	2,9
10 min	6,4
12 hrs	9,6

12 hours after tightening of the bolts an axial tensile force is applied to the joints, corresponding to 80 % and 60 % of the characteristic static resistance of the joint. As it can be seen in Table 3-2 the loss of pretension over time does not change significantly. The loss of pretension refers to the force present in the bolts at the time the tensile load is applied to the joint.

The six specimens - three for each load case - are kept under static loading for a period of four months. During this time the forces in the bolts are measured constantly.

Table 3-2: Average loss of pretension [%] after applying a tensile load

	Loss of pretension after the tensile load is applied			Total loss after tightening
Time after loading	**300 kN**	**225 kN**	**average**	**average**
2 hrs	0,4	0,4	0,4	10,0
24 hrs	1,0	0,8	0,9	10,5
1 week	2,1	1,5	1,8	11,4
15 weeks	2,5	3,3	2,9	12,5

3.3.2 Relaxation tests

In this test as well, the loss of pretension force in the bolts, from the installation until eight weeks after tightening, is monitored constantly. A total number of 3 specimens, containing 3 bolts each, are tested. Depending on the number of coated surfaces of the main plate these tests are named as R2, R1 and R0, meaning two, one and no coated surface respectively.

Table 3-3: Average loss of pretension [%] depending on no. of coated surfaces

	No. of coated surfaces		
Time after loading	**R2**	**R1**	**R0**
10 s	2,8	3,0	2,8
10 min	4,5	4,4	3,4
12 hrs	6,4	5,8	3,9
12 hrs +2 hrs	6,5	5,8	3,9
12 hrs + 24 hrs	6,9	6,2	4,0
12 hrs + 1 week	7,5	6,5	4,0

3.3.3 Extrapolation for 20 years

The average losses of pretension for all tests are plotted versus time, cp. Figure 3.3-1. This diagram shows an extrapolation for 20 years of the losses as percentage of the maximum pretension force at bolt tightening in a logarithmic scale. For R0, R1 and R2 losses of 4,8 %, 8,8 % and 10,5 % of the initial pretension are expected. For LT much higher losses are calculated; up to 16,8 %.

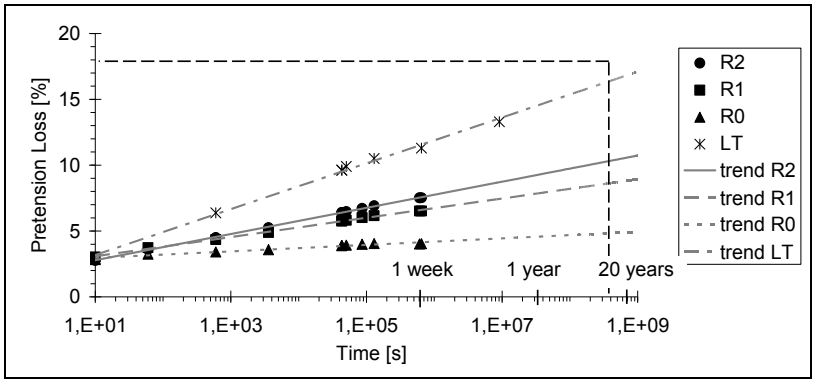

Figure 3.3-1: Extrapolated average losses of pretension [%] versus time

Comparing the trends for R0, R1 and R2 an influence of the surface coating is evident. Specimens in the long-term tests consist of two single plates, which are each painted with the primer on both sides plus an additional cover plate without coating. This ends up with 4 coated surfaces. Extrapolation of the loss of pretension acc. to the number of covered surfaces is shown in Table 3-4.

Table 3-4: Predicted average loss of pretension [%] depending on the no. of coated surfaces after 20 years

	R0	**R1**	**R2**	**LT**
20 years	4,8	8,8	10,5	16,8

This means that the primer dominantly influences the loss of pretension in the static test.

From the average losses of pretension for the long-term tests shown in Figure 3.3-1 a statistical evaluation according to EN 1990 [27] is done to obtain characteristic values, cp. Figure 3.3-2. Approximating these values by a trend allows the prediction of the characteristic loss of pretension after 20 years.

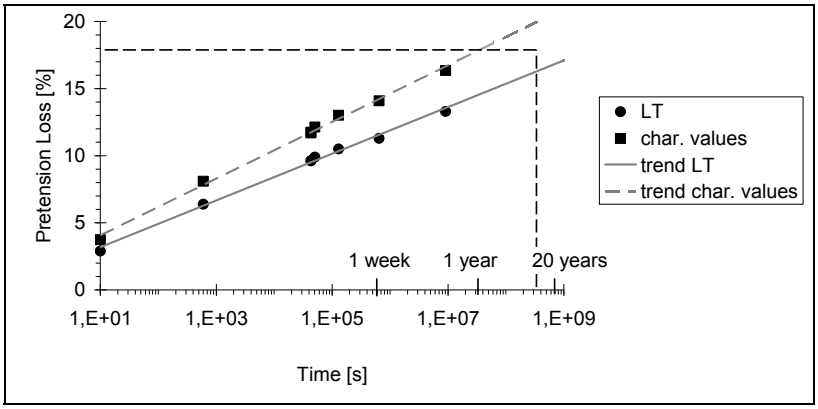

Figure 3.3-2: Extrapolated characteristic and average losses of pretension [%] versus time

The function of the trend line for the characteristic values can then be included in formula 3-1 and leads to formula 3-2.

3.4 Conclusions

Based on the segment test results for TCB M30 with a grip length of 58 mm, carried out under corrosion free conditions, a tentative recommendation for the estimation of the remaining force in the pretensioned bolt is:

$$F_{p,C,lt} = F_{p,C} \cdot \left[1 - \frac{0,9165 \cdot \ln\left(\frac{t}{31,536 \cdot 10^6} \right) + 1,9602}{100} \right] \qquad (3\text{-}2)$$

Where

$F_{p,C,lt}$ is the pretension force in a certain period of time (long term),

$F_{p,C}$ is the initial pretension force, according to EN-1993-1-8,

t is the time in years after the pretensioning.

Formula 3-2 gives an indication of the pretension force in a bolt of the friction connection that would remain if the influence of the corrosion and the cyclic load is be neglected.

The performed tests lead to the following conclusions about the reduction of forces in pretensioned bolts:

1. A load applied on a joint with pretensioned bolts does not increase the loss of pretension significantly.

2. A coating on the surfaces of the jointed plates increases the loss of pretension, which means that the losses of pretension over time can be quantified depending on the number of coated plate surfaces.

4 INFLUENCE OF BOLT TYPE AND DIMENSIONS ON LOSS OF PRETENSION

The loss of pretension depends on various factors, such as bolt material and material of the clamping package. To investigate the influence of the type of bolt the following tests have been carried out. Here, the reduction in clamping force is checked for standard bolts in combination with NordLock washers, Friedberg HV Rändel and Huck BobTail lockbolts. The latter ones are tested in two variations; longer and shorter grip length, to understand the contribution of the length of the bolt shank on the loss of pretension.

4.1 Performed tests

The same tests as described in chapter 3.3.2 have also been carried out for other types of bolts than TCB to examine the loss of pretension in various types of bolts. The specimens all have the same configuration, see Figure 4.1-1, but vary in dimensions, which are adapted to the diameter of the bolts and their clamping lengths.

For a comparison of various types of fasteners of size M30, standard structural bolts in combination with pairs of NordLock washers have been tested additionally to the tests with TCB in chapter 3. In size M20 tests have been performed with Huck BobTail lockbolts and Friedberg HV Rändel. The experiments with Huck bolts have been carried out in two variations: One specimen had a thickness of the clamping package of 40 mm = 37 mm main plate plus 3 mm cover plate, the other one of 18 mm = 15 mm main plate plus 3 mm cover plate. The latter ones are the same thicknesses as used for the tests with Friedberg HV Rändel bolts.

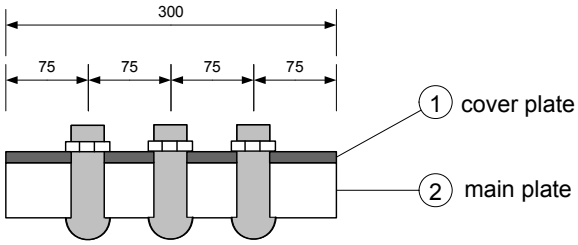

Figure 4.1-1: Specimen for relaxation tests

All plates have the same dimensions of 100 mm width and 300 mm length. The diameter of the holes varies between 33 mm for M30 bolts and 23 mm for M20 bolts. Just for the fitted Friedberg bolts the hole diameters were smaller; 20,1 mm.

4.2 Tests with standard structural bolts and NordLock washers

Already during tightening of the bolts problems have arisen. The original plan has been to tighten the bolts according to the Swedish codes. This means to screw the nut by hand in the first place and then all the way with a machine. But by doing so, the surfaces of the washer pairs facing the plate surfaces have gripped into it and started to turn themselves. Due to the applied power, the washer pairs have overrun. To prevent from this, tightening has to be done very carefully in a stepwise manner.

The specimen with one surface coating looses the most pretension force, whereas the specimen with two coated surfaces undergoes the least. These observations are unreasonable and imply the conclusion that these tests are either not well performed or that the special washers equal out the influence of the surface coating. To ensure the first or the second hypothesis, further tests are necessary.

However, pretension force losses of 8 – 9 % of the maximum tightening force are higher than the ones monitored for the same kind of specimen using TCB, see chapter 3.3.2. Whether this is a general fact or just applies to these tests, needs to be checked in additional tests. The findings here imply a tentative recommendation for the use of TCB instead of structural bolts in combination with NordLock washers. In order to draw a general conclusion, further tests of these washers are necessary.

Table 4-1: Loss of pretension for standard structural bolts with NordLock washers in % of the maximum pretension force

	NordLock		
	R2	**R1**	**R0**
after 10 seconds	1,84	2,58	1,80
after 60 seconds	4,74	3,73	4,50
after 10 minutes	5,68	5,73	6,52
after 1 hour	6,79	7,48	7,40
after 12 hours	7,74	8,59	8,23
after 12+2min	7,74	8,59	8,23
after 12+2 hours	7,79	8,65	8,27
after 24 hours	7,91	8,76	8,35
after 36 hours	8,06	8,93	8,45
after 1 week	8,50	9,49	8,77

4.3 Tests with Friedberg HV Rändel

Inserting the bolts into the fitted holes turns out to be problematic. The idea is to pull the bolt into the hole by tightening the nut from the other end. But by doing so with specimen R2F, breaking-noises appear. However, from visible inspection it is not recognisable if the bolt is broken. Nevertheless, the monitored strains prove that both of the bolts or strain gauges are damaged, cp. Table 4-2.

Table 4-2: Loss of pretension for Friedberg HV Rändel in % of the maximum pretension force

	Friedberg		
	R2	R1	R0
after 10 seconds	31,31	3,26	1,08
after 60 seconds	77,71	19,10	33,97
after 10 minutes	78,90	21,69	35,20
after 1 hour	93,04	22,92	35,43
after 12 hours	93,24	22,93	35,70
after 12+2min	93,24	22,93	35,70
after 12+2 hours	93,25	22,92	35,71
after 24 hours	93,26	22,90	35,71
after 36 hours	93,30	22,91	35,74
after 1 week	93,36	22,94	35,80

The same is valid for the specimens R1F and R0F. Although the losses of pretension seem to be reasonable directly after tightening, they increase extremely during the first couple of minutes. The data achieved from these tests is not reliable.

4.4 Tests with Huck BobTail lockbolts

Two variations of tests have been carried out with Huck BobTail lockbolts; one of them had a clamping package length of 40 mm and is named as “long”, whereas the other one had a clamping package length of 18 mm and is labelled as “short”. Although it seems to be unreasonable that for the specimens with only one coated surface the losses of pretension are higher than the for the specimens with two coated surfaces, it does make sense that the longer bolts show lower losses than the shorter ones, see Table 4-3.

The values in general seem to be quite high. But since each test result consists of the average value of three bolts per specimen and two replicates, they are assumed to be reliable. Besides, the test with Huck bolts of 1” in diameter, described further below (see chapter 5.2), achieve similar values.

Table 4-3: Loss of pretension for long and short Huck BobTail lockbolts in % of the maximum pretension force

	Huck long			Huck short		
	R2	**R1**	**R0**	**R2**	**R1**	**R0**
after 10 seconds	18,32	23,65	23,00	37,85	42,17	33,38
after 60 seconds	17,80	23,66	23,34	38,24	42,17	38,07
after 10 minutes	18,15	23,69	23,39	38,53	42,21	38,58
after 1 hour	18,63	23,81	23,63	38,97	42,37	39,06
after 12 hours	19,21	24,24	24,09	39,68	42,90	39,83
after 12+2min	19,21	24,25	24,09	39,68	42,90	39,83
after 12+2 hours	19,24	24,28	24,12	39,73	42,95	39,87
after 24 hours	19,38	24,40	24,25	39,45	43,10	40,02
after 36 hours	19,46	24,51	24,34	39,64	43,26	40,19
after 1 week	20,01	25,01	24,82	40,41	43,93	40,85

5 INFLUENCE OF LOADING ON LOSS OF PRETENSION IN BOLTED CONNECTIONS

A common problem in bolted connections is the self-loosening effect of bolts over time. Therefore, the remaining strength in a slip resistant connection can only roughly be estimated for a certain point of time. A possible solution to avoid self loosening is the use of lockbolts, which have been studied in order to achieve recommendations for connections which are "free from maintenance". The pretension force in the bolt unavoidably reduces over time due to creep of primer, forces in bolts and in plates. These effects are experimentally studied. For all types of connections this effect is very important and in this chapter the focus is brought on lap joints, where the influence of various types of loading is examined. In contrast to chapter 3, which also deals with friction connections, the test specimens here are symmetric double shear lap joints and have round holes of normal clearance in all plates instead of a long open slotted one, to meet the requirements for lattice towers.

5.1 Performed tests

For these tests 6 specimens have been prepared. All of them are used to check the loss of pretension in bolted connections over time. They are all tightened with Huck Bobtail lockbolts (see chapter 1.2.2) of 1" in diameter, which is equal to 25,4 mm. Further information about the material properties and behaviour of this type of bolt can be found in Annex D, where additional tests on the bolt itself are described. The specimens differ in the number of galvanized surfaces and in the clamping length of the used bolts: In three of the specimens longer bolts with additional extension sleeves are used.

Those two test pieces, which are galvanized on all surfaces, are used for further investigation, in which the specimens undergo external loading. Purpose is to get a first indication of the loss of pretension in the bolts during loading of the specimen, since it is a known fact that a variation of stresses perpendicular to the bolts reduces the thickness of the clamping package and thereby decreases the strains in the bolts, which correspond directly to their forces.

The applied loading is static or cyclic, respectively. Various stress ranges are considered in the cyclic loading. All tests are performed indoors at constant room temperature to exclude other influences on the loss of pretension in the bolts.

The strains in the bolts, from which forces can be calculated by help of the data achieved in the calibration of the strain gauges (see Annex B), are constantly monitored. After performance of the tests, the friction coefficient μ is evaluated from the results of a static test.

5.1.1 Setup

As the drawing in Figure 5.1-1 shows, two different test-series are performed on double shear lap joints; series 1 for long bolts with extension sleeves, series 2 for shorter bolts without extension sleeves. In both cases the plates are bolted together by a group of three lockbolts. The normal sized holes have a diameter of 28 mm. The plates in these experiments are fabricated of hot dip galvanized S355 steel and have a width of 110 mm.

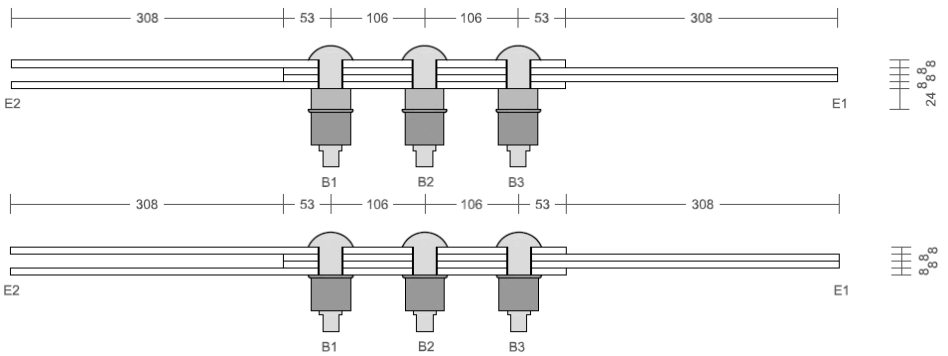

Figure 5.1-1: Test setup with and without extension sleeves

Purpose of the sleeves, which can be seen in the upper drawing of Figure 5.1-1, is to raise the thickness of the connection, so that it meets the grip length of the bolts, which are investigated to see if they loose less pretension than shorter bolts. For each grip length three tests are carried out. They differ in the number of galvanized surfaces; either eight, four or no surfaces have a zinc protection layer, which faces the outside of the connections. In tests RuH-S_4 and RuH-4 all plate surfaces are galvanized. For tests RuH-S_0 and RuH_0 all plate surfaces are grit blasted only, whereas tests RuH-S_2 and RuH_2 have galvanized surfaces on the outside and grit blasted surfaces on the inside of the connected plates. Average thickness of the galvanization is 0,25 mm.

5.1.2 Denotation

All tests are named according to the same system: The “Ru” for relaxation tests in the first place is followed by “H” as an indication for Huck BobTail lockbolts. Depending on the fact whether long bolts plus sleeves were used or not the test notation includes a “S”. The final number 4 gives an indication of the number of galvanized surfaces in the test specimen: A 4 equals eight galvanized surfaces, a 2 equals four galvanized surfaces and a 0 means that no galvanization can be found on the plates.

As an example, the specimen

RuH-S_4

describes a relaxation test with long Huck bolts and additional extension sleeve, where all of the surfaces is galvanized.

In short:

Ru	relaxation test
H	Huck BobTail lockbolt
S	including an extension sleeve
4	number of galvanized surfaces is eight

5.1.3 Sleeves

The steel producer provided the original extension sleeves, as they are used in the original lattice tower connection. Purpose of these is to raise the thickness of the connection so that it meets the grip length of the bolts.

The sleeves were originally fabricated by Fa. Mutzenbach in Germany. The original sleeves are too long for the grip length of the long Huck BobTail lockbolts, so that they are shortened to a length of 24 mm. By this the original surface finishing of the sleeves is taken away at one end. Their nominal grade is S355J0.

5.1.4 Surface preparation

Some of the plate surfaces are galvanized. The surface finishing has been prepared by the steel producer. For more information about the thickness of the galvanization layer a thickness measurement is carried out on the specimen for the static test (RuH-S_4).

The actual plate thickness as well as the thickness of the galvanization layer influences the results of the tests. The originally planned plate thickness is 8 mm plus the additional galvanization layer. To obtain the actual values of plate thickness and of the thickness of the galvanization layer, 55 mm long plates are cut off at the ends of the specimens. The resulting small plates are measured in three points on each side, assuming that the thickness variation is the same over the full plate length, cp. Figure 5.1-2:

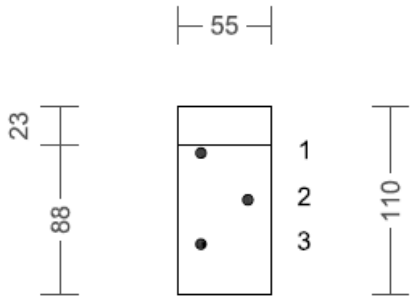

Figure 5.1-2: Measurement points per plate surface

The thickness measurements are performed as follows: First, the complete plate thickness is measured. Then the galvanization on one side of the plate is removed by placing the plate in a 30 % - salt acid for 11 minutes. To protect the galvanization layer on the other side of the plate this surface is coated with beeswax, which can be easily removed by heating it up. After removing the first galvanization layer another thickness measurement is performed. If the galvanization has completely been removed is carefully checked under a microscope. The difference in measurement one and two adds up to the thickness of the galvanization layer of side A. Then, the same procedure is performed again on the other side of the plate, side B. In total this is conducted 4 x 2 times, for four plates and two sides A and B each. The results can be seen in Table 5-1.

Table 5-1: Plate thickness measurements [mm]

Specimen	measured point 1	2	3	average value of point 1, 2 & 3	layer thickness
1A1	8,51	8,50	8,49	8,50	
1A2	8,22	8,23	8,22	8,22	0,28
1B1	8,22	8,23	8,22	8,22	
1B2	7,98	7,98	7,99	7,98	0,24
2A1	8,47	8,49	8,48	8,48	
2A2	8,24	8,23	8,23	8,23	0,25
2B1	8,24	8,23	8,23	8,23	
2B2	7,96	7,97	7,96	7,96	0,27
3A1	8,51	8,52	8,52	8,51	
3A2	8,25	8,24	8,24	8,24	0,27
3B1	8,25	8,24	8,24	8,24	
3B2	8,01	7,99	8,00	8,00	0,24
4A1	8,41	8,43	8,41	8,41	
4A2	8,16	8,17	8,16	8,16	0,25
4B1	8,16	8,17	8,16	8,16	
4B2	7,93	7,92	7,93	7,93	0,24

The name of the measured specimen includes first the number of the measured plate 1 - 4, then the side A or B and finally if it is the first measurement with galvanization (1) or the one after the galvanization has been taken away (2).

The galvanization layer has a thickness that varies between 0,236 and 0,276 mm, which results in an average thickness of 0,25425 mm.

Due to these results, it can be concluded that specimens with eight galvanized surfaces have a total coating thickness of 2,034 mm and the ones with four galvanized surfaces 1,017 mm in average, cp. Table 5-2.

Table 5-2: Average galvanization thickness per specimen [mm]

Specimen	No. of galvanized surfaces	Total galvanization thickness [mm]
RuH-S_4	8	2,034
RuH-S_2	4	1,017
RuH-S_0	0	0
RuH_4	8	2,034
RuH_2	4	1,017
RuH_0	0	0

5.1.5 Test procedure

By inserting strain gauges into the bolt shanks the axial deformation of the bolts is constantly monitored during the ongoing experiments. The forces in the bolts can be calculated from the measured strains due to a calibration, which is performed in advance of the tests. The according data can be found in Annex B.

The bolts are tightened one after the other without lubrication, starting with the one in the middle (B2), followed by the one to the left (B1) and concluded with the last one (B3). After four weeks of monitoring the strains in the specimens, the two ones with eight galvanized surfaces, RuH-S_4 and RuH_4 are set

under external loading – static and cyclic loading, respectively, while the clamping force in the other specimens is monitored for another 36 weeks.

5.2 Relaxation tests

Before the test specimens RuH-S_4 and RuH_4 are set in the machine to apply axial loading they are kept under constant indoor conditions to monitor the loss of pretension during a period of about four weeks to check the bolts' performance without external loading. The bolts of other specimens, RuH-S_2, RuH-S_0, RuH_2 and RuH_0, are tightened at the same time, but the monitoring of their behaviour goes on for 42 weeks in total, without any external load application at all.

In series 1 long Huck BobTail lockbolts of diameter 1" are used, commercially named as BT8R-DT32-32 (hereinafter referred to as "long"), whereas in series 2 shorter Huck BobTail lockbolts, trade name BT8R-DT32-16 (hereinafter referred to as "short") connect the plates.

The exact description about which bolts are engaged in which specimen can be seen in Table 5-3.

Table 5-3: Bolts per test specimen

Specimen	Bolt Name		
	B1	**B2**	**B3**
RuH-S_4	H30	(H32)	H40
RuH-S_2	H31	(H33)	H41
RuH-S_0	H35	H37	H38
RuH_4	H46	H47	(H51)
RuH_2	H57	H55	H58
RuH_0	H63	H60	H62

The tests RuH-S_4, RuH-S_2, RuH-S_0 contain extension sleeves and are therefore performed with long bolts, whereas in tests RuH_4, RuH_2, RuH_0 the short bolts are inserted.

5.2.1 Test data

Checking the measured data during testing reveals that strains in all bolts look reasonable, besides the ones monitored for bolt H51 in specimen RuH_4. Here the losses seem to be too big. The assumed reason for this is that the strain gauge is not working well or even might have been destroyed during bolt tightening. For further interpretation of the test results the data of bolt H51 is excluded. The same goes for bolt H33, which later on shows unreasonable strains. Bolt H32 does not show unreasonable results, as long as the overall performance is regarded. But the measured strains appeared to be very sensitive to movement of the attached cables, so that this data as well is not taken into account for the evaluation of the tests.

5.2.2 Results

With help of strain gauge calibrations, which have been performed in advance of the tests, the monitored strains in the bolts can be transferred into bolt forces. Table 5-4 shows the bolt force per test setup as an average of the three bolts per specimen. In case of the tests RuH-S_4, RuH-S_2 and RuH_4 the average consists of only 2 bolts, since it is found that the third bolts do not work properly.

Alcoa Fastening Systems guarantees a clamping force of 284 kN for bolts of 1”-diameter independent of the length of the shank. It is significant that most of the average bolt forces drop below this level one minute after tightening of the bolts and in all cases after 10 minutes.

A typical curve for the development of forces in Huck BobTail lockbolts illustrates Figure 5.2-1. Here, the bolt forces for test specimen RuH-S_0 are shown. Noteworthy is, that the bolts loose comparably much of the maximum force already during the installation process: about 50 - 60 kN, which equals more than 15 % of the initial clamping force. Another remarkable fact is, that the bolts are obviously not influenced by each others’ tightening as much as has been observed by Husson for TCB bolts [8]: The tested TCB loose about 5 – 10 kN each directly after tightening and the same amount again when one of the other bolts is installed. This equals losses of the maximum pretension of 2,5 – 5 %.

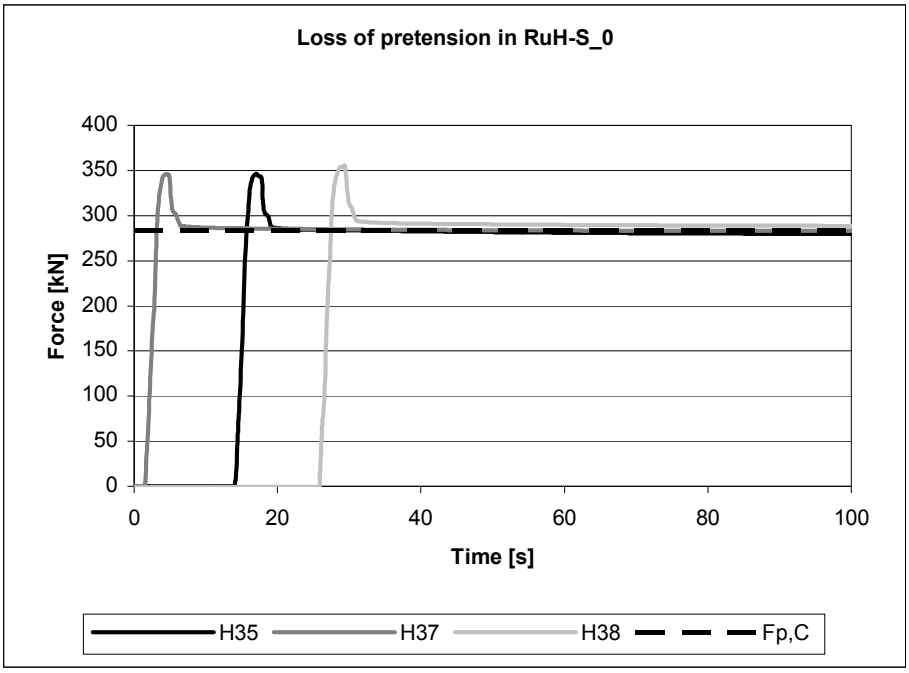

Figure 5.2-1:Loss of pretension [kN] in Huck BobTail lockbolts during tightening

Table 5-4 shows the average bolt forces per test specimen which have been monitored during tightening and thereafter. For specimens RuH-S_4 and RuH_4 measured values for a period of four weeks are available, whereas the clamping force in specimens RuH-S_2, RuH-S_0, RuH_2 and RuH_0 has been recorded for 40 weeks.

Table 5-5 shows the same results as Table 5-4, but they are recalculated into losses of pretension in % of the maximum load, which was achieved directly after swaging the bolts.

Table 5-4: Average bolt force [kN] per test-setup

average actual force [kN]	Huck long			Huck short		
per bolt type	RuH-S_4	RuH-S_2	RuH-S_0	RuH_4	RuH_2	RuH_0
maximum pretension force	350,28	372,44	349,39	381,60	379,77	382,98
after 10 seconds	286,80	296,83	287,01	282,98	282,37	282,81
after 60 seconds	282,62	292,75	284,13	277,07	277,17	278,82
after 10 minutes	277,44	288,65	283,81	271,59	273,79	278,63
after 1 hour	272,80	285,29	283,09	266,16	270,04	277,25
after 12 hours	268,33	282,31	282,24	259,68	265,56	275,14
after 24 hours	266,78	282,28	281,85	257,93	264,39	274,53
after 1 week	262,93	281,21	281,05	253,60	261,10	272,68
after 4 weeks	259,44	279,64	280,14	249,88	258,21	270,96
after 8 weeks	-	282,04	279,60	-	257,00	270,21
after 12 weeks	-	281,35	279,33	-	255,89	269,41
after 16 weeks	-	280,75	278,96	-	255,09	268,77
after 20 weeks	-	280,35	278,77	-	254,52	268,58
after 24 weeks	-	279,83	278,42	-	254,01	268,13
after 28 weeks	-	279,95	278,70	-	253,84	268,12
after 32 weeks	-	280,12	278,98	-	253,99	268,24
after 36 weeks	-	279,88	278,93	-	253,44	267,87
after 40 weeks	-	279,36	278,64	-	252,82	267,31

Table 5-5: Average losses of pretension [%] per test-setup

average losses [%]	Huck long			Huck short		
per bolt type	RuH-S_4	RuH-S_2	RuH-S_0	RuH_4	RuH_2	RuH_0
after 10 seconds	18,12	20,30	17,85	25,84	25,65	26,16
after 60 seconds	19,31	21,39	18,67	27,39	27,02	27,20
after 10 minutes	20,79	22,50	18,77	28,83	27,91	27,25
after 1 hour	22,12	23,40	18,97	30,25	28,89	27,61
after 12 hours	23,39	24,20	19,22	31,95	30,07	28,16
after 24 hours	23,84	24,21	19,33	32,41	30,38	28,32
after 1 week	24,94	24,50	19,56	33,54	31,24	28,80
after 4 weeks	25,93	24,92	19,82	34,52	32,01	29,25
after 8 weeks	-	25,15	19,97	-	32,33	29,45
after 12 weeks	-	25,34	20,05	-	32,62	29,66
after 16 weeks	-	25,52	20,15	-	32,83	29,82
after 20 weeks	-	25,62	20,21	-	32,98	29,87
after 24 weeks	-	25,77	20,31	-	33,11	29,99
after 28 weeks	-	25,72	20,23	-	33,16	29,99
after 32 weeks	-	25,66	20,15	-	33,12	29,96
after 36 weeks	-	25,70	20,17	-	33,26	30,06
after 40 weeks	-	25,86	20,25	-	33,42	30,20

For an easier comparison the numbers given in Table 5-5 are as well given in relative losses compared to the losses 10 s after tightening, see Table 5-6.

Table 5-6: Relative losses of pretension [%] per test-setup in comparison to losses 10 seconds after tightening

average losses [%]	Huck long			Huck short		
per bolt type	RuH-S_4	RuH-S_2	RuH-S_0	RuH_4	RuH_2	RuH_0
after 10 seconds	0,00	0,00	0,00	0,00	0,00	0,00
after 60 seconds	1,19	1,09	0,83	1,55	1,37	1,04
after 10 minutes	2,67	2,20	0,92	2,99	2,26	1,09
after 1 hour	4,00	3,10	1,12	4,41	3,25	1,45
after 12 hours	5,27	3,90	1,37	6,11	4,43	2,00
after 24 hours	5,72	3,91	1,48	6,57	4,73	2,16
after 1 week	6,82	4,20	1,71	7,70	5,60	2,64
after 4 weeks	7,81	4,62	1,97	8,68	6,36	3,09
after 8 weeks	-	4,85	2,12	-	6,68	3,29
after 12 weeks	-	5,05	2,20	-	6,97	3,50
after 16 weeks	-	5,22	2,31	-	7,18	3,67
after 20 weeks	-	5,32	2,36	-	7,33	3,72
after 24 weeks	-	5,48	2,46	-	7,47	3,83
after 28 weeks	-	5,42	2,38	-	7,51	3,84
after 32 weeks	-	5,36	2,30	-	7,47	3,81
after 36 weeks	-	5,40	2,32	-	7,61	3,90
after 40 weeks	-	5,56	2,40	-	7,78	4,05

These values clearly show that specimens with more coated surfaces provoke higher losses of the pretension force in the bolts. Comparing the results achieved after four weeks of measuring shows that for long Huck bolts the specimens with eight galvanized surfaces loose in average 7,81 % of the pretension force, which they had 10 seconds after tightening, while specimens with four galvanized surfaces loose only 4,62 % and specimens without any galvanization at all only 1,97 %. The same trend is valid for the shorter bolts: Here, the test specimens with eight galvanized surfaces loose 8,68 % of the pretension force in comparison to the losses 10 seconds after tightening, whereas for four galvanized surfaces only 6,36 % of losses are monitored and the bolts connecting plates without any galvanization at all 3,09 % of losses are measured.

Furthermore, another trend becomes obvious in Table 5-6: Longer bolts loose less of their pretension force than shorter bolts. While the long bolts in the

specimens with eight galvanized surfaces loose only 7,81 %, the short ones in the same type of specimen loose 8,68 %. This tendency is also found for the other variations of the test.

Checking the results for the ongoing measurements in the specimens with four galvanized surfaces and without galvanization at all reveals that, although the speed of the reduction in clamping force reduces, the bolt forces still decrease. This is a result, which contrasts previous findings described in literature [32], where the loss of pretension has been found to be nearly stable after 12 days.

Keeping in mind the varying surface conditions in the tests both series show the same trend: For the tests with long bolts as well as for the tests with short bolts the loss of pretension grows if the specimen contains galvanized surfaces. Figure 5.2-2 and Figure 5.2-3 show the losses of pretension in relativity to the initial losses 10 seconds after tightening of the bolts. Here, an extrapolation of the loss of pretension in the bolts for the life time of a tower structure of 20 years can be found.

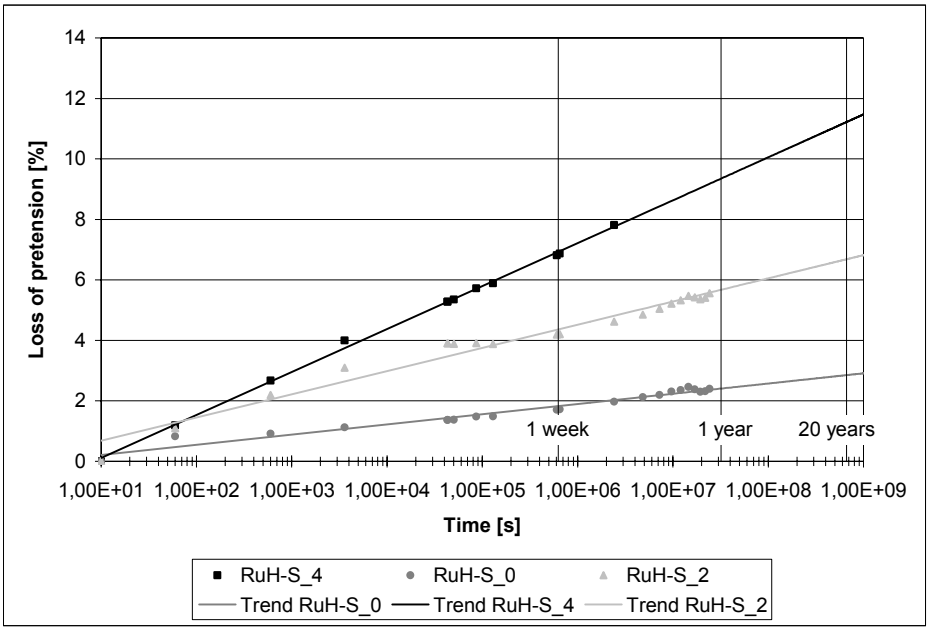

Figure 5.2-2: Average losses of pretension [%] of long Huck bolts depending on the surface finishing, extrapolated for 20 years

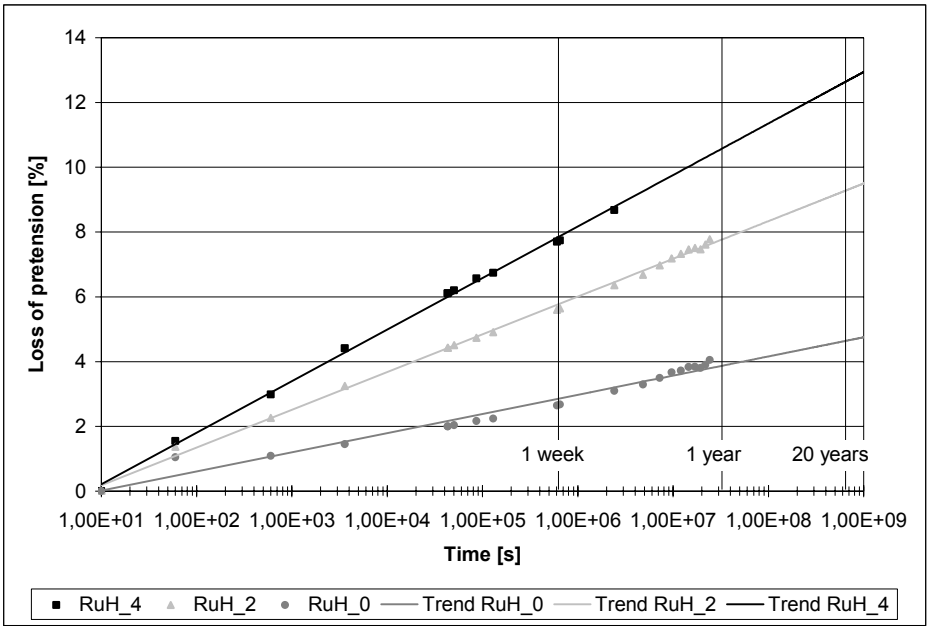

Figure 5.2-3: Average losses of pretension [%] of short Huck bolts depending on the surface finishing, extrapolated for 20 years

5.2.3 Comparison to Eurocode 3

Under the terms of EN 1993, part 1-8 [34] the preloading force $F_{p,C}$ is calculated according to the following formula:

$$F_{p,C} = 0,7 \cdot f_{ub} \cdot A_s \qquad (5\text{-}1)$$

For a tensile stress area A_s = 405,37 mm^2 and a ultimate strength f_{ub} = 1000 N/mm^2 (bolts are originally of grade 8, which is assumed to have equal properties as 10.9 bolts) this gives a preloading force of $F_{p,C}$ = 283,76 kN, which is equal to the clamping load guaranteed by Alcoa Fastening Systems.

The forces in the bolts reach this preload and even higher values during the tightening process. But the initial losses are that high that the average forces in the bolts drop below 300 kN 10 seconds after the maximum load has been reached. One minute later most of them drop below the guaranteed 284 kN.

Figure 5.2-4 and Figure 5.2-5 show the development of the pretension forces in the bolts depending on the varying surface conditions in comparison with the design load given by Eurocode 3 according to formula 5-1.

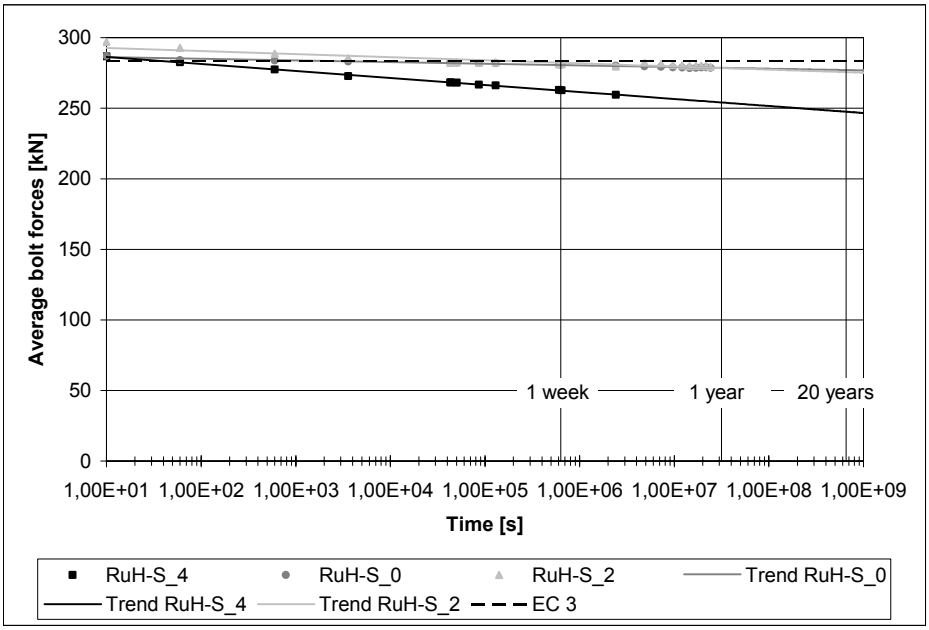

Figure 5.2-4: Average bolt forces [kN] of long Huck bolts depending on the surface finishing extrapolated for 20 years in comparison with EC 3

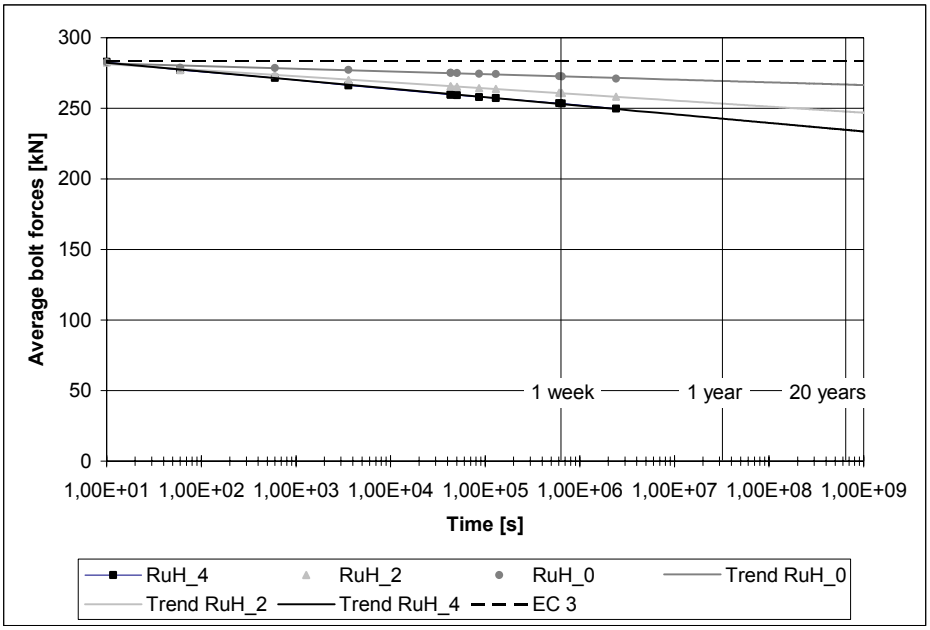

Figure 5.2-5: Average bolt forces [kN] of short Huck bolts depending on the surface finishing extrapolated for 20 years in comparison with EC 3

5.2.4 Conclusions

The pretension in the bolts is measured constantly over time. The results given in the paragraphs above are the average of the measured values per type of test specimen, from which a general design value of the remaining pretension force $F_{p,C,lt}$ during a period of time should be evaluated, using a general formula acc. to EN 1990 [33] and the initial pretension force $F_{p,C}$ acc. to EN 1993-1-8 [34].

$$F_{p,C,lt} = F_{p,C} - m_x \cdot (1 + k_n \cdot \frac{s_X}{m_X}) \qquad (5\text{-}2)$$

Where

$F_{p,C,lt}$ is the remaining pretension force after a certain time

$F_{p,C}$ it the initial pretension force as calculated acc. to EC 3 [34]

m_x is the mean loss of pretension force in bolts,

k_n is the factor given for the 5% characteristic value,

$V_x = s_x/m_x$ is the coefficient of variation of the pretension losses.

Based on preliminary segment test results, carried out under corrosion free conditions, design values can be achieved, see Figure 5.2-6.

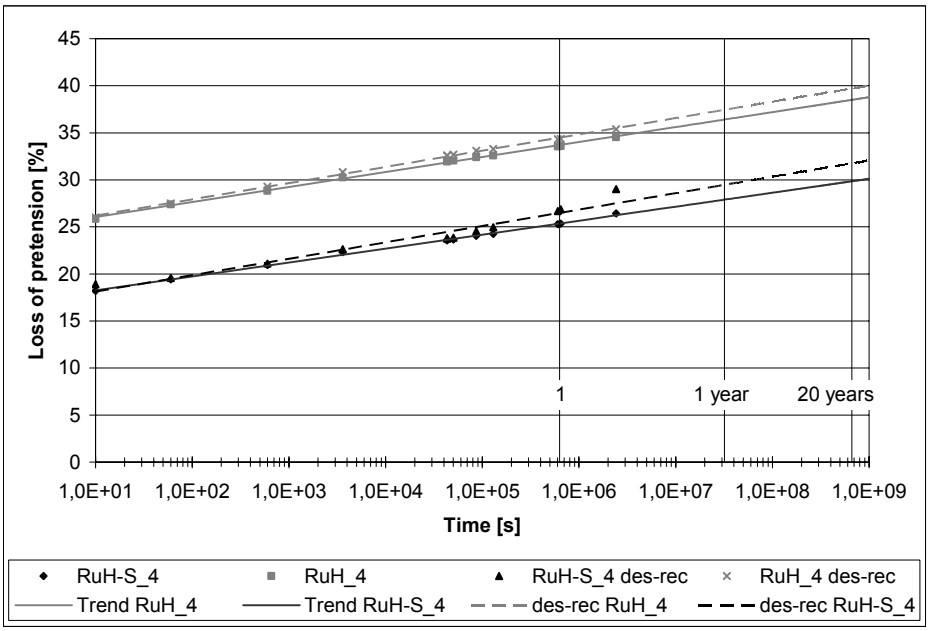

Figure 5.2-6: Test data and design recommendations for specimens with 4 galvanized surfaces

Therefore, a tentative recommendation on estimation of the remaining force in the pretensioned bolt is:

$$F_{\mathrm{p,C,with\ sleeve}} = F_{\mathrm{p,C}} \cdot \left[1 - \frac{0,7578 \cdot \ln\left(\frac{t}{31,536 \cdot 10^6} \right) + 16,459}{100} \right] \qquad (5\text{-}3)$$

$$F_{\mathrm{p,C,without\ sleeve}} = F_{\mathrm{p,C}} \cdot \left[1 - \frac{0,7517 \cdot \ln\left(\frac{t}{31,536 \cdot 10^6} \right) + 24,458}{100} \right] \qquad (5\text{-}4)$$

Where

$F_{\mathrm{p,C,xx}}$ is the pretension force in a certain period of time for either bolts with or without sleeves,

$F_{\mathrm{p,C}}$ is the initial pretension force, according to EN-1993-1-8 [34],

t is the time in years after the pretensioning.

Formulas 5-3 and 5-4 give an indication of the pretension force in a bolt of the friction connection that would remain if the influence of the corrosion and the cyclic load is neglected. They are valid in the most common case that all surfaces are galvanized.

The performed tests lead to the following conclusions about the reduction of forces in pretensioned bolts:

1. A longer bolt with extension sleeve leads to less losses of pretension force compared to a shorter bolt without extension sleeve.

2. A coating on the surfaces of the jointed plates increases the loss of pretension, which means that the losses of pretension over time can be quantified depending on the number of coated plate surfaces.

5.2.5 Discussion

The number of tests described above is quite limited, which leads to a very conservative recommendation for the design. Since the obtained results are based on only maximum three bolts per specimen type, a k_n value of 3,37 had to be taken as factor given for the 5 % characteristic value. The more data to rely on is available the smaller k_n can be chosen, so that for an increasing number of tests it can be reduced, for example k_n = 1,92 for 10 tests, see Table 5-7.

Table 5-7: Values of k_n for the 5 % characteristic value with unknown variance [33]

Number of tests n	3	4	5	6	8	10	20	30	∞
Fractile factor k_n	3,37	2,63	2,33	2,18	2,00	1,92	1,76	1,73	1,64

The tests have been carried out during a limited period of time of four and 40 weeks, respectively, which give only an idea of the behaviour of prestressed bolts over time and do not necessarily lead to safe approximations. Though it is possible to extrapolate the data for the loss of pretension for a period of 20 years, which is set as the life time of a tower, this has to be regarded with caution: Creep-behaviour is usually divided into primary, secondary and tertiary stage, where only the behaviour in the second phase can be considered as linear. Otherwise creep-behaviour is highly non-linear.

5.3 Static test

5.3.1 Static resistance of the connection

The static test is performed on specimen RuH-S_4, which means long bolts with extension sleeves, where all surfaces are galvanized. The expected static resistance of the connection $F_{s,Rd}$ is calculated according to EC3 [24]:

$$F_{s,Rd} = \frac{k_s \cdot n \cdot \mu}{\gamma_{M3}} \cdot F_{p,C} \qquad (5\text{-}5)$$

Where

$F_{s,Rd}$ is the static design resistance of the joint,

k_s is the coefficient depending on the type of hole, for normal holes 1,0,

n is the number of friction surfaces, here taken as 2,

μ is the slip factor, here assumed to be 0,4,

γ_{M3} is the partial coefficient, here taken as 1,0,

$F_{p,C}$ is the pretension force for the sum of all bolts in the joint.

The partial factor γ_{M3} is given as 1,25 by the Eurocode. But since the actual resistance shall be calculated safety values are not taken into account.

The actual pretension force per bolt $F_{p,C}$ is calculated according to the following formula taken from EC 3 [34]:

$$F_{p,C} = 0,7 \cdot f_{ub} \cdot A_s \qquad (5\text{-}6)$$

Where

f_{ub} is the ultimate strength of the bolt, here 1000 N/mm^2,

A_s is the tensile stress area of the bolt, here 405,37 mm^2.

As a friction coefficient is not available for this certain connection, it is primarily assumed to be 0,4. It is decided to take out the bolt in the middle, since the monitored strains seem to be unreasonable and it is assumed that the strain gauge is damaged. The static resistance therefore ends up at 454 kN.

5.3.2 Test protocol

The test is performed at Complab in Luleå. Its purpose is to find out about the maximum static resistance of this specific connection as well as to achieve a value for the friction coefficient. An INSTRON load frame with a capacity of 600 kN and adjustable hydraulic grips is used, cp. Figure 5.3-2.

The static test is performed on specimen RuH-S_4. It is first loaded in load control, spread 0,4 kN/s, until ~ 80 % of the assumed static resistance is reached; 275 kN – in the very beginning a slip coefficient of 0,2 was assumed, which would have let to a maximum static resistance of 340 kN. Then the load is kept constant for 5 hours. After that the load is increased, but the specimen seems to move in the machine grips. So the test is stopped. After removal of the galvanization at the grip region the testing proceeds by applying the load all the way. Since the specimen does not show any slip until the maximum machine load of 577 kN is reached, one of the bolts has to be taken away. The decision is to take out the bolt in the middle, B2, since it reacts sensitively to any movement of the cable connecting the strain gauge with the monitoring computer.

At the next try bolt B2 had been removed. The specimen is constantly loaded in load control of 0,5 kN/s until a load of 300 kN is reached. Then the way of load application is changed to stroke control. Now the machine progresses with 0,5 μm/s. Figure 5.3-1 shows how the specimen reacts.

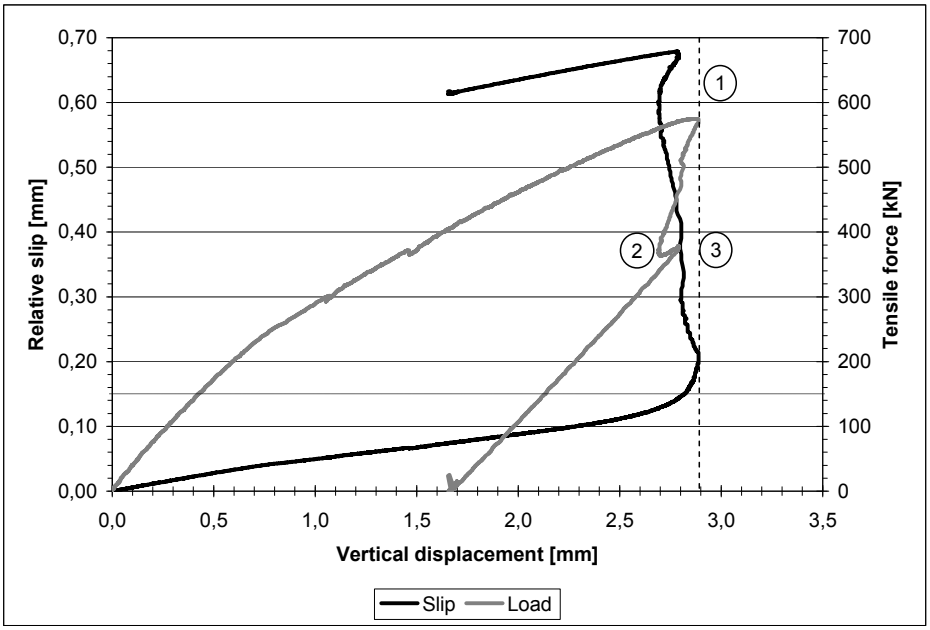

Figure 5.3-1: Relative slip and applied force vs. vertical displacement in static test

In the beginning the load-displacement curve behaves more or less linearly. At a machine stroke of about 0,7 mm the graph bends a little, but progresses linearly even beyond this point. Reason for this bending is most probably microslip, since yielding of the plates is expected not below an applied force of 624,8 kN based on the gross cross-section. Macroslip appears at the same time as the ultimate load is reached (point 1). Whereas the slip grows from this time on, the bearable load reduces until it starts to grow again in point 2.

In point 3 the unloading of the specimen started.

5.3.3 Actual static resistance

Purpose of the test is to find out about the maximum static resistance of this specific connection as well as to achieve a value for the friction coefficient, cp. Figure 5.3-2.

The test specimen resists an applied tensile force of 573 kN until a slip of 0,15 mm occurs. According the calculations in advance the expected static resistance for a connection with two pretensioned bolts and an assumed slip coefficient of 0,4 the specimen is supposed to withstand an axial load of 454 kN, which it does.

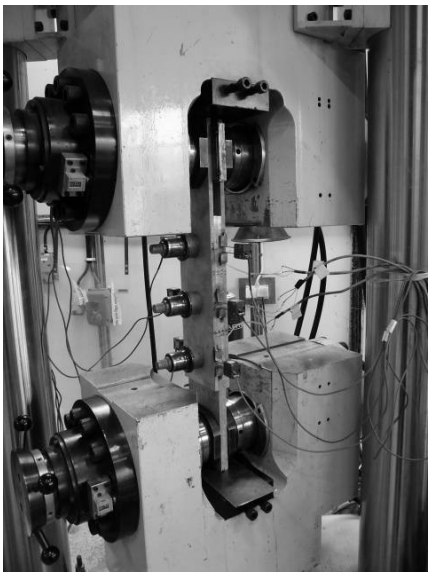

Figure 5.3-2: Picture of the test rig for the performed static and fatigue test

Calculating the same formula with the actual average bolt pretension force of 237 kN, which is monitored in the beginning of the test, a static resistance of 379 kN can be expected. The achieved static resistance proofs that the primarily assumed friction coefficient of μ = 0,4 is too low and underestimates the surface conditions of the specimen.

5.3.4 Slip behaviour and friction coefficient

According to EC0, part 2 the slip of 0,15 mm is the failure criterion for a slip resistant connection [20]. During both the static and the fatigue test the relative slip between outer and inner plates has been measured constantly by the help

of Crack Opening Devices (COD). *Figure 5.3-3* shows the slip development in relation to the applied load in the static test.

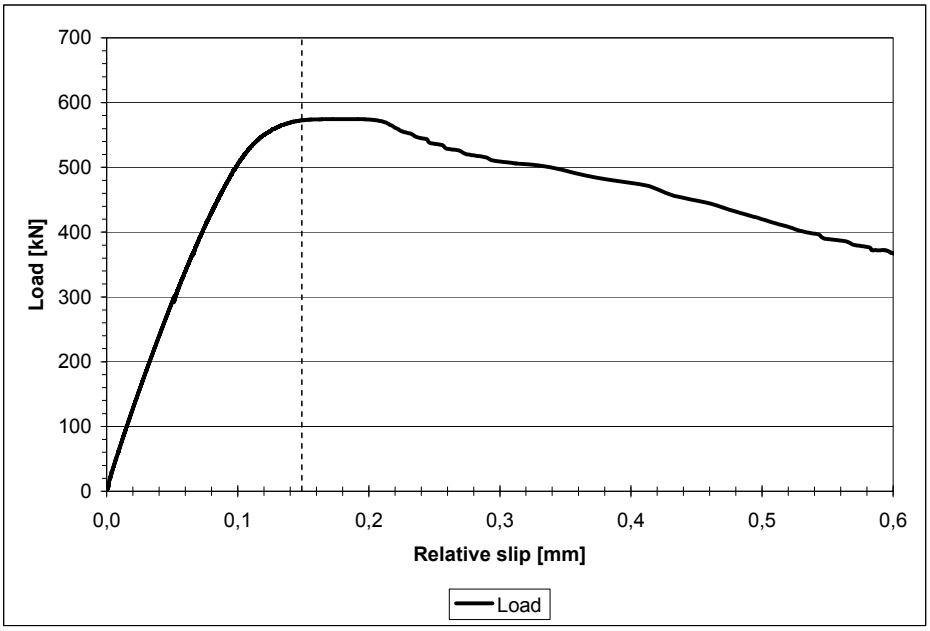

Figure 5.3-3: Applied load vs. relative slip in static test

Simultaneously as the maximum static resistance is reached, the slip criterion of 0,15 mm appears. While the load on the specimen cannot be increased, the slip grows. The slip is calculated as the average of the CODs.

Based on this data a slip factor of 0,5 is calculated as the ratio between slip resistance F_{max} and initial clamping force $F_{p,initial}$, which is assumed to be the bolt force 10 seconds after tightening, divided by 2 due to two friction surfaces where slip can occur, cp. formula 5-7.

$$\mu_{slip} = \frac{F_{max}}{n \cdot F_{p,initial}} = \frac{574,64}{2 \cdot (286,44 + 285,87)} = 0,50 \qquad (5\text{-}7)$$

Note that this slip factor is not evaluated in accordance with EC0, part 2 and should therefore not be compared directly to values available in literature.

The friction coefficient can be calculated by dividing the slip resistance F_{max} by $F_{p,actual}$, the sum of bolt forces at the time major slip occurs. In this case here this has to be divided by two due to the two friction surfaces. Therefore the friction coefficient ends up to be 0,62 in this case, see formula 5-8.

$$\mu_{friction} = \frac{F_{max}}{n \cdot F_{p,actual}} = \frac{574,64}{2 \cdot (229,89 + 230,10)} = 0,62 \qquad (5\text{-}8)$$

5.3.5 Results

Table 5-5 shows the results from pure relaxation of the bolts after tightening recalculated into losses of pretension in % of the maximum load, which were achieved directly after swaging the bolts. These numbers do not include any external loading.

During the static test the bolts also loose some of their pretension. Based on the maximum bolt forces when the bolts were tightened, B1 looses additional 2,29 % and B3 1,96 % of its forces until the maximum applied load of 574,64 kN is reached. This means that the forces in the bolts are more or less stable during load application, see Figure 5.3-4.

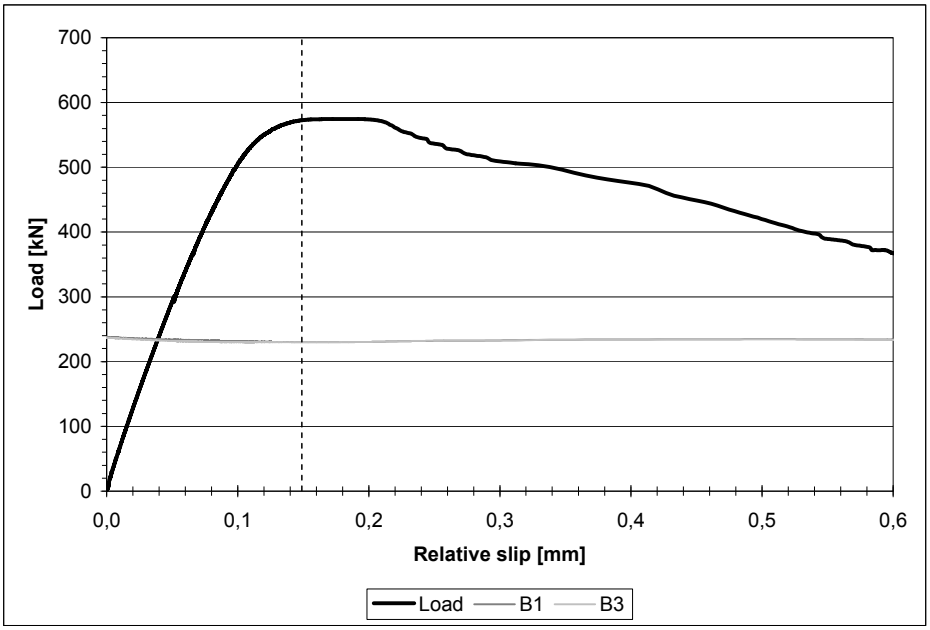

Figure 5.3-4: Bolt forces in comparison to applied load versus relative slip

Compared to losses of more than 25 % during the first four weeks from pure relaxation, these further losses seem to be negligible.

5.4 Test with cyclic loading

It is a well known fact, that cyclic loading induces micro settlements in the thread of a bolt shank and thereby generates a loss of pretension force. To get a first indication about the losses of pretension during dynamic loading, specimen RuH-4 is exposed to a cyclic load variation. The loading program is a modified version of the loading program developed at the University of Hannover in Germany [36]. Their procedure is chosen on the basis of real wind loads acting on the structure during the life time of a tower. In the test described here, the frequency is changed from 3 to 5 Hz after a couple 50000 cycles, cp. *Table 5-8*. Each load level starts with a few cycles to check if everything works well. Then the remaining number of the 50000 cycles per interval is carried out.

According to Table 8.1 in Eurocode 3, part 1-9 [23] the specimen is described as “Double covered symmetrical joint with preloaded high strength bolts” and shall therefore be detail category 112, which indicates the reference fatigue strength $\Delta\sigma_C$. The reference fatigue strength thus is $\Delta\sigma_C$ = 112 N/mm^2 and represents a fatigue strength at 2 million cycles.

Table 5-8: Loading program for cyclic test RuH_4

load step [-]	load level [kN]	no. of cycles [-]	frequency [Hz]	load step [-]	load level [kN]	no. of cycles [-]	frequency [Hz]
1	40-140	50000	1,00	11	40-290	50000	5,00
2	40-140	50000	3,00	12	40-340	50000	5,00
3	40-190	50000	1,00	13	40-390	50000	1,00
4	40-190	50000	3,00	14	40-390	50000	5,00
5	40-240	50000	1,00	15	40-440	50000	1,00
6	40-240	50000	3,00	16	40-440	50000	5,00
7	40-290	50000	1,00	17	40-490	50000	1,00
8	40-290	50000	3,00	18	40-490	50000	5,00
9	40-340	50000	1,00				
10	40-340	50000	3,00				

5.4.1 Results

Table 5-9 shows the losses of pretension in the bolts during the application of a cyclic load according to Table 5-8. The specimen fails due to a fatigue crack in the plate, which initiates from the point, where one of the CODs is welded to the plates, see Figure 5.4-1. Failure occurs after about 49000 cycles in load-step 40 - 490 kN applied with a frequency of 1 Hz, so a total number of 849000 cycles is carried out. The final failure of the specimen does not depend on the joint.

Increasing the amplitude of loading results into an increase in loss of pretension in the bolts. Not in all, but in most of the cases the loss of pretension rises with growing frequency.

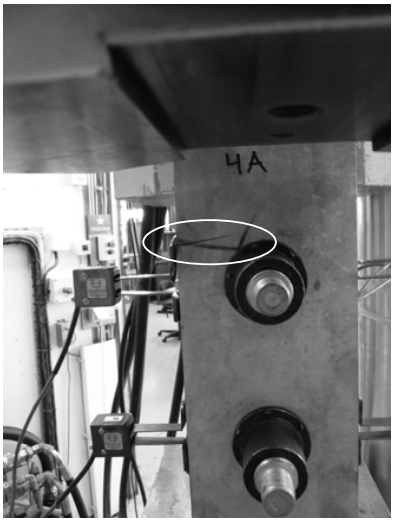

Figure 5.4-1:Failure of specimen under cyclic loading

Table 5-9: Cumulative losses of pretension [%] during cyclic loading

load step [-]	load level [kN]	no of cycles [-]	total no of cycles [-]	frequency [Hz]	B1 [%]	B2 [%]	average [%]
1	40-140	50000	50000	1,00	0,59	0,65	0,62
2	40-140	50000	100000	3,00	0,56	0,61	0,58
3	40-190	50000	150000	1,00	1,03	1,02	1,02
4	40-190	50000	200000	3,00	1,03	1,02	1,02
5	40-240	50000	250000	1,00	1,49	1,31	1,40
6	40-240	50000	300000	3,00	1,55	1,36	1,46
7	40-290	50000	350000	1,00	2,13	1,70	1,91
8	40-290	50000	400000	3,00	2,15	1,72	1,93
9	40-340	50000	450000	1,00	2,84	2,11	2,47
10	40-340	50000	500000	3,00	2,98	2,21	2,59
11	40-290	50000	550000	5,00	2,76	1,91	2,33
12	40-340	50000	600000	5,00	3,04	2,24	2,64
13	40-390	50000	650000	1,00	3,89	2,71	3,30
14	40-390	50000	700000	5,00	3,96	2,74	3,35
15	40-440	50000	750000	1,00	5,06	3,44	4,25
16	40-440	50000	800000	5,00	5,00	3,37	4,18
17	40-490	49000	849000	1,00	5,94	4,08	5,01

Also for this test the results from the pure relaxation tests can be found in Table 5-4 to Table 5-6. During the cyclic loading the bolts also loose some of their pretension. Based on the bolt forces when the test was started, B1 looses additional 5,94 % and B2 4,08 % of its forces. The development of the forces during cyclic loading can be followed in Figure 5.4-2. This figure shows also that the strain gauge in B3 did not work properly, since it shows almost no forces in the bolt, which is not correct. As a matter of fact, all bolt forces show values well below the pretension force requested by Eurocode. This has already been observed during the previous relaxation tests, see chapter 5.2.2.

The design value for the accumulation of damage D_d can be calculated according to the Palmgren-Miner-Rule [23]:

$$D_d = \sum_i^n \frac{n_{Ei}}{N_{Ri}} \leq 1 \qquad (5\text{-}9)$$

Where

n_{Ei} is the number of cycles associated with the stress range $\gamma_{Ff}\Delta\sigma$i for band 1 in the factored spectrum

N_{Ri} is the endurance (in cycles) obtained from the factored $\Delta\sigma_C/\gamma_{Mf}N_R$ curve for a stress range of $\gamma_{Ff}\Delta\sigma_i$

In this case the accumulated damage D is equal to 0,186, with m = 3 for a fatigue detail class of 112. Safety factors and partial coefficients are not taken into account.

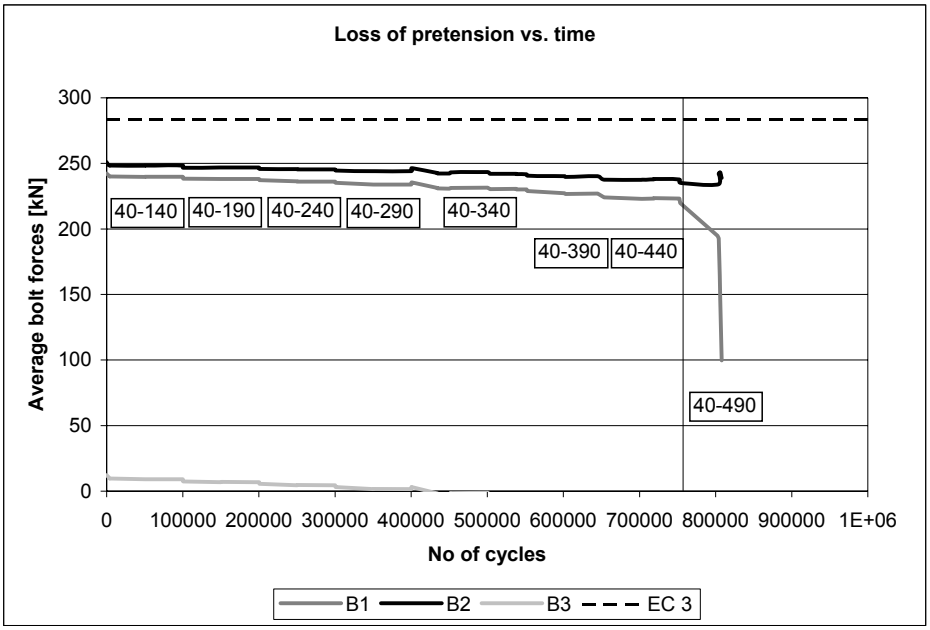

Figure 5.4-2: Development of bolt forces during cyclic loading, various load-intervals are marked

For this case the S-N curve looks as shown in Figure 5.4-3.

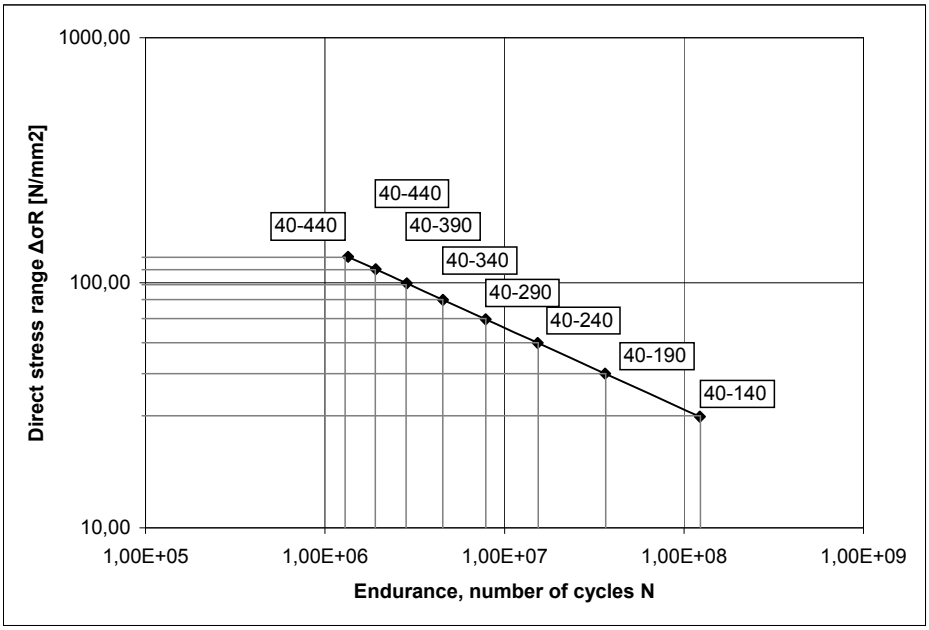

Figure 5.4-3:S-N Curve for test with cyclic loading, various load-intervals are marked

5.5 Conclusions

As has been shown in the paragraphs above it is possible to quantify the loss of pretension in a connection depending on the number of galvanized surfaces. The more plate surfaces are galvanized, the bigger is the loss of pretension, see chapter 5.2. Besides this, it is also possible to calculate the loss of pretension force for the future of the bolts with the help on an extrapolation of the achieved test results, cp. formulas 5-3 and 5-4. This can then also be used as recommendation for the design of such joints.

Additionally, it was found that the longer lockbolts perform better than the short ones. Including the extensional sleeve between clamped plates and the nut leads to about 7 % less loss of pretension of than short lockbolts where the nut is in direct contact with the clamping package.

From the test with a variation of cyclic load can be concluded that the additional losses due to external loading are small compared to the losses resulting from pure relaxation; an average loss of 5,01 % vs. 34,52 %. This is, of course, obtained in laboratory conditions.

6 FINITE ELEMENT ANALYSIS OF THE STATIC TEST

The use of finite element analysis is a convenient method to study the behaviour of structures or details of structures as for example connections. It enhances the possibility to easily investigate more details compared to performed tests in a laboratory such as the distribution of contact pressure or stresses in a plate. Those and other parameters are difficult and sometimes impossible to obtain in a test. Once the finite element model is calibrated with help of a test or other calculation methods, it even offers the great capability of performing large parametric studies to check the influence of different parameters. Thus, enormous savings in time and money can be achieved when performing those large numerical studies rather than performing a large amount of tests. Over the past years the increased performance of computers and the availability of high performance clusters have led to an even bigger benefit. This chapter focuses on modelling the static test (cp. chapter 5.3). The influence of different materials and possible assembling tolerances on the resistance is investigated.

6.1 Description of finite element models

Figure 6.1-1 shows a three dimensional finite element (FE) model including the meshed parts of a symmetric double shear lap joint, the static test described in chapter 5.3. The model consists of three different parts: bolt, sleeve and plate. Plates and sleeves are modelled with realistic dimensions whereas the bolt's head and nut are simplified as cylinders with height of 15 mm and diameter of 30,8 mm in order to easily obtain a good mesh. Thus, the contact pressure distribution, especially on the side where the head is directly in

contact with the plate, is influenced by this. However, the effect on the distribution at the friction surfaces is negligible. Due to the fact, that the middle bolt B2 is removed from the setup during the performance of the original test, it is not considered in the FE analysis. The mesh around the holes is refined in order to ensure that the contact pressure can be well distributed, cp. Figure 6.1-1. To obtain a good mesh in Abaqus for these circular parts, so called partitions have to be created to divide the part into different meshable areas. Swept meshing with hex elements as shape is found to be appropriate. This means, that Abaqus creates a mesh on one side of the region and then copies the nodes of that mesh until the target side is reached [38].

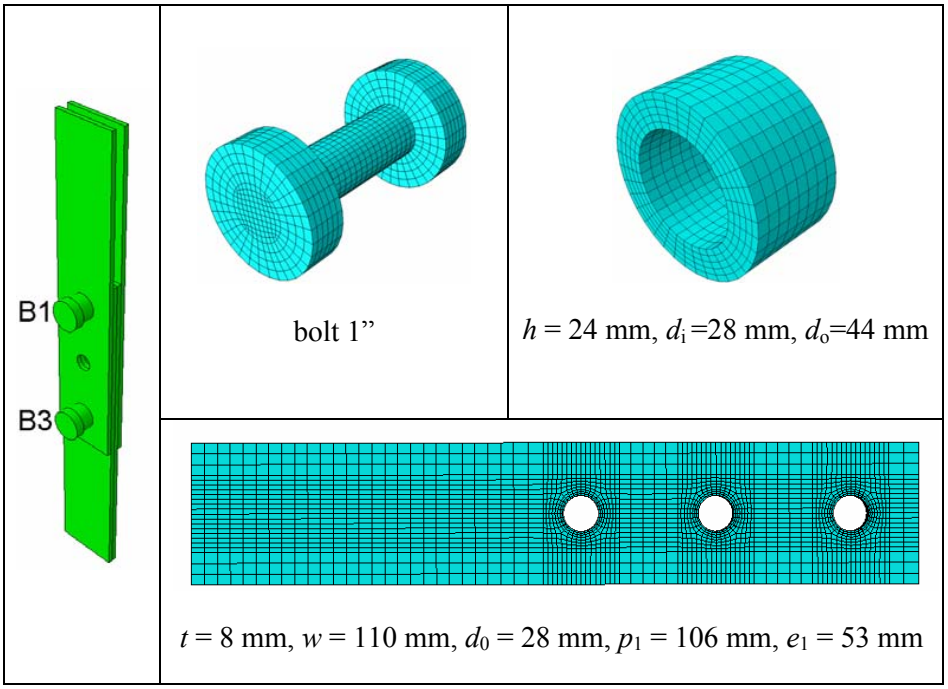

Figure 6.1-1: Finite Element model of the static test

The commercial software Abaqus (version 6.10-2) is used both for creating and analyzing the different models.

6.1.1 Mechanical properties

Two different stress-strain relationships are considered in the FE models. Figure 6.1-2 shows an elastic-plastic relationship allowing for strain hardening to be used for structural steel (sleeve and plate) based on Swedish regulations for steel structures [37]. The Young's modulus is taken as 210 GPa and Poisson's ratio as 0,3 respectively.

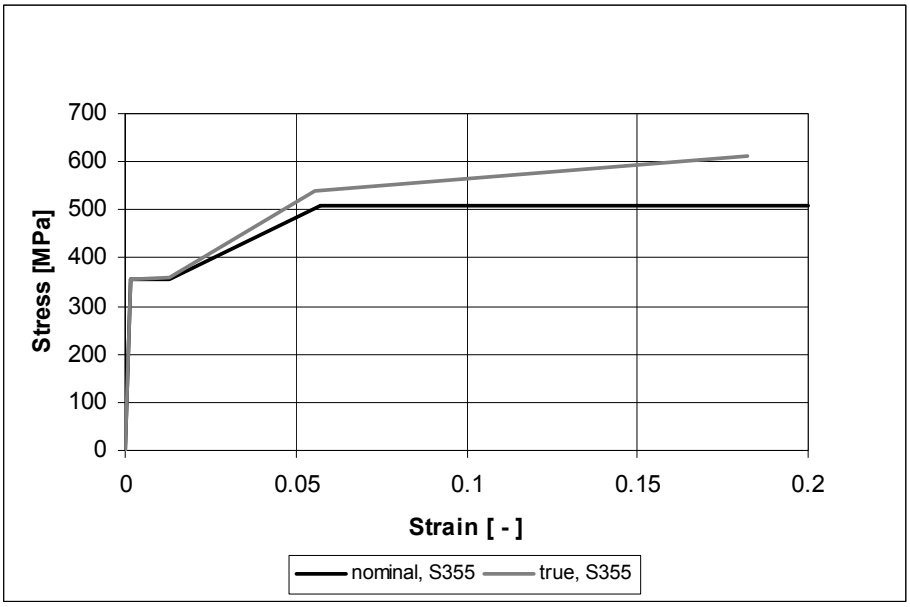

Figure 6.1-2: Nominal and true stress – strain relationship of steel S355

Annex D, Figure D-3 shows results from material testing of M25,4/1" Huck BobTail lockbolts, which have been used for the static test. They clearly verify that all bolts are in the elastic range after the pretension is applied in the experiment. Therefore, a Young's modulus of 210 GPa and Poisson's ratio of 0,3 are considered. Since the equivalent bolt stiffness in tension of the Huck BobTail lockbolts used in the static test is unknown, it has been planned to carry out tensile tests of those bolts. By the time, these FE calculations are finalized, the results have not been available yet. To take the smaller tensile

stiffness of the bolts into account, it is assumed that modelling of the tensile stress area of the bolt is sufficient at this stage.

Generally, true stress and true strain values are to be used in Abaqus as input data to define non-linear material properties. Tensile test data of ductile materials are always presented showing nominal stresses and strains and they need to be converted to true stresses and strains, respectively [38]. The equation shown below describes the relationship used to translate nominal strain to true strain.

$$\varepsilon_{true} = \ln (1 + \varepsilon_{nom}) \qquad (6\text{-}1)$$

Where

ε_{true} are the true strains,

ε_{nom} are the nominal strains.

The relationship between true stress and nominal stress is established by considering the incompressible nature of metal plasticity and assuming an incompressible elastic response, which then leads to the following relationship.

$$\sigma_{true} = \sigma_{nom}(1 + \varepsilon_{nom}) \qquad (6\text{-}2)$$

Where

σ_{true} are the true stresses,

σ_{nom} are the nominal stresses,

ε_{nom} are the nominal strains.

6.1.2 Contact interactions

Many different possible interactions need to be considered in a connection, which lead to a complex numerical problem. Abaqus/Standard provides three different approaches for defining contact: “general contact”, “contact pairs” and “contact elements”. The first two types are surface based and are recommended to be used if possible [38]. The general contact tool is a very powerful option, introduced in recent Abaqus versions, which allows for self-contact. In this case no contact surfaces need to be specified manually, but depending on the considered problem size it may extent the time for the calculation. If for example in a model with a lot of nodes only a few possible contact interactions exist, they shall preferably be specified manually in order to avoid that Abaqus checks whether new contact problems arise during all the calculation process. “General contact” can only be used with a “finite-sliding”, “surface-to-surface” formulation, whereas, if “contact pairs” are chosen, “small-sliding” and “node-to-surface” formulations become available.

For all calculations carried out within this thesis the “general contact” formulation is used. As tangential behaviour a friction coefficient equal to 0,62 calculated from the static test described in chapter 5.3 is assumed using the basic Coulomb friction model. For normal behaviour “hard” contact is introduced, which means that contact pressure can be transmitted if surfaces are in contact, but also a separation of contact surfaces is allowed. A more detailed discussion about mechanical and frictional behaviour can be found in a previous study [8].

Finite element models including contact problems are very sensitive to any applied load and may have problems to converge numerically at the beginning of a calculation. The reason is that the contact is not fully established as long as there is zero force in the model and therefore, depending on boundary conditions, rigid body modes may exist. Convergence may be achieved by introducing a small load first before the actual load is applied. It can be necessary to stabilize the model by activating damping in normal and/or tangential direction.

For any interaction it is crucial to choose appropriate master and slave surfaces. Usually the master surface should be the surface of the stiffer body or should have a coarser mesh than the slave surface. If not followed the solution may become quite time consuming [38]. In case the “general contact” option is used, Abaqus itself assigns master and slave roles.

6.1.3 Element types

For all different parts of the model the continuum element type C3D8R is used. This is an eight-node brick element with first order reduced integration. The reason for choosing a reduced integration element is, that it uses a lower order integration to form element stiffness and thus reduces the overall computation time especially in three dimensions. The shear locking phenomenon observed in C3D8 elements does not appear, since it just has one integration point at the centroid. The disadvantage of these elements is, that they are prone to hourglassing. These elements can therefore deform in such a manner that the strain calculated at the integration point is equal to zero, which further leads to uncontrolled distortion. C3D8R elements can still be used but with a reasonably fine mesh: At least four elements through the thickness are recommended [38]. A cost effective alternative, if bending dominates, is to use incompatible mode elements such as C3D8I. In addition to the standard degrees of freedom these elements possess internally added incompatible deformation modes. They eliminate the causes for a very stiff bending response seen in regular first order displacement elements. They can also be used to model bending with just one element over thickness without hourglassing. Incompatible modes can be used in a mesh in combination with other regular continuum elements. Hourglassing can normally be recognized in deformed shape plots or the Abaqus in-built hourglass control can be used. It has to be verified that the artificial energy used is small (<1 %) in relation to the internal energy [38].

6.1.4 Simulation procedure

The analysis has been performed in the following three sequential steps:

Pretension

The bolts are preloaded to the same level as the bolts at the beginning of the test, see chapter 5.3.3. In the finite element analysis this is done by applying a concentrated load, which is a self-equilibrating force carried across the pretension section in the shank, to the pretension node [38]. This internal section is defined as the middle of the shank, cp. Figure 6.1-3.

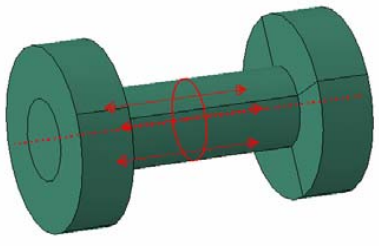

Figure 6.1-3: Application of preload in the bolt

Fixing the bolt length

After applying the pretension to the bolts, their length is fixed at their current position, so that the force in the bolt changes according to the response of the model in the subsequent analysis.

External load

The last step contains the external load, which is applied to the model through a displacement at the end of the plates.

6.1.5 Boundary conditions

During the first two steps all three translational degrees of freedom (DOF) at both top and bottom of the specimen are restrained as can be seen in Figure 6.1-4.

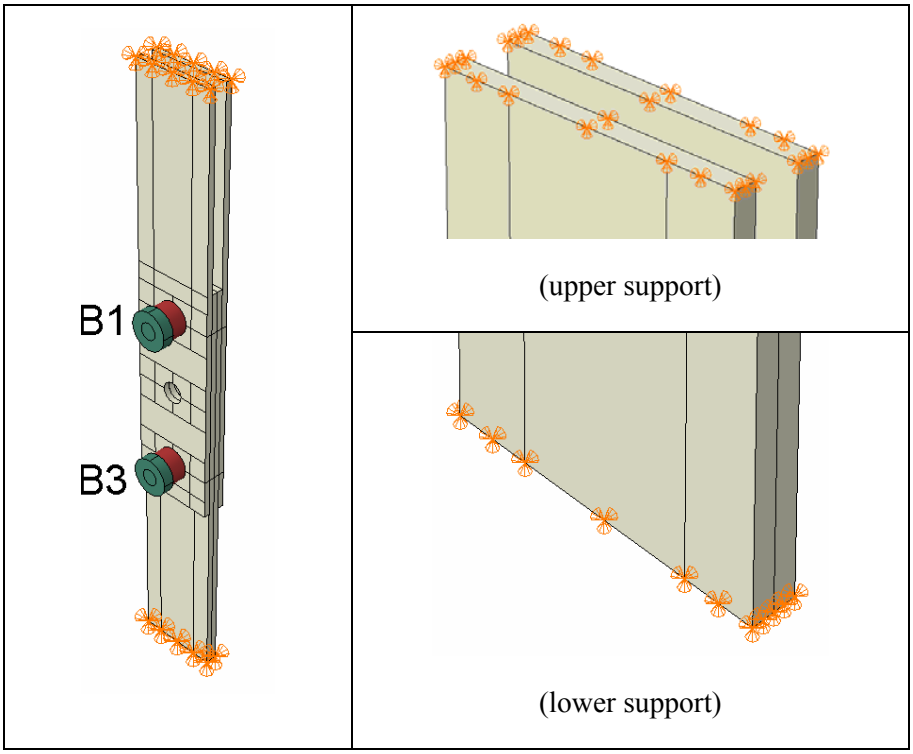

Figure 6.1-4: Boundary conditions – pretension of bolts step

After the pretension forces in the bolts are successfully reached, the DOF in longitudinal direction of the plates at the bottom is released and a longitudinal displacement is applied to represent a tensile load, acting on the friction connection, cp. Figure 6.1-5.

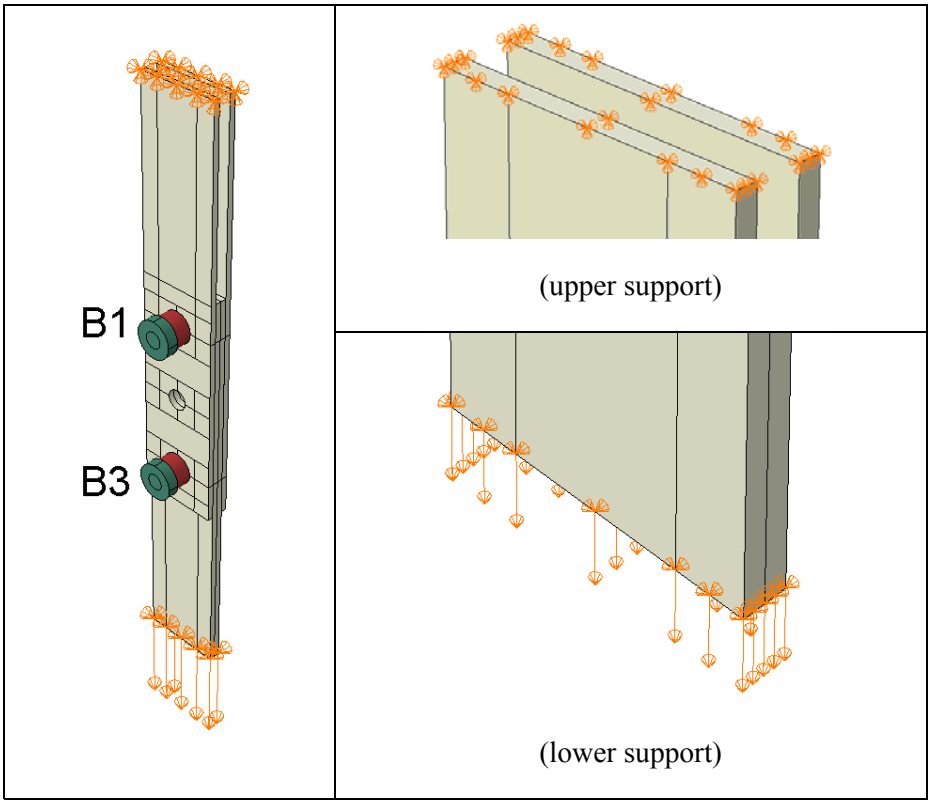

Figure 6.1-5: Boundary conditions – external loading step

6.1.6 Parallel processing

Abaqus offers the possibility of parallel processing. This means, more than one central processing unit (CPU) can be used for calculating. Big savings in terms of time may be achieved. For a typical model, as the one presented here, including a fine mesh, small increments to get a smooth load vs. slip curve and without use of symmetry, a calculation using two CPUs takes approx. 464 minutes compared to 133 minutes with 12 CPUs. Using even a high performance cluster, which allows the calculation of various jobs at the same time due to many available CPUs, makes finite element modelling more and more attractive compared to past years.

6.2 Results

According to EN 1090-2 [20] failure of a friction connection (slip resistance) is defined as the load, which leads to a slip of 0,15 mm. EN1993-1-8 [34] specifies at ultimate limit state that the design shear load should not exceed the design slip resistance, nor the design bearing resistance. Furthermore, the design plastic resistance of the net cross-section at the bolt holes has to be checked. Possible bearing failure, which may occur after the bolt gets in contact with the plates, is not taken into account in the following since the position of the bolts is assumed to be coaxial in all calculations.

6.2.1 Slip resistance

Figure 6.2-1 shows a comparison of the applied load and the average slip in the specimen. The average slip in the test is defined as the averaged measurement of four CODs, which are capturing the relative movements of the plates at two sides and for each bolt during the test. In the finite element analyses (FEA) the average slip is defined by two values at one side, since the specimen is modelled with a perfect symmetry and therefore bending due to position tolerances cannot occur. Figure 6.2-1 clearly shows that the slip resistance is slightly underestimated and the stiffness in the FEA is considerably higher than in the actual test after a load of about 100 kN is reached. The slip resistance during the test is 574,6 kN. Compared to the resistance of 542,1 kN obtained by Abaqus, this leads to a difference of about 5,6 %. The characteristic slip resistance $F_{s,R}$ according to Eurocode 3 part 1-8 [34] is calculated to 593,1 kN, whereas the characteristic plastic resistance of the net cross-section at the bolt holes $N_{net,R}$ is equal to 465,8 kN.

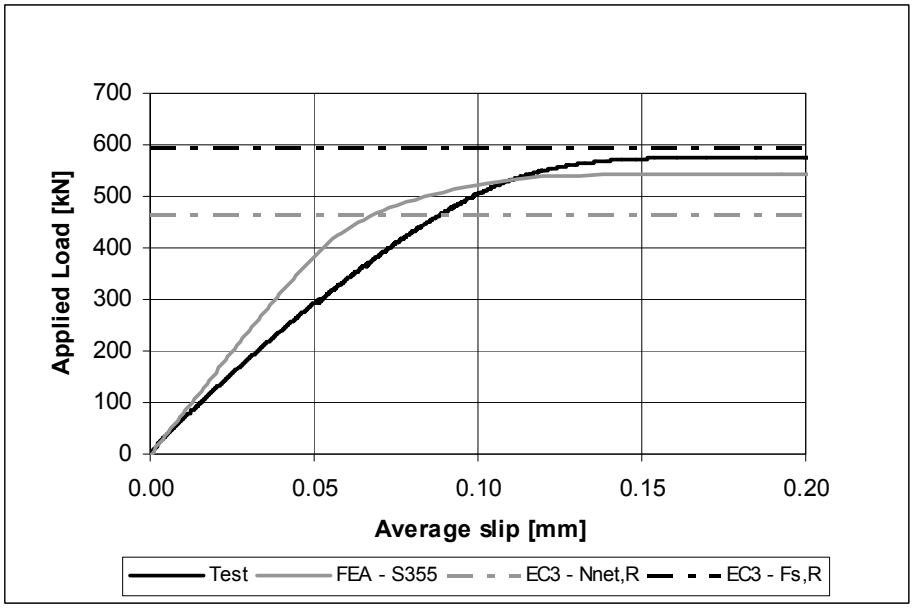

Figure 6.2-1: Applied load vs. average slip, S355

It should be noted that the friction coefficient determined from the static test is based on the total load and the loss of pretension in both of the bolts at 0,15 mm slip. It does not reflect any non-linearity of the friction coefficient during the test, which may be present depending on the state of the contact surfaces, in particular size of asperities and level of changes of the roughness due to contact pressure. Thus, it is very likely in an experiment that the friction coefficient is not constant. This micro mechanism is not further investigated. The friction between two surfaces is modelled at macro level, which explains the discrepancy in stiffness between FEA and experiments.

6.2.2 Loss of pretension in bolts

As mentioned before the finite element calculations consider a perfect roughness of the coating and are represented by a constant friction coefficient. Therefore, a simple direct correlation between the loss of pretension in the two bolts and the slip resistance can be observed. It is therefore expected that for higher losses of pretension in the bolts during a test less slip resistance at failure slip of 0,15 mm occur. Abaqus offers a simple recording of applied bolt

loads. A "history output" monitoring the reaction force at each pretension node, which is defined as the total force across the specified pretension section, is available.

Figure 6.2-2 and Figure 6.2-3 clearly indicate that the bolts in the FEA loose more pretension force than measured in the test, which therefore leads to an underestimation of the total resistance of the joint.

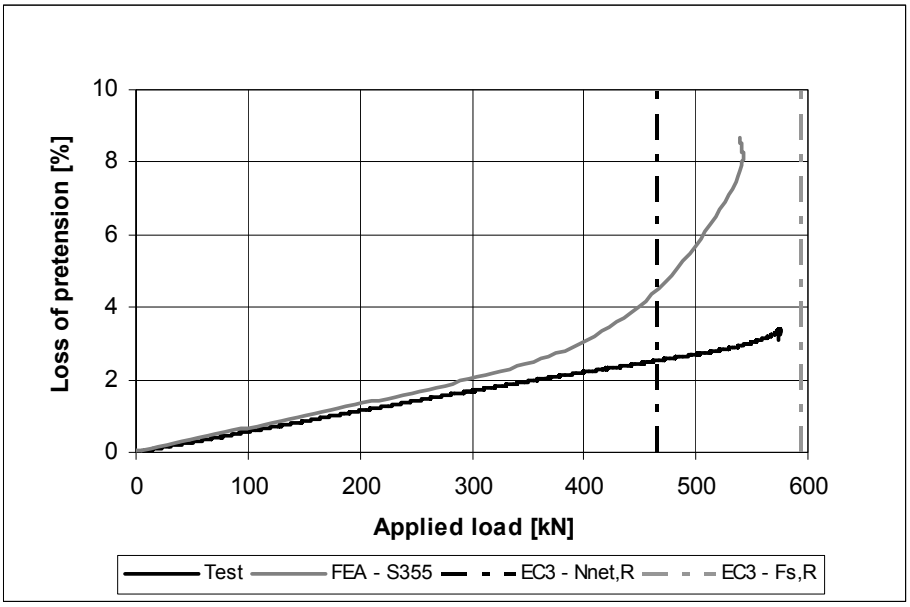

Figure 6.2-2: Loss of pretension –bolt B1, S355

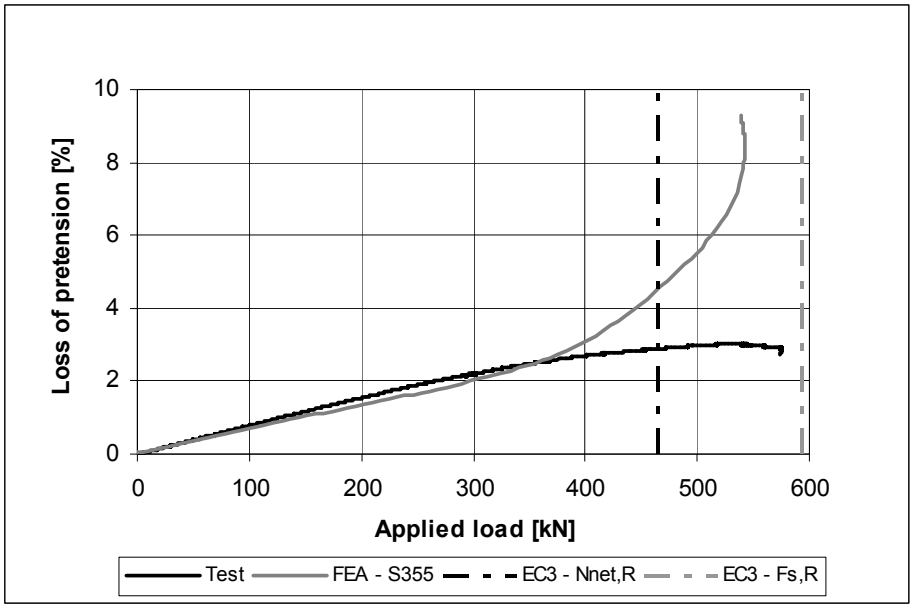

Figure 6.2-3: Loss of pretension – bolt B3, S355

Possible reasons for this discrepancy are, among others, the non-uniformity of the friction coefficient and the influence of the joined plates. A possible effect of the material of the joined plates on the slip resistance can be found in chapter 6.2.4.

6.2.3 Contact pressure distribution

Figure 6.2-4 and Figure 6.2-5 clearly show how the contact pressure in the friction surface changes during the test. After pretensioning the contact pressure is perfectly distributed around the holes, cp. Figure 6.2-4.

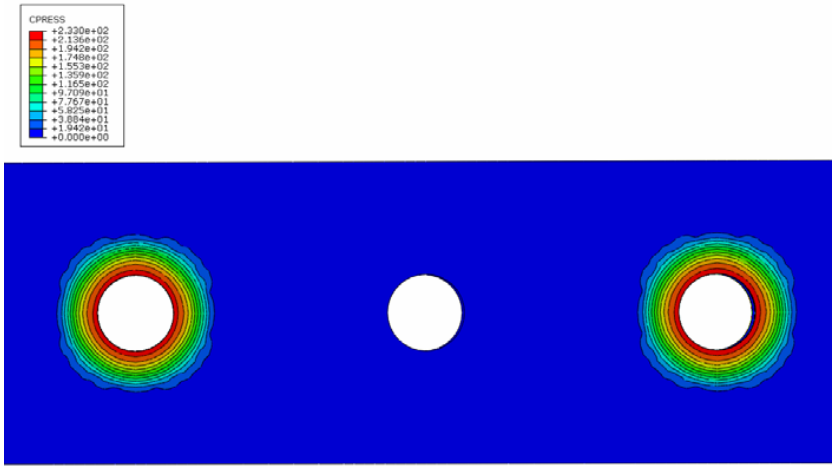

Figure 6.2-4: Contact pressure distribution around bolt B3 and B1 – after pretensioning, S355

From Figure 6.2-5 can be seen that the area which is contact changes during the test. At a slip of 0,15 mm the contact stresses are not evenly spread any more.

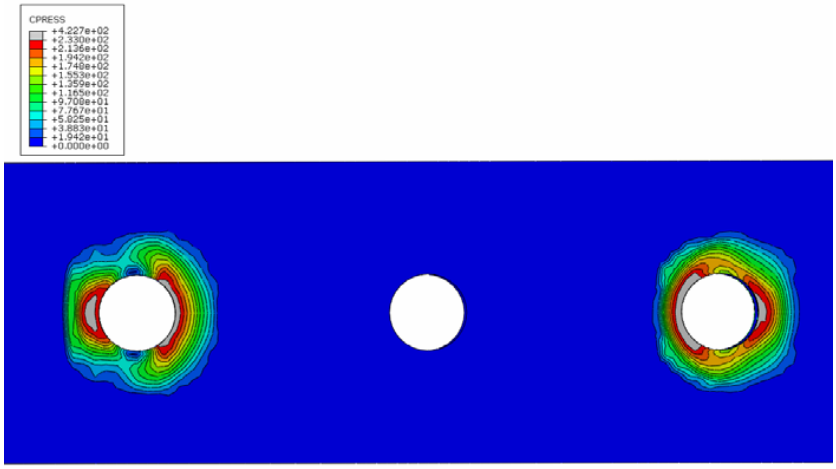

Figure 6.2-5:Contact pressure distribution around bolt B3 and B1– 0,15 mm slip, S355

Since a sleeve is used between nut and plate to obtain a larger clamping length for the bolts, the stress pattern through the thickness of the plate is not perfectly symmetric. However, Figure 6.2-6 emphasizes that the influence of the friction surface on the stresses is small and an almost perfect shape of a pressure cone is be obtained.

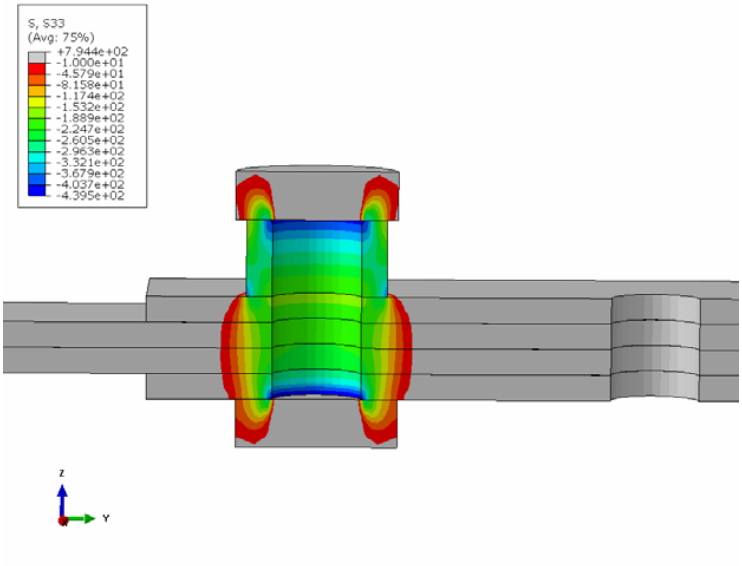

Figure 6.2-6: Stress distribution through thickness – after pretensioning, S355

For the sake of comparison Figure 6.2-7 shows a perfect stress distribution for a configuration without sleeves.

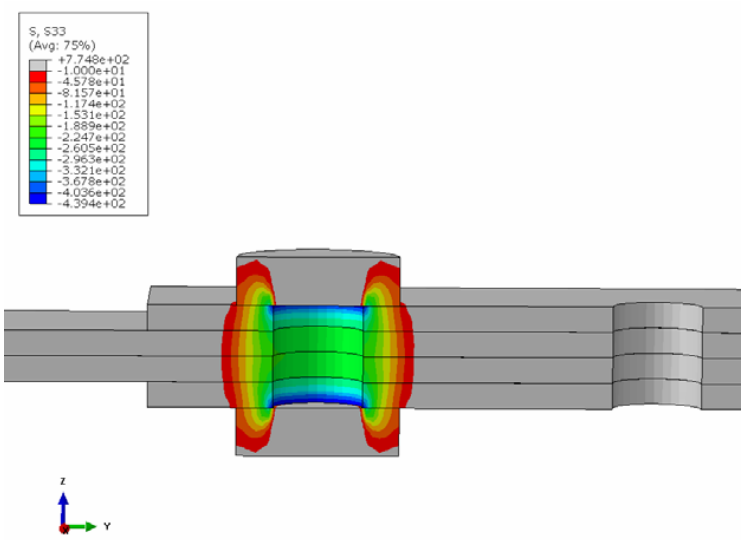

Figure 6.2-7:Stress distribution through thickness without sleeves – after pretensioning, S355

6.2.4 Parametric study based on material properties of the plates

In chapter 6.2.2 it has been observed, that the bolts in the finite element analysis based on a nominal steel grade of S355 of the plates loose more pretension force compared to the bolts in the actual test. This leads to a lower slip resistance of the joint in the FEA. Independently of consequences related to the appearance of surface coatings, this parametric study only investigates the influence of the material of the connected plates on the loss of pretension in the bolts.

When a steel plate is stretched, it will contract in the directions transverse to the applied load. This phenomenon is known as Poisson effect. While the total thickness of the clamped package of plates decreases in the area of the bolts, a certain loss of pretension in the bolts can be observed. Figure 6.2-8 and Figure 6.2-9 clearly visualize this effect. While the total thickness of the clamping package decreases – positive values in Figure 6.2-8 describe a decrease – the bolt looses pretension force at the same time. The reduction of the total plate

thickness in the joint is obtained as average at each hole as the relative change of the two outermost plates.

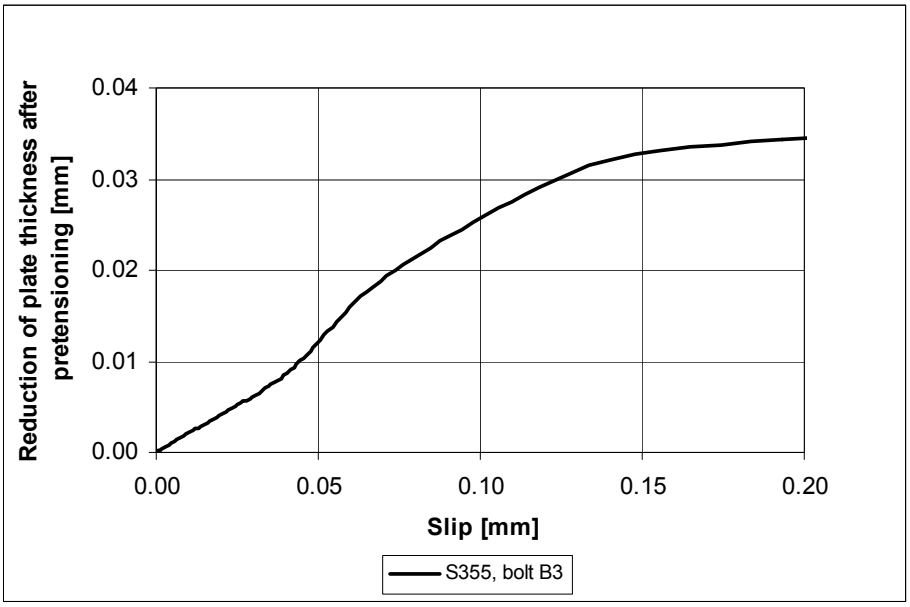

Figure 6.2-8: Reduction of plate thickness during loading – bolt B3, S355

Since the finite element model considers a constant friction coefficient and no asperity of the coated surfaces is taken into account, stretching of the plates visualized by Figure 6.2-8 can directly be set into relation to the loss of pretension, cp. Figure 6.2-9.

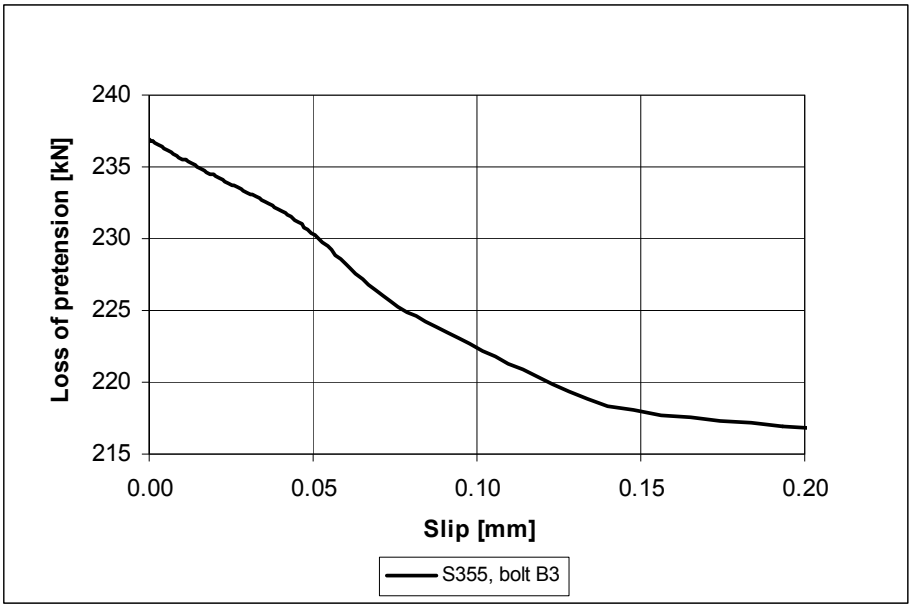

Figure 6.2-9: Loss of pretension – bolt B3, S355

Considering the applied load on the plate and bearing in mind the reduction in area due to the bolt holes, it is realistic that the plates start yielding around the holes although force is transferred through friction to the other plates. Formula 6-3 shows the nominal force needed for yielding of material grade S355, considering just an axial force.

$$N_{\text{net,R}} = f_{\text{y}} \cdot A_{\text{net}} = 355 \cdot 10^{-3} \cdot (110 - 28) \cdot 2 \cdot 8 = 465{,}8 \text{ kN} \qquad \textit{(6-3)}$$

Where

$N_{\text{net,R}}$ is the characteristic plastic resistance of the net cross-section,

f_{y} is the yield strength of the plate material,

A_{net} is the net cross-section of the clamping package.

In Figure 6.2-1 can be seen that around this load level in the FE model a change in stiffness occurs due to first yielding in the plates. Figure 6.2-10 and Figure 6.2-11 emphasize clearly that yielding around the lower hole has started. Considering that the plastification depends on the material used, one may assume that the loss of pretension and therefore also the total slip resistance are related to the material properties of the plates and not only to the surface coatings. The comparison of experimental and FE results shown in Figure 6.2-1 indicates that the yield strength of the plates is higher than the nominal. This is rather realistic and leads to a parametric study based on different nominal steel grades (S235, S275, S355, S450 and S690) as presented below.

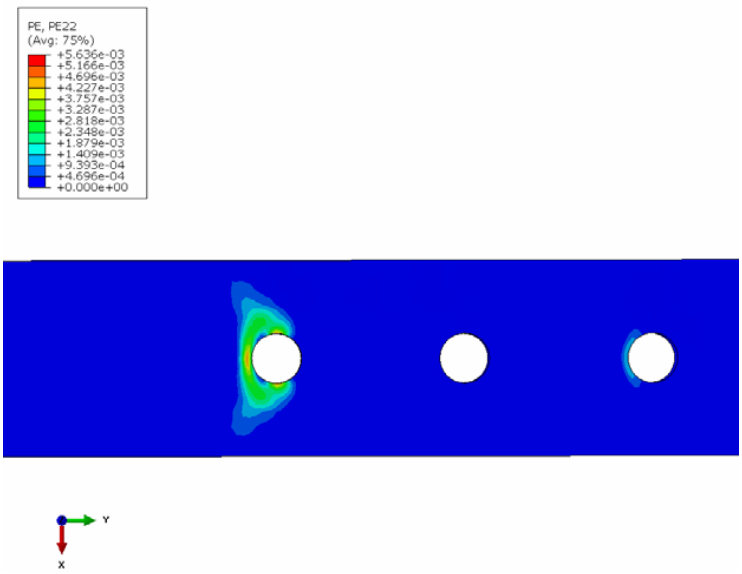

Figure 6.2-10: Plastic strains in longitudinal direction – 0,15 mm slip, S355

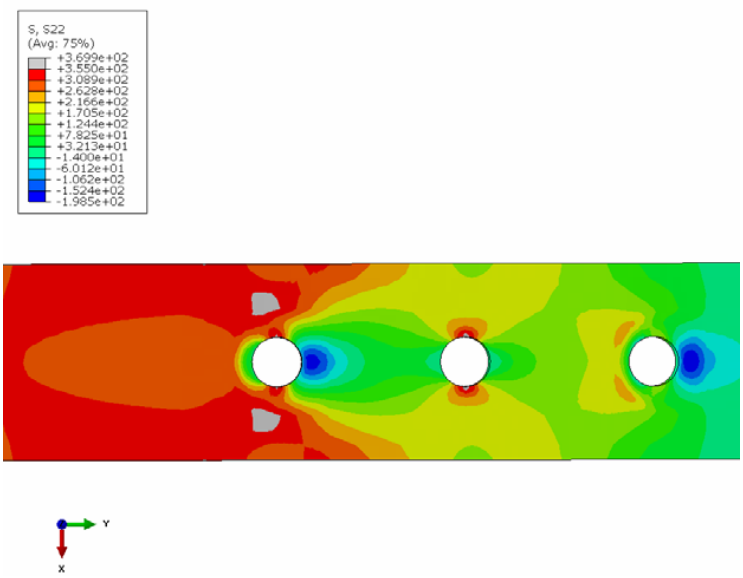

Figure 6.2-11: Stresses in longitudinal direction – 0,15 mm slip, S355

Figure 6.2-12 and Table 6-1 illustrate that a scattering in resistance, varying from 390,6 kN for S235 to 570,5 kN for S690, exists depending on the yield stresses of the plates. A look on the behaviour of the inner plates demonstrates that the area where yielding occurs, as Figure 6.2-13 and Figure 6.2-14 show for S235, is increased compared to the results with steel S355. Furthermore, a large loss of pretension for the two bolts of 22,0 % and 13,1 %, respectively, is observed. Those losses have to be related mainly to the yielding of the plates. Table 6-1 shows a comparison of the characteristic resistances according to EN1993-1-8 [34] and Abaqus. The resistance in Abaqus is defined at 0,15 mm slip. The resistance against bearing is listed for the sake of completeness, it is not considered in any numerical calculation performed by Abaqus. The ratio Abaqus/EC is always based on the smallest Eurocode value [34], [39]. It can be observed that for this joint configuration according to [34], [39] only for S690 the slip resistance governs, otherwise the plastic resistance of the net cross-section of the plates. Abaqus models always show slip failure influenced by material properties. Characteristic predictions according to [34], [39] are unsafe for S450 and S690.

Table 6-1: Characteristic resistances from parametric study on material properties of plates

Material	$N_{net,R}$ [kN]	$F_{b,R}$ [kN]	$F_{s,R}$ [kN]	Abaqus [kN]	Abaqus/EC [-]
S235	308,3	(923,1)	593,1	390,6	1,27
S275	360,8	(1102,6)	593,1	449,9	1,25
S355	465,8	(1307,7)	593,1	542,1	1,16
S450	577,3	(1410,3)	593,1	562,2	0,97
S690	905,3	(1974,4)	593,1	570,5	0,96

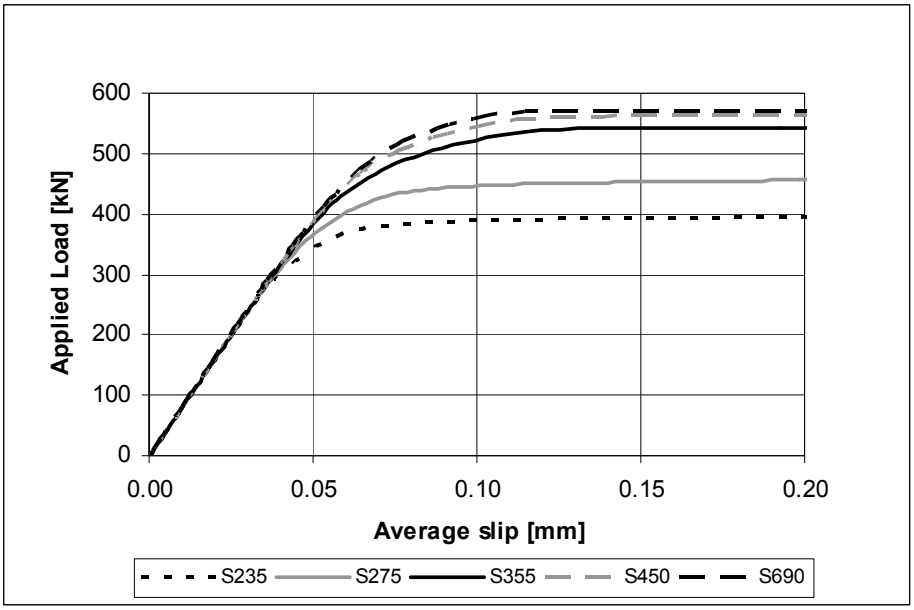

Figure 6.2-12: Comparison of load vs. slip curves for different materials

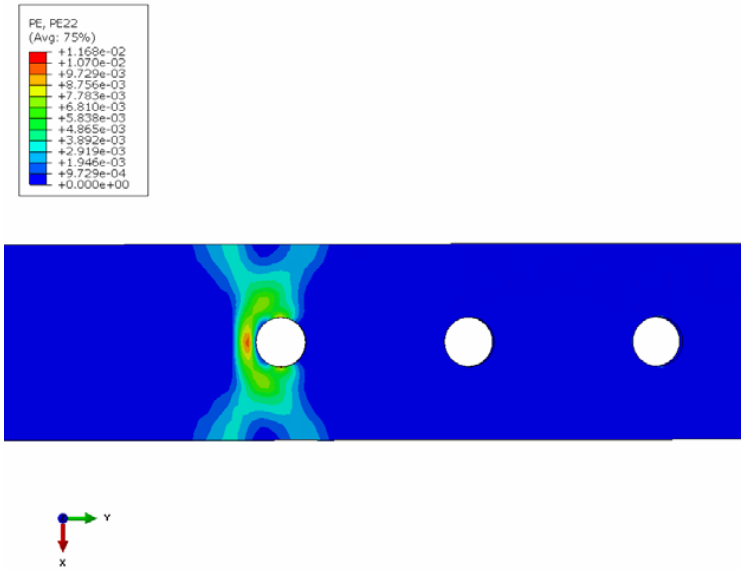

Figure 6.2-13: Plastic strains in longitudinal direction – 0,15 mm slip, S235

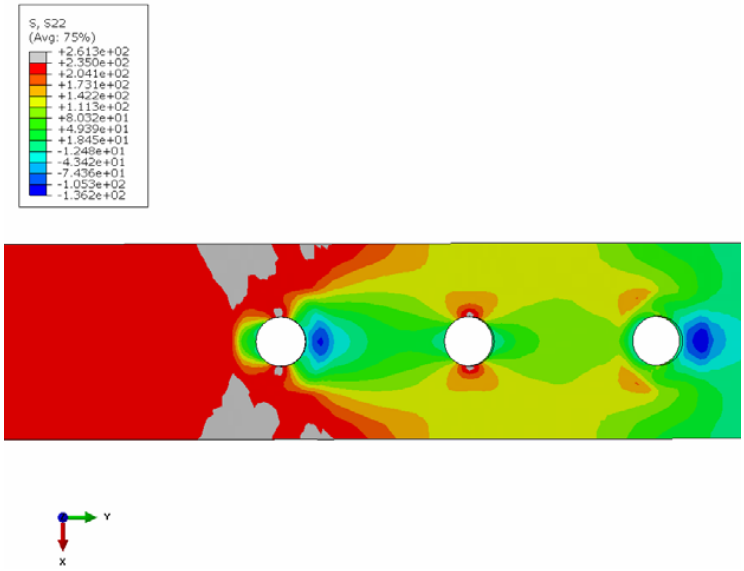

Figure 6.2-14: Stresses in longitudinal direction – 0,15 mm slip, S235

Table 6-2 summarizes the results obtained from this parametric study with regard to longitudinal stresses and loss of pretension. The gross stress is defined as the applied load divided by the gross area of the plates. This is the minimum stress in the plate due to external loading. The net stress considers the reduction in area due to the hole and therefore represents an upper theoretical bound. The expected maximum stress at the hole is obtained around the holes of the inner plates in the FE model. If the ratio of this stress to the yield stress is larger than one, yielding has started and a higher loss of pretension can be expected. Its magnitude cannot be predicted by those ratios since the distribution of stresses, especially above yield stress, governs the loss of pretension in the bolts. However, Table 6-2 shows that for this specific test a loss of pretension up to 22 % may be expected.

Table 6-2: Results of parametric study on material properties of plates – at 0,15 mm slip

Material	σ_{gross} **[MPa]**	σ_{net} **[MPa]**	$\sigma_{max,hole}$ **[MPa]**	$\frac{\sigma_{net}}{f_y}$ **[-]**	$\frac{\sigma_{max,hole}}{f_y}$ **[-]**	**Loss of pretension [%]**
S235	221,9	297,7	247,5	1,27	1,05	22,0
S275	255,6	342,9	290,3	1,25	1,05	17,2
S355	308,0	413,2	367,6	1,16	1,04	8,1
S450	319,4	428,5	427,1	0,97	0,97	5,1
S690	324,1	434,8	624,2	0,63	0,90	3,9

6.2.5 Parametric study to access level of assembling tolerances

In chapter 6.2.4 has been shown that the stress level in the plates plays an important role in a friction connection since it influences the loss of pretension in the bolts. This chapter deals with assembling tolerances which are generally

needed to fit together two parts during the execution phase. For the kind of connection considered previously, it seems to be realistic to initially have a gap between the inner and outer plates, cp. Figure 6.2-15. This gap may be closed by applied pretension forces into the bolts, which will cause additional bending stresses in the outer plate.

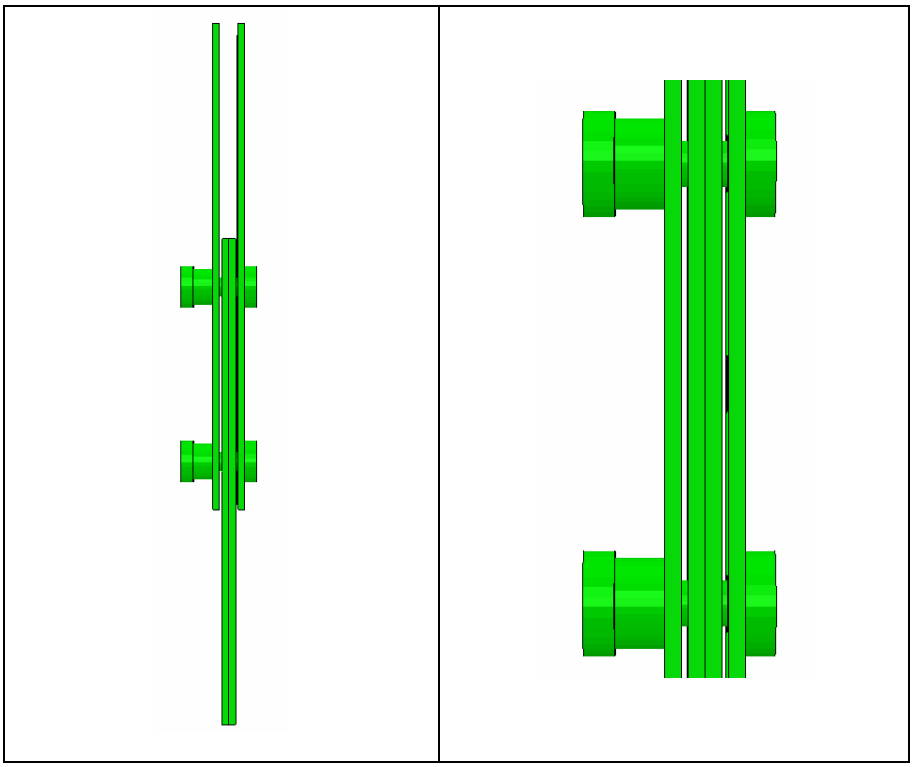

Figure 6.2-15: Detail of assembling tolerances

A parametric study is carried out with two different steel grades (S355 and S450) and gaps of one, two and three mm on each side in order to investigate the effect on the slip resistance. Figure 6.2-16 and Figure 6.2-17 clearly quantify the expected trend, the bigger gap is used the lower resistance can be achieved. A reduction of resistance up to 26,9 % at a slip level of 0,15 mm is

shown on Figure 6.2-16 and Figure 6.2-17. It can also be observed that the defined failure does not correspond to the ultimate load. The specimens can still increase their load until they reach a level where mainly slip occurs without increasing the load. When a gap of 3 mm is used for S355, the results from Abaqus are even below the lower boundary defined in this case as plastic resistance of the net cross-section, meaning that such gap would be out of tolerances. Eurocode [34] overestimates the resistance in this case by 17 %.

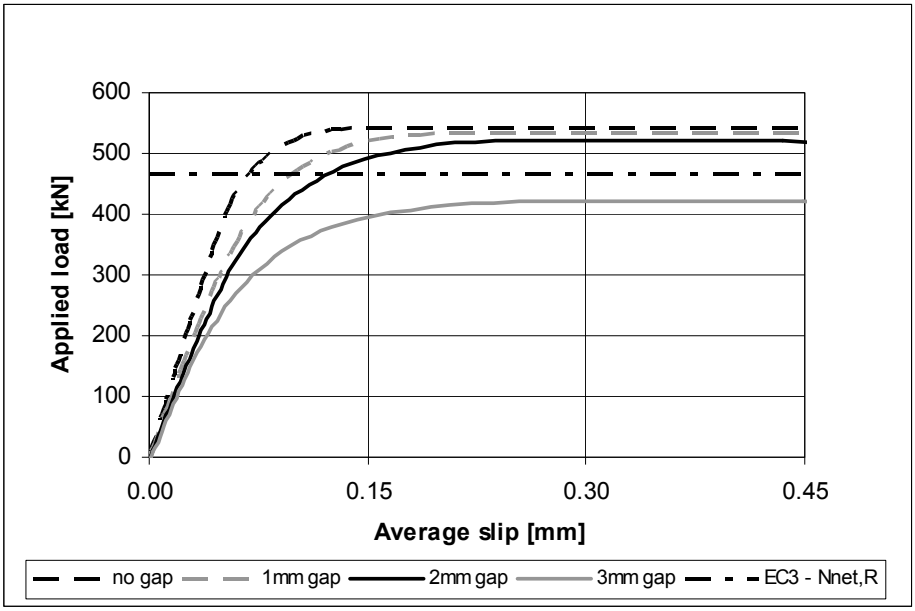

Figure 6.2-16: Comparison of load vs. slip curves for different gaps, S355

As can be seen in Figure 6.2-17 for S450 all considered models would be out of tolerances. According to [34] the resistance is overestimated by 2,7 % for no gap, 8,7 % for 1 mm gap, 15,8 % for 2 mm gap and 39,2 % for a gap of 3 mm.

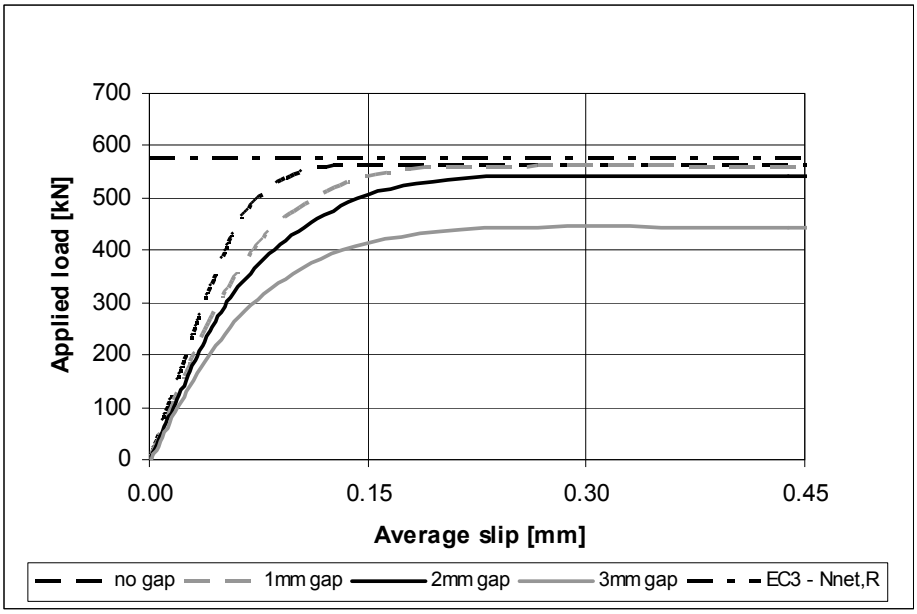

Figure 6.2-17: Comparison of load vs. slip curves for different gaps, S450

6.3 Conclusions

It is shown that the prediction of the slip resistance of the static test by FEA is in good agreement with the experimentally obtained results. The achieved accuracy is equal to 5,6 % for nominal steel properties of grade S355. A complete agreement cannot be accurately predicted due to changing surface conditions.

Additionally, it is demonstrated that the slip resistance depends on the material grade of the connected plates. Premature yielding around the holes results into higher losses of pretension in the bolts and therefore lower total slip resistance.

Assembling tolerances have a negative effect on the total resistance. The bigger the modelled gap the lower resistance is achieved. However, the ultimate load is larger than the one obtained at a slip of 0,15 mm.

Characteristic resistances according to [34], [39] are overestimated compared to FEA for S450 and S690. However, different governing failure modes are

observed. Whereas according to [34], [39] the plastic resistance of the net cross-section is dominating, finite element calculations clearly show slip failure. This means that a new recommendation for high strength steel is necessary.

7 FINITE ELEMENT ANALYSIS OF A SINGLE LAP JOINT

In chapter 6 a finite element model has been benchmarked and parametric studies have been carried out based on a symmetric friction connection with two shear planes. This chapter focuses on modelling of a friction connection with a single shear plane based on the previous calculations. The same parameters as for the symmetric connection are investigated and compared to existing design rules [34], [39]. A comparison of symmetric and asymmetric friction connections based on the finite element calculations will be shown.

7.1 Description of finite element models

Figure 7.1-1 shows a three dimensional finite element (FE) model including the meshed parts of a single shear lap joint. It is based on the previously described model of a symmetric friction connection. Dimensions of plates and bolts remain the same. The sleeve is elongated by 16 mm to compensate the two removed plates compared to the symmetric test. All other properties as material, friction coefficient, magnitude of pretension force etc. are used as in the static test and will not be specified in detail again.

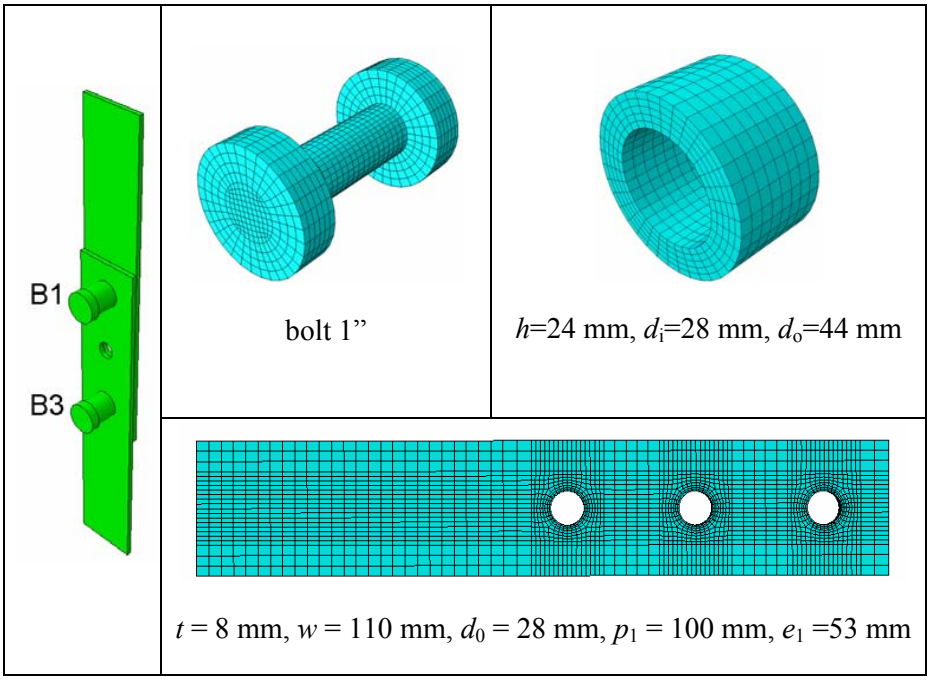

Figure 7.1-1: Finite Element model of a single shear lap joint

7.2 Results

From chapter 6 can be seen that the slip resistance varies depending on material properties of the joined plates and assembling tolerances. For the sake of comparison a similar investigation of a single shear lap joint is carried out. The failure criterion is defined as 0,15 mm slip for all numerical calculations. Practical importance of this chapter is in understanding of the so called HISTWIN joint [19], a lap joint used in tubular towers.

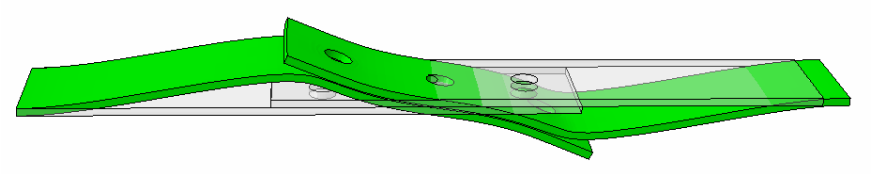

Figure 7.2-1: Deformed shape of a single shear lap joint – scale factor 20

Figure 7.2-1 shows the general deformed shape of a single shear lap joint. It is obvious that so called “secondary bending” occurs due the eccentricity, when loaded in tension.

7.2.1 Parametric study based on material properties of the plates

As has been explained in chapter 6.2.4 the total thickness of the joined plates is decreasing in the area of the bolts due to Poisson’s effect while loaded. Figure 7.2-2 and Figure 7.2-3 visualize that this also holds for the single shear lap joint. While the total thickness of the connected plates decreases – positive values in Figure 7.2-2 mean a decrease – the bolt looses pretension force at the same time. The reduction of plate thickness is measured at each hole as the relative change of the two outermost points on each plate. As simplification the rotation of the two plates, which occurs due to secondary bending, is neglected for determination of the reduction.

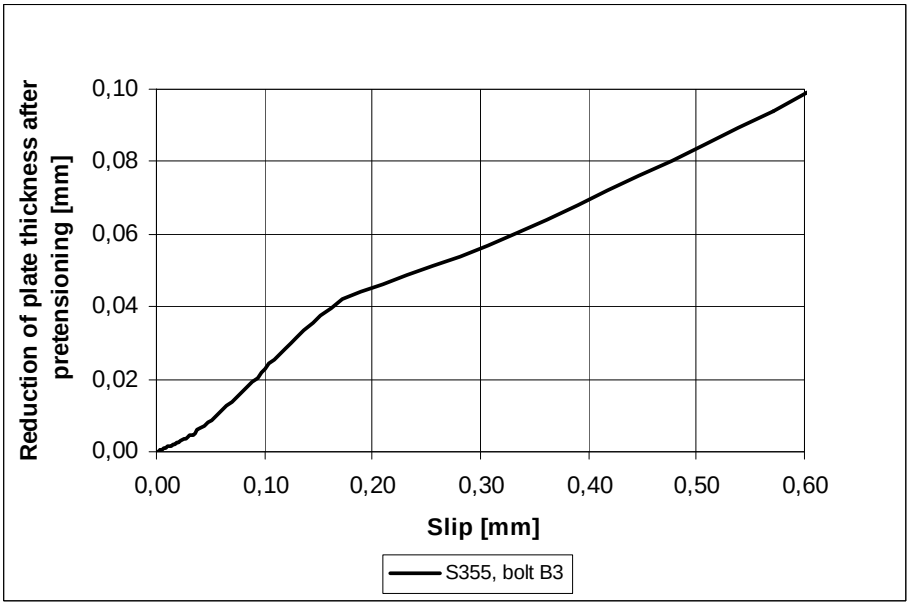

Figure 7.2-2: Reduction of plate thickness during loading – bolt B3, S355

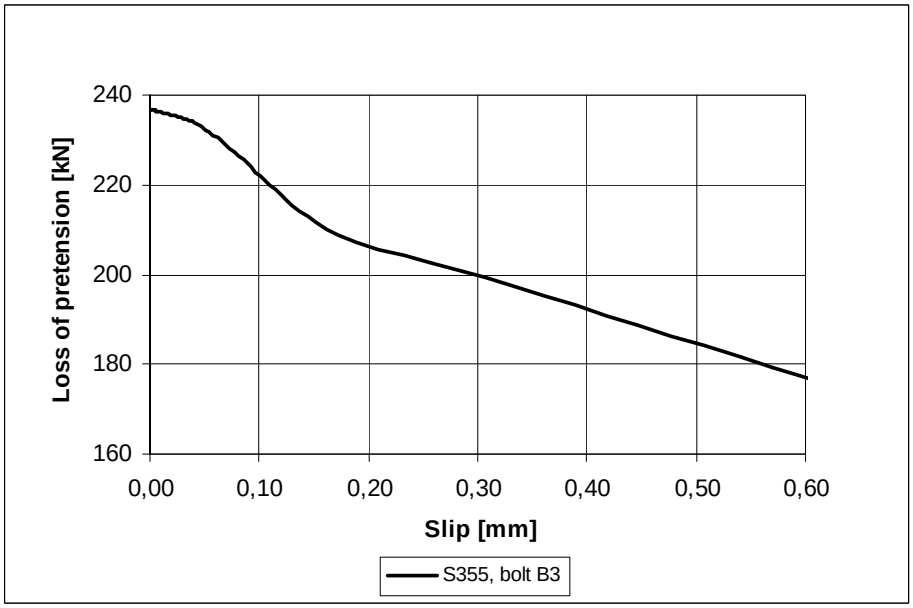

Figure 7.2-3: Loss of pretension – bolt B3, S355

Considering the applied load on the plate and bearing the reduction in area due to the bolt holes in mind, it is realistic that the plates start yielding around the holes although force is transferred through friction to the other plates. However, yielding may start even earlier due to secondary bending. It can clearly be seen in Figure 7.2-4 to Figure 7.2-6 that high stresses arise from this bending.

As mentioned before, yielding depends on the material used. Thus, for the single shear lap joint it is also expected that the loss of pretension and therefore the total slip resistance are related to the material properties of the plates.

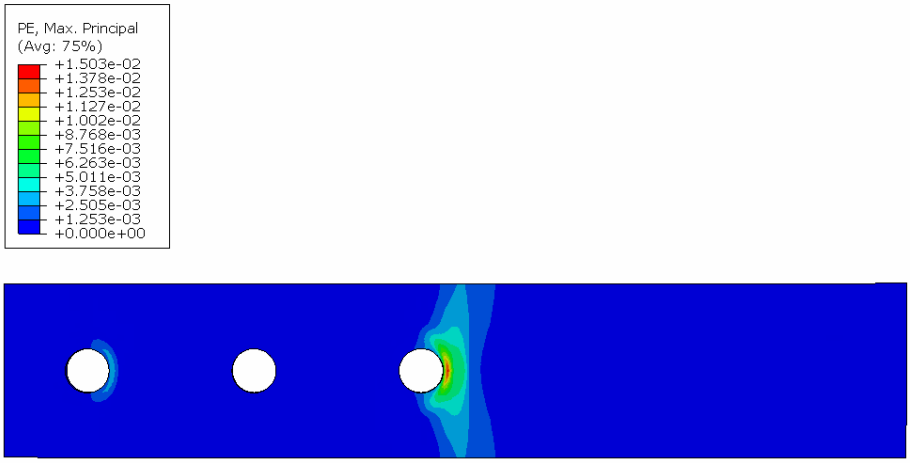

Figure 7.2-4: Plastic strains – 0,15 mm slip, S355

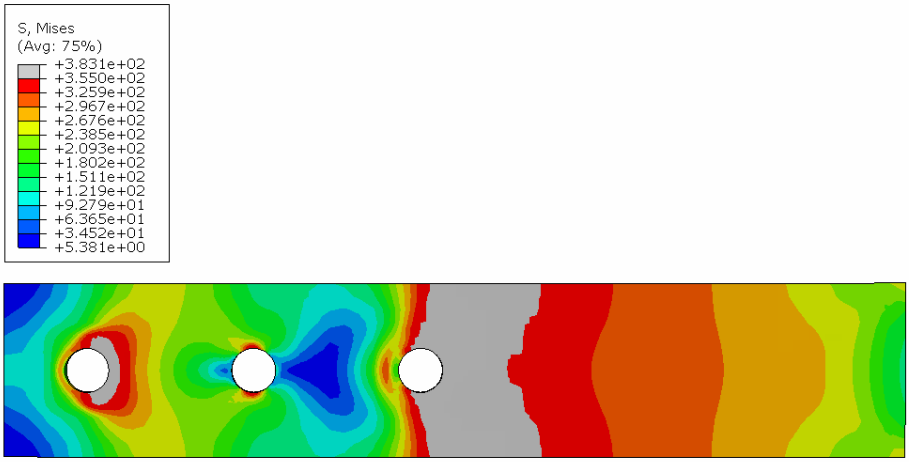

Figure 7.2-5: Von Mises Stresses – 0,15 mm slip, S355

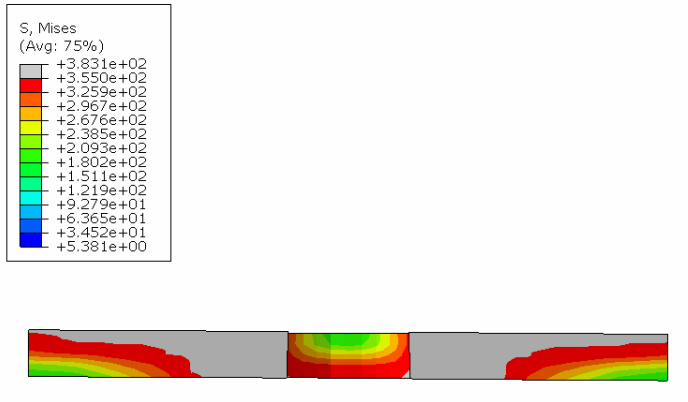

Figure 7.2-6: Von Mises Stresses through thickness– 0,15 mm slip, S355

In the following, results of a parametric study based on different nominal steel grades (S235, S275, S355, S450 and S690) are presented.

Table 7-1: Characteristic resistances from parametric study on material properties of plates

Material	$N_{net,R}$ **[kN]**	$F_{b,R}$ **[kN]**	$F_{s,R}$ **[kN]**	**Abaqus [kN]**	**Abaqus/EC [-]**
S235	154,2	(461,6)	296,6	195,0	1,26
S275	180,4	(551,3)	296,6	223,2	1,24
S355	232,9	(653,9)	296,6	266,5	1,14
S450	288,6	(705,2)	296,6	288,6	1,00
S690	452,6	(987,2)	296,6	300,0	1,01

The characteristic slip resistance according to [34] is equal to 296,6 kN. Even the design slip resistance (237,3 kN) overestimates the resistance obtained by FEA for S235 and S275. However, with regard to the characteristic plastic resistance of the net cross-section all results are on the safe side, cp. Table 7-1.

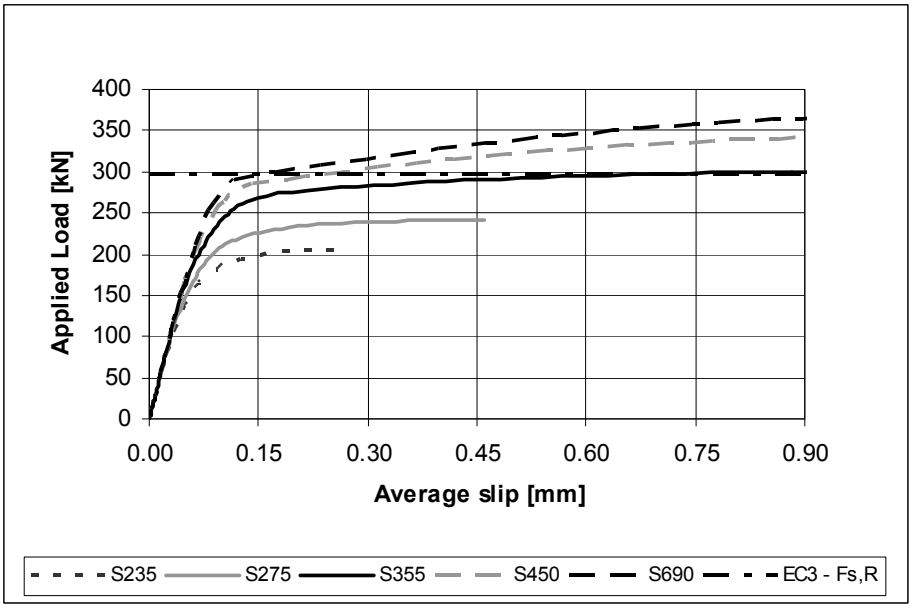

Figure 7.2-7: Comparison of load vs. slip curves for different materials

Figure 7.2-7 illustrates that a scattering in slip resistance, varying from 195,0 kN for S235 to 300,0 kN for S690, exists depending on the yield strength of the plates. Furthermore, none of the considered materials has reached a flat plateau, where just slip occurs without increase of load, at the defined failure criterion of 0,15 mm. This indicates that the ultimate slip resistance of the connection will be higher.

Table 7-2: Results from parametric study on material properties of plates

Material	σ_{gross} **[MPa]**	σ_{net} **[MPa]**	$\sigma_{\max,hole}$ **[MPa]**	$\frac{\sigma_{net}}{f_y}$ **[-]**	$\frac{\sigma_{\max,hole}}{f_y}$ **[-]**	**Loss of pretension [%]**
S235	221,5	297,2	115,8	1,26	0,49	21,8
S275	253,7	340,3	186,0	1,24	0,68	18,1
S355	302,8	406,2	303,4	1,14	0,85	10,7
S450	328,0	440,0	386,3	1,00	0,86	5,9
S690	340,9	457,3	574,8	0,66	0,83	2,5

Table 7-2 summarizes the results obtained from this parametric study with regard to longitudinal stresses and loss of pretension. The gross stress is defined as the applied load divided by the gross area of the plates. This is the nominal longitudinal stress in the plate due to external loading. The net stress considers the reduction in area due to the hole, neglecting the influence of secondary bending stresses. The expected maximum stress at the hole is obtained around the holes of the plates in the FE model in exactly the same way as for the double shear lap joint. It can be seen that the ratio of this stress to the yield stress is always smaller than one. This fact and Figure 7.2-4 emphasize that plastification is shifted away from the hole. Major reason for that is secondary bending. However, Table 7-2 shows that for this specific specimen configuration a loss of pretension up to 21,8 % may be expected.

7.2.2 Parametric study to access level of assembling tolerances

In chapter 6.2.5 it has been shown that the effect of assembling tolerances in terms of gaps between the plates may have a significant influence on the slip resistance of a symmetric double shear friction connection. A reduction of resistance up to 26,9 % at a slip level of 0,15 mm is recognized for a specific connection configuration.

This chapter deals with assembling tolerances for a single shear lap joint. For this kind of connection, it seems to be realistic to have a gap between the two connected plates before assembling, cp. Figure 7.2-8. This gap may be closed by applying pretension forces into the bolts and therefore causes additional bending stresses in the plates. As tensile load is applied on the plates, secondary bending stresses arise due to the eccentricity of the two plates.

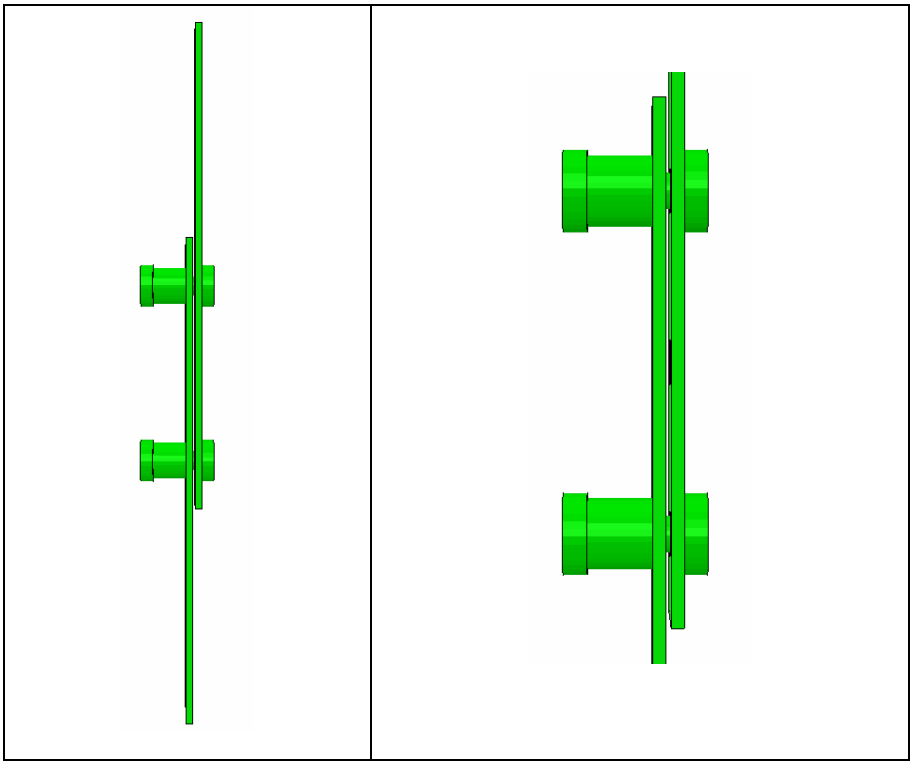

Figure 7.2-8: Detail of assembling tolerances

A parametric study has been carried out with two different steel grades (S355 and S450) and gaps between the two plates of one, two and three mm in order to investigate the effect on the slip resistance. Figure 7.2-9 and Figure 7.2-10 clearly prove the bigger gap is used the lower resistance can be achieved. A

reduction of resistance up to 10,7 % at a slip level of 0,15 mm is identified. It can also be observed that the defined failure does not correspond to the ultimate load. The specimens can still increase their load after a slip level of 0,15 mm is reached.

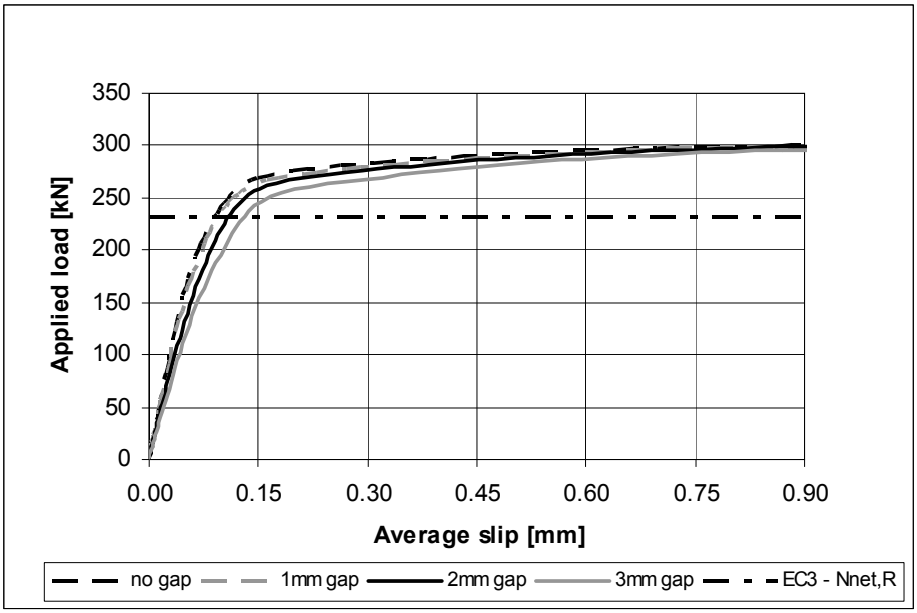

Figure 7.2-9: Comparison of load vs. slip curves for different gaps, S355

Figure 7.2-9 clearly visualizes that in this case with regard to the lower boundary according to [34], plastic resistance of the net cross-section, even assembling tolerances up to 3 mm are on the safe side. Contrary to those results Figure 7.2-10 shows that this doesn't hold for S450. [34] overestimates the resistance by 3,0 % for 1 mm gap, 6,4 % for 2 mm gap and 11,0 % for a gap of 3 mm.

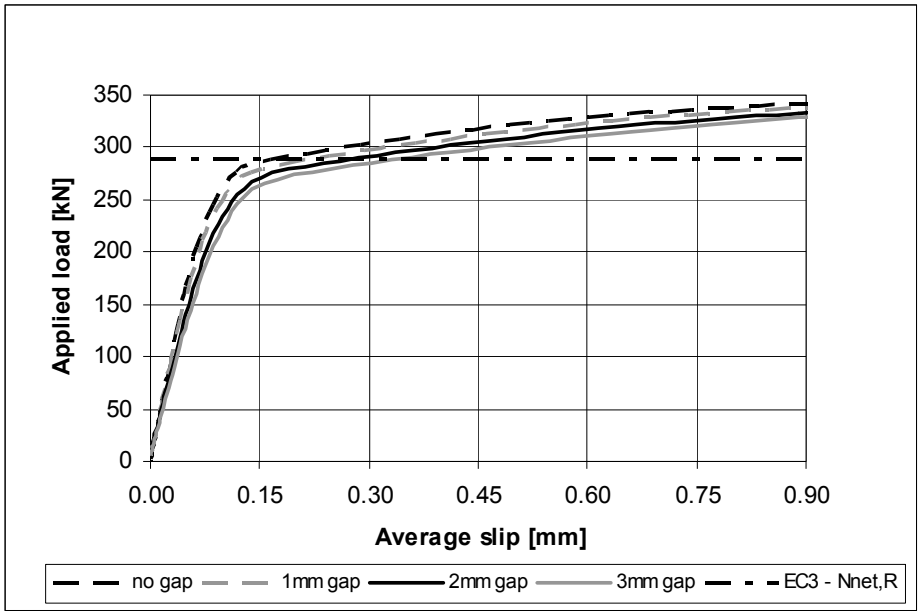

Figure 7.2-10: Comparison of load vs. slip curves for different gaps, S450

7.3 Conclusions

The slip resistance depends on the steel grade of the connected plates. It is shown that the slip resistance of a single shear lap joint depends on the material grade of the connected plates. Premature yielding around the holes results into higher losses of pretension in the bolts and therefore reduces the slip resistance.

Assembling tolerances have a negative effect on the total resistance. The bigger the modelled gap the lower resistance is achieved. However, the joint sustains higher load when the slip of 0,15 mm is passed. This effect becomes more obvious with increased material grades. Clear plateaus, where major slip occurs without increase of load, are not obtained due to secondary bending effects.

Characteristic resistances according to [34], [39] are on the safe side compared to FEA for all considered materials, but assembling gaps may result into unsafe estimations.

7.4 Comparison of single and double shear lap joint

The previous chapters have described the influence of material properties of the plates and possible gaps during assembly on the slip resistance. Table 7-3 clearly shows that both single and double shear lap joint have very similar nominal stress level and loss of pretension at a slip level of 0,15 mm.

Table 7-3: Comparison of single and double shear joints without gaps

Material	σ_{gross} **[MPa]**		**Loss of pretension [%]**	
	single shear lap joint	**double shear lap joint**	**single shear lap joint**	**double shear lap joint**
S235	221,5	221,9	21,8	22,0
S275	253,7	255,6	18,1	17,2
S355	302,8	308,0	10,7	8,1
S450	328,0	319,4	5,9	5,1
S690	340,9	324,1	2,5	3,9

One major difference is related to the failure mechanisms. The double shear lap joint has a symmetric configuration and the ultimate resistance corresponds to the defined slip criterion of 0,15 mm. A clear plateau can be observed, cp. Figure 6.2-12, where major slip occurs without increasing the load. The single shear lap joint behaves differently since it is an asymmetric connection, where secondary bending occurs, when loaded in tension. This leads to a "post critical" resistance, which could be achieved after 0,15 mm of slip, cp. Figure 7.2-7. For a single shear lap joint the area where major yielding occurs is shifted away from the reduced cross-section due to the secondary bending effect.

Both types of connections have shown that assembling tolerances may reduce the slip resistance. However, the influence on a single shear lap joint is

considerably lower (reduction of up to 10,7 %) compared to a double shear lap joint (reduction of up to 26,9 %).

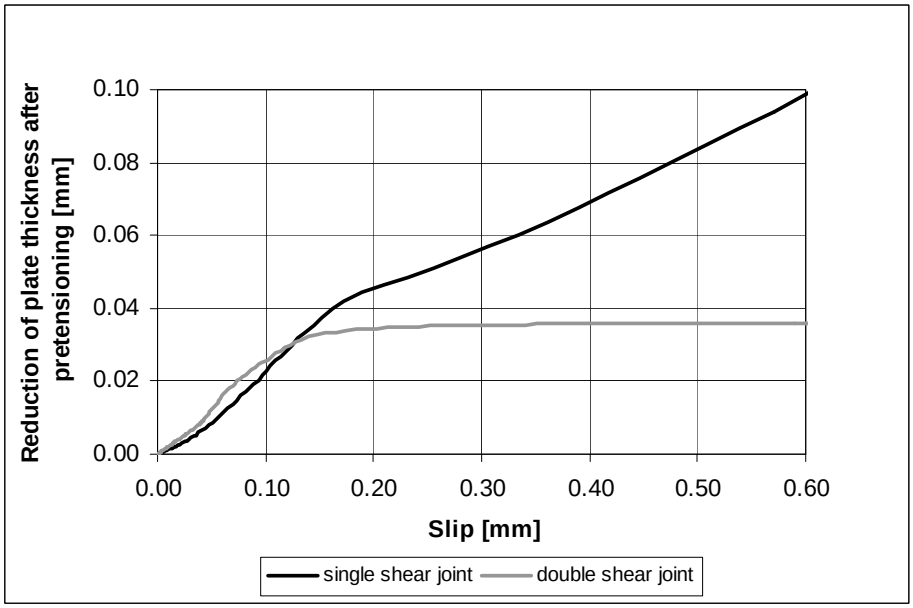

Figure 7.4-1: Comparison of reduction of plate thickness vs. slip curves without gaps, S355

Figure 7.2-1 indicates the different behaviour of a single and double shear lap joint. For a double shear lap joint major slip occurs after the maximum load is obtained and the reduction in plate thickness remains constant.

8 CONCLUSIONS

Pure relaxation tests and relaxation tests in combination with external loading have been performed to understand the pretension behaviour in friction connections. It has been shown that bolts loose some of their pretension force over time; most of it during the first couple of hours. As the test results prove, this mainly depends on the tightening process, the type of bolt, the clamping length of the bolt and the coating of the clamping package. For certain combinations design recommendations as consequences of test results are given. But it should be kept in mind, that these recommendations can just be seen as tentative, since the number of tests that they are based on is comparably small. The loss of pretension in TCB joining two plates coated with Temasil 90 under a static load, for example, can be calculated according to formula 8-1.

$$F_{p,C,lt} = F_{p,C} \cdot \left[1 - \frac{0,9165 \cdot \ln\left(\frac{t}{31,536 \cdot 10^6} \right) + 1,9602}{100} \right] \tag{8-1}$$

Where

$F_{p,C,lt}$ is the pretension force in a certain period of time (long term),

$F_{p,C}$ is the initial pretension force, according to EN-1993-1-8,

t is the time in years after the pretensioning.

Similar calculations for Huck BobTail lockbolts tightening galvanized plates can be found in chapter 5.

These recommendations are based on a perfectly closed joint without initial gap. The numerical calculations show, that if the plates have to be assembled with a gap between them, as it can be the case at any construction site, the resistance of a friction grip connection is further reduced. It is found that the influence of the gap in a single shear lap joint, as for example in tubular towers, is smaller than in double shear lap joints as they are used in lattice towers. Assembling tolerances have anyhow a negative effect on the total resistance. The bigger the modelled gap, the lower resistance is achieved. Additionally, assembling tolerances may result into unsafe estimations acc. to EN 1993-1-8 [34]. And while the characteristic resistances calculated according to EN 1993-1-8 [34] are on the safe side for a single lap joint, they may overestimate the actual resistance of double lap joints for S450 and S690 in comparison with the results from finite element analysis.

The prediction of the slip resistance of the static test modelled in finite elements is in good agreement with the experimentally obtained results. The achieved accuracy is equal to 5,6 % for nominal steel properties of grade S355. A complete agreement cannot be accurately predicted due to changing surface conditions.

The final slip resistance of the regarded structure depends on the material grade of the connected plates. Premature yielding around the holes results into higher losses of pretension in the bolts and therefore lower total slip resistance. In order to avoid this phenomenon, higher steel grades may be used.

All these findings imply that a friction joint in any kind of structure should be checked and maintained regularly. Although some bolts exist, which are claimed to be vibration proof and safe against self loosening, they may not provide the pretension force, which has been assumed in the design of the structure. Besides, the design for slip resistance in EN 1993-1-8 [34] does not consider any parameters such as material properties of the plates or assembling tolerances. Both have a major influence on the behaviour of the joint, as has been shown by experimental and numerical investigation.

9 OUTLOOK

The recommendations given in chapter 8 are based on tests, which have been carried out at Luleå University of Technology during the last couple of years. The tests vary in type of bolt, the coating thickness of surface paint, thickness of the clamping package and load application. However, the number of performed tests is comparably small, so that the above given formulas can just be seen as tentative recommendations for design, which give a first indication of the bolts' behaviour. It is recommended to do further investigations before giving out more general design recommendations. Besides, the data in some tests accounts for maximum one to four weeks of testing. To verify an extrapolation of the bolts' behaviour during a life time of a tower structure, longer lasting tests should be done. The most reasonable results would be achieved by monitoring the behaviour of bolts in real tower applications.

Besides, the recommendations given above are just valid for very specific cases. To generalize and validate them for any combination of bolt type, clamped material, dimension, and coating, further investigations are necessary.

This work has helped to verify the use of friction connections instead of flange connections in tubular towers. Thereby, the limiting criterion – not taking into account the transportation issue – for steel tubular towers shifts from the fatigue sensitivity of the flange connection to the stability resistance of the tower shells. However, the design of tubular towers with friction connections justifies a use of higher strength steel grades, but further research towards a more economical application is recommended.

All numerical investigations carried out are based on a benchmarked finite element model of one double shear lap joint experiment. A testing programme,

checking some of the effects discussed above, is necessary to confirm effects as loss of pretension based on material properties of the plates or influence of assembling tolerances. More numerical analyses need to be performed to investigate the influence of other parameters as thickness of plates, level of pretension, bolt diameter, number of bolts, position of bolts or variation of plate's width, which may influence the overall response of the connections. Furthermore, the design of friction connections according to EN 1993-1-8 [34] as it is present today does not take all influencing parameters into account and should be modified in future. A possible solution could be to aim for a design slip resistance based on yield strength, rather than designing separately for slip resistance and plastic resistance of the net-cross section of the plate.

In addition to the afore mentioned, it might be interesting to also check the difference in resistance of single and double shear lap joints using oversized or long slotted holes.

References

[1] Vinnova Analys VA 2009:08: Vindkraften tar fart – En strukturell revolution?

[2] Sahin, A. D.: Progress and recent trends in wind energy, *Progress in Energy and Combustion Science*, Vol. 30, Issue 5: pp. 501 – 543, 2004

[3] Word Wind Energy association 2008, www.wwindea.org, last visit 11/04/11

[4] Krohn, S., Danish Wind Industry Association, 2003

[5] Engström, S., Lyrner, T., Hassanzadeh, M., Stalin, T., Johansson, J.: "Tall towers for large wind turbines – Report from Vindforsk project V – 342 Höga tron för vindkraftverk", Elforsk rapport 10:48, 2010

[6] High strength steel tower for wind turbine (HISTWIN) – Draft Final Report, Period of Reference 01/07/06 – 30/06/09, 2010

[7] Heistermann, C., Husson, W., Veljkovic, M.: "Flange connection vs. friction connection in towers for wind turbines", *Proc. of Nordic steel and construction conference (NSCC 2009)*, pp. 296 – 303, Malmö, Sweden, 2009

[8] Husson, W.: Friction Connections with Slotted Holes for Wind Towers; Luleå University of Technology, Luleå, 2008

[9] SeeBA Energiesysteme GmbH, Tielger Allee 60, 32351 Stemwede, Germany. www.seeba-online.de, Last visit: 2011-03-15

[10] Garzon, O., Heistermann, T., Veljkovic, M.: "A study of an axially compressed cold-formed folded plate", *Proc. of 6th International conference on Thin Walled Structures (ICTWS2011)*, to be published, Timisoara, Romania, 2011

[11] BTM-6C strain gauge, Tokyo Sokki Kenkyujo Co. Ltd.

[12] Naumes, J., Pak, D.: HISTWIN – WP 2.5 – Large Scale 4-Point-Bening Tests, Perfomance check of various assembling joints, 8 static tests, Background document, 30/03/2009

[13] Ryan, I.: Evaluation of the high strength "bolt for pre-loading" product type "TCB" and its use in France. *Centre Technique Industriel de la Construction Metallique*, CTICM N°2001-07, 2001

[14] Cosgrove, T. C.: Tension Control Bolts, Grade S10T in Friction Grip Connections; The Steel Construction Institute, Ascot, England, 2004

[15] Tension Control Bolts Limited 2008, Whitchurch Business Park, Shakespeare Way, Whitchurch. Shropshire, SY13 1LJ England. www.tcbolts.co.uk, last visit 2011-04-11

[16] Alcoa Fastening Systems, "Bobtail – Huck's next generation lockbolt. No pintail, fast installation, vibration resistant. ½"-1", 12mm-20mm", AF1032 0410 2.5M. 2010

[17] Nord-Lock – Bolt Securing System, Technical Information, www.nord-lock.com, last visit 2011-04-11

[18] August Friedberg GmbH, Achternbergstr. 38a, 45884 Gelsenkirchen, Germany, www.august-friedberg.de, last visit 2011-04-11

[19] High steel tubular towers for wind turbines (HISTWIN2) – Grant Agreement No RFSR-CT-2010-00031

[20] EN 1090-2:2008: E, "Execution of steel structures and aluminium structures – Part 2: Technical requirements for steel structures", European Committee for Standardisation, Brussels, 2008

[21] Petersen, C.: „Nachweis der Betriebsfestigkeit exzentrisch beanspruchter Ringflanschverbindungen", *Stahlbau*, Vol. 67, pp. 191 – 203, Enrst & Sohn, 1998

[22] Seidel, M.: "Zur Bemessung geschraubter Ringflanschverbindungen von Windenergieanlagen", Dissertation, Universität Hannover, Institut für Stahlbau, 2001

[23] EN 1993-1-9: "Eurocode – Design of steel structures – Part 1-9: Fatigue", CEN, European Committee for Standardization, Brussels, Belgium, 2004

[24] EN 1993 (E): "Eurocode – Design of steel structures", CEN, European Committee for Standardization, Brussels, Belgium, 2005

[25] Germanischer Lloyd WindEnergy: Guideline for the certification of wind turbines, Edition 2003 with supplement 2004

[26] Bickford, J. H.: "An introduction to the design and behaviour of bolted joints - 3rd edition, revised and expanded", Marcel Dekker, Inc., New York, USA, 1995

[27] Friede, R., Lange, J.: "Loss of preload in bolted connections due to embedding and self loosening", *Proc. Stability and ductility of steel structures (SDSS'Rio 2010)*, pp. 287 – 293, Rio de Janeiro, Brazil, 2010

[28] Katzung, W., Pfeiffer, H. Schneider, A.: "Zum Vorspannkraftabfall in planmäßig vorgespannten Schraubenverbindungen mit beschichteten Kontaktflächen", *Stahlbau*, Vol. 65, Issue 9, pp. 307 – 311, Ernst & Sohn, 1996

[29] Sedlacek, G., Kammel, C.: "Zum Dauerverhalten von GV-Verbindungen in verzinkten Konstruktionen – Erfahrungen mit Vorspannkraftverlusten", *Stahlbau*, Vol. 70, Issue 12, pp. 917 – 926, Ernst & Sohn, 2001

[30] VDI 2230, Part 1: Systematic calculation of high duty bolted joints – Joints with one cylindrical bolt, VDI-Richtlinien, Beuth Verlag, Berlin, Germany, 2003

[31] Veljkovic, M., Limam, M., Heistermann, C., Rebelo, C., Simões da Silva, L.: "Feasibility study of friction connections in tubular towers for wind turbines", Proc. of the International Symposium "Steel Structures: Culture & Sustainability 2010", pp. , Istanbul, Turkey, 2010

[32] DeWolf, J. T., Yang, J.: "Relaxation in high-strength bolted connections with galvanized steel", Final report, Project 96-4, JHR 98-262University of Connecticut, Storrs, Connecticut, USA, 1998

[33] EN 1990: "Eurocode – Basis of structural design", CEN, European Committee for Standardization, Brussels, Belgium, 2002

[34] EN 1993-1-8:2005: E, "Eurocode 3 - Design of Steel Structures, Part 1-8 Design of Joints", European Committee for Standardisation, Brussels, 2005

[35] Heistermann, C, Heistermann, T, Veljkovic, M, "Remaining pretension force in a friction connection", Proc. 4th Intl. Conference on Steel & Composite Structures (ICSCS'10), pp. 275-279, Sydney, 2010

[36] Schaumann, P., Rutkowski, T.: "Ergebnisbericht der Verfahrensprüfung zur Ermittlung des Reibkoeffizienten im Zusammenhang mit der Typengenehmigung der Gittermaste für die Windenergieanlage MD/S70, MD/S77", University of Hannover, Hannover, Germany, 200

[37] Swedish Institute of Steel Construction: "Swedish Regulations for Steel Structures, BSK", Publication 118, Stockholm, Sweden, 1989

[38] Abaqus Analysis User's manual version 6.10, Dassault Systèmes Simulia Corp., Providence, 2010

[39] EN 1993-1-12:2007: E, "Eurocode 3 - Design of Steel Structures, Part 1-12 Additional rules for the extension of EN 1993 up to steel grades S700", European Committee for Standardisation, Brussels, 2007

Annex

A. Overview of performed tests

B. Calibration data of the bolts

C. Bolt force diagrams

D. Material testing of Huck BobTail lockbolts 1”/M25,4

E. Data sheets about Huck 1”/M25,4, Huck M20, Friedberg HV Rändel

F. Product information sheet for Temasil 90 by Tikkurila Coatings

G. Input data from Abaqus calculations

A OVERVIEW OF PERFORMED TESTS

The following Table A-1 and Table A-2 shall give a general overview on the tests carried out within the scope of this thesis. Here, information about the name of the specimen, type and size of the tested bolt, hole diameter, plate dimensions and surface preparations can be found.

Table A-1: Relaxation tests, RuH-S_4 with static loading, RuH_4 with cyclic loading (chapter 5)

specimen	bolt	bolt diameter	hole diameter	plate thickness	no. of painted surface
surface finishing: grit blasted (G70, Sa 2 ½) + hot dip galvanization					
RuH-S_4	Huck long	M25,4 (1”)	28	4 * 8 + 24 (sleeve)	8
RuH-S_2	Huck long	M25,4 (1”)	28	4 * 8 + 24 (sleeve)	4
RuH-S_0	Huck long	M25,4 (1”)	28	4 * 8 + 24 (sleeve)	0
RuH_4	Huck short	M25,4 (1”)	28	4 * 8	8
RuH_2	Huck short	M25,4 (1”)	28	4 * 8	4
RuH_0	Huck short	M25,4 (1”)	28	4 * 8	0

Table A-2: Pure relaxation tests (chapters 3 and 4)

specimen	bolt	bolt diameter	hole diameter	plate thickness	no. of painted surface
surface finishing: grit blasted (G70, Sa 2 ½) + zinc rich primer					
R2	TCB	M30	33	50+8	2
R1	TCB	M30	33	50+8	1
R0	TCB	M30	33	50+8	0
R2N-1	standard+NL	M30	33	50+8	2
R2N-2	standard+NL	M30	33	50+8	2
R1N-1	standard+NL	M30	33	50+8	1
R0N-1	standard+NL	M30	33	50+8	0
R2F-1	Friedberg	M20	20,1	16+3	2
R1F-1	Friedberg	M20	20,1	16+3	1
R0F-1	Friedberg	M20	20,1	16+3	0
R2H-1	Huck short	M20	22	16+3	2
R2H-2	Huck short	M20	22	16+3	2
R1H-1	Huck short	M20	22	16+3	1
R1H-2	Huck short	M20	22	16+3	1
R0H-1	Huck short	M20	22	16+3	0
R0H-2	Huck short	M20	22	16+3	0
RL2H-1	Huck long	M20	22	37+3	2
RL2H-2	Huck long	M20	22	37+3	2
RL1H-1	Huck long	M20	22	37+3	1
RL1H-2	Huck long	M20	22	37+3	1
RL0H-1	Huck long	M20	22	37+3	0
RL0H-2	Huck long	M20	22	37+3	0

B CALIBRATION DATA OF THE BOLTS

In all bolts used in the above described tests strain gauges are inserted to measure the change of the shaft length during testing. By this, inferences on the actual forces in the bolt can be drawn due to the calibration, which has been carried out in advance. For this calibration, the strain gauges has to be glued into the shaft of the bolts. The position of the strain gauge inside the shank of the bolts, given as the distance from the head of the bolt depending on the type of bolt, can be seen in Table B-1.

The calibration of the strain gauges in the bolts is always performed in the same way: The head of the bolt is mounted in one grip of a tensile testing machine while lower end of the shank is engaged into a special extended nut, which is also fixed in the tensile testing machine, cp. Figure B-1. Then the machine pulls the bolt with a load control rate of 5 kN/s until a certain force is reached. This force varies depending on the diameter of the bolt: For M30 TCB and standard structural bolts it is 420 kN, for M20 Friedberg HV Rändel and Huck BobTail lockbolts it is 180 kN and for M25,4/1” Huck BobTail lockbolts the maximum calibration load is 280 kN. When this specific load level is reached, the load is kept constant for about 300 seconds. By this, it shall not only be checked if bolt and strain gauge perform linearly, but also if the strain gauge is properly installed in the bolt. If the monitored stroke of the machine does not remain stable, an indication is given that either bolt or strain gauge does not perform well.

Table B-1: Strain gauge position depending on type of bolt

Type of bolt	diameter	clamping length [mm]	depth of bore hole as distance from the head of the bolt [mm]	position of the strain gauge as distance from the head of the bolt [mm]
TCB	M30	58	50	45
standard + NL	M30	58	50	45
Friedberg	M20	19	30	23
Huck BobTail	M20	19	34	30
Huck BobTail	M20	40	40	36
Huck BobTail	M25,4/1”	32	40	28
Huck BobTail	M25,4/1”	56	55	51

After keeping the load constant for five minutes, unloading starts with the same loading rate until the zero load level is reached again. Then the loading-unloading process is repeated at least twice, but these times the stop at peak load level last just for 30 seconds. From the achieved data the ration between applied load and strains in the bolts calculated with the method of least squares. If it shows a completely linear behaviour all the way to the maximum load during all load cycles, the bolt is approved for testing.

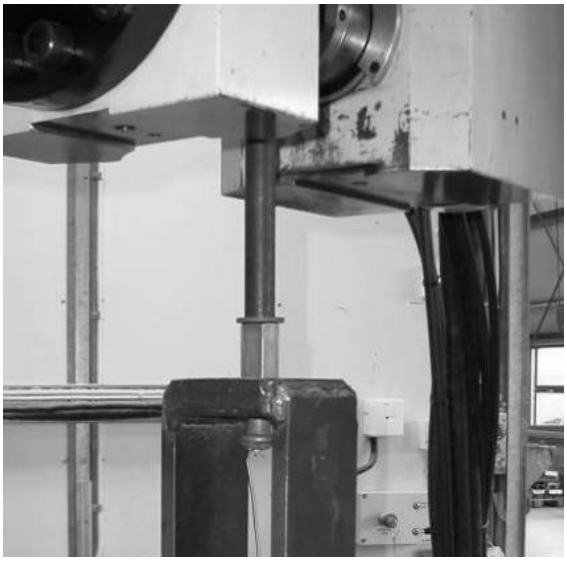

Figure B-1: Bolt calibration, here a TCB as an example [8]

As an example for bolt calibration the calibration curve and the load-displacement diagram for T1 are shown in Figure B-2 and Figure B-3. All bolts used in the performed tests are proven to behave linearly up to the calibrated load level. The parameters for the gradient a and the y-intercept b are given in Table B-2 to Table B-8 for all used bolts.

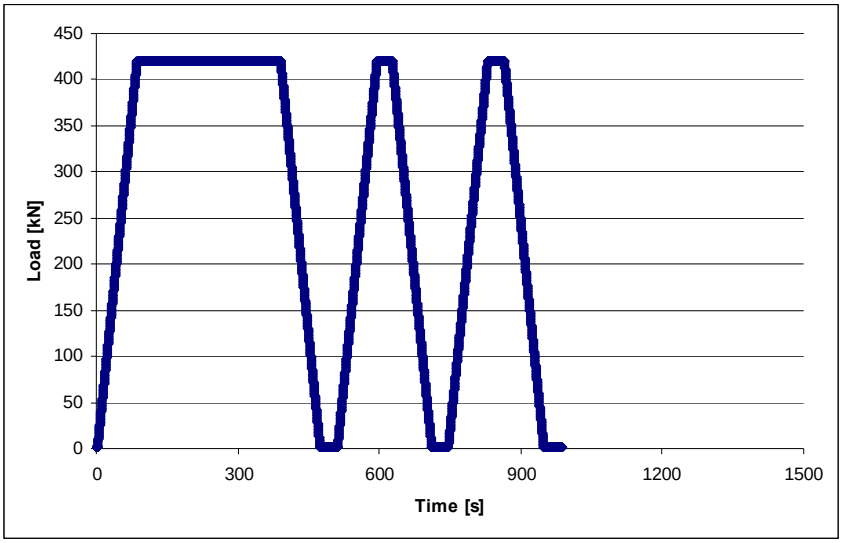

Figure B-2: Calibration curve for T1

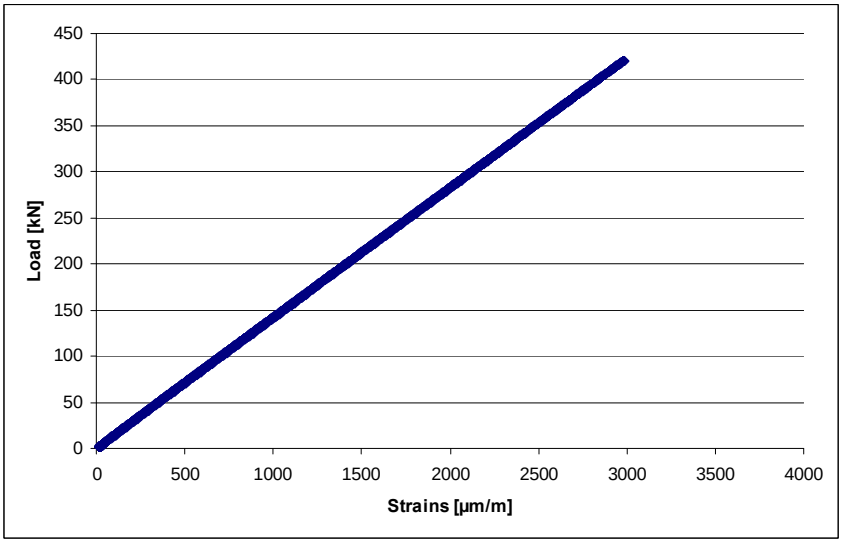

Figure B-3: Load-displacement diagram for T1

Table B-2: Calibration data of TCB M30 bolts for pure relaxation tests (chapter 3)

name of the specimen	position of the bolt	name of the bolt	calibration curve			
			a [N/µm/m]	b [kN]	rsq	
R2	B1	T1	0,14	0,53	1,0000	TCB M30
	B2	T3	0,14	0,01	1,0000	TCB M30
	B3	T4	0,14	0,96	1,0000	TCB M30
R1	B1	T5	0,14	-2,36	1,0000	TCB M30
	B2	T6	0,14	-1,51	1,0000	TCB M30
	B3	T7	0,14	-3,42	1,0000	TCB M30
R0	B1	T8	0,14	0,34	1,0000	TCB M30
	B2	T9	0,14	-1,91	1,0000	TCB M30
	B3	T10	0,14	-0,60	1,0000	TCB M30

Table B-3: Calibration data of standard structural M30 bolts in combination with NordLock washers for pure relaxation tests (chapter 4)

name of the specimen	position of the bolt	name of the bolt	calibration curve			
			a [N/µm/m]	b [kN]	rsq	
R2N-1	B1	N1	0,13	-1,81	1,0000	standard + NL M30
	B2	N2	0,12	-1,21	1,0000	standard + NL M30
	B3	N3	0,13	-0,08	1,0000	standard + NL M30
R1N-1	B1	N4	0,13	2,41	1,0000	standard + NL M30
	B2	N6	0,12	-0,95	1,0000	standard + NL M30
	B3	N8	0,12	-7,23	0,9999	standard + NL M30
R0N-1	B1	N13	0,13	2,87	1,0000	standard + NL M30
	B2	N11	0,12	-2,90	1,0000	standard + NL M30
	B3	N9	0,12	2,30	1,0000	standard + NL M30
R2N-2	B1	N17	0,13	2,90	1,0000	standard + NL M30
	B2	N15	0,12	-3,44	1,0000	standard + NL M30
	B3	N14	0,12	0,11	1,0000	standard + NL M30

Table B-4: Calibration data of Friedberg HV Rändel M20 bolts for pure relaxation tests (chapter 4)

name of the specimen	position of the bolt	name of the bolt	calibration curve			
			a [N/µm/m]	b [kN]	rsq	
R2F-1	B1	F10	0,07	-1,83	1,0000	Friedberg, M20
	B2	F7	0,07	-0,59	0,9999	Friedberg, M20
R1F-1	B1	F13	0,07	-2,80	0,9999	Friedberg, M20
	B2	F12	0,07	-2,80	0,9999	Friedberg, M20
R0F-1	B1	F16	0,07	-1,24	1,0000	Friedberg, M20
	B2	F15	0,07	2,03	0,9999	Friedberg, M20

Table B-5: Calibration data of long Huck M20 BobTail lock bolts for pure relaxation tests (chapter 4)

name of the specimen	position of the bolt	name of the bolt	calibration curve			
			a [N/µm/m]	b [kN]	rsq	
RL2H-1	B1	H1	0,05	1,47	1,0000	Huck M20, l_k = 40 mm
	B2	H2	0,05	1,94	1,0000	Huck M20, l_k = 40 mm
	B3	H3	0,05	0,51	1,0000	Huck M20, l_k = 40 mm
RL2H-2	B1	H19	0,05	2,08	1,0000	Huck M20, l_k = 40 mm
	B2	H5	0,05	1,71	1,0000	Huck M20, l_k = 40 mm
	B3	H4	0,05	2,51	1,0000	Huck M20, l_k = 40 mm
RL1H-1	B1	H9	0,05	0,38	1,0000	Huck M20, l_k = 40 mm
	B2	H8	0,05	1,87	1,0000	Huck M20, l_k = 40 mm
	B3	H7	0,05	2,15	1,0000	Huck M20, l_k = 40 mm
RL1H-2	B1	H12	0,05	1,06	1,0000	Huck M20, l_k = 40 mm
	B2	H11	0,05	1,87	1,0000	Huck M20, l_k = 40 mm
	B3	H10	0,06	1,46	1,0000	Huck M20, l_k = 40 mm
RL0H-1	B1	H15	0,05	1,65	1,0000	Huck M20, l_k = 40 mm
	B2	H14	0,05	0,46	1,0000	Huck M20, l_k = 40 mm
	B3	H13	0,05	1,66	1,0000	Huck M20, l_k = 40 mm
RL0H-2	B1	H18	0,05	1,34	1,0000	Huck M20, l_k = 40 mm
	B2	H17	0,05	2,35	1,0000	Huck M20, l_k = 40 mm
	B3	H16	0,05	2,10	1,0000	Huck M20, l_k = 40 mm

Table B-6: Calibration data of short Huck M20 BobTail lock bolts for pure relaxation tests (chapter 4)

name of the specimen	position of the bolt	name of the bolt	calibration curve			
			a [N/µm/m]	b [kN]	rsq	
R0H-1	B1	Hk4	0,05	-0,78	1,0000	Huck M20, l_k = 19 mm
	B2	Hk5	0,06	-4,07	0,9999	Huck M20, l_k = 19 mm
	B3	Hk6	0,05	-0,36	1,0000	Huck M20, l_k = 19 mm
R1H-1	B1	Hk8	0,06	-6,81	0,9994	Huck M20, l_k = 19 mm
	B2	Hk10	0,06	1,31	1,0000	Huck M20, l_k = 19 mm
	B3	Hk12	0,06	-1,33	0,9999	Huck M20, l_k = 19 mm
R2H-1	B1	Hk14	0,07	-36,97	0,9939	Huck M20, l_k = 19 mm
	B2	Hk15	0,06	0,45	1,0000	Huck M20, l_k = 19 mm
	B3	Hk16	0,06	0,03	1,0000	Huck M20, l_k = 19 mm
R0H-2	B1	Hk18	0,05	-9,38	0,9991	Huck M20, l_k = 19 mm
	B2	Hk19	0,05	-0,64	0,9999	Huck M20, l_k = 19 mm
	B3	Hk20	0,06	2,08	0,9999	Huck M20, l_k = 19 mm
R1H-2	B1	Hk21	0,06	1,13	1,0000	Huck M20, l_k = 19 mm
	B2	Hk22	0,06	0,74	0,9999	Huck M20, l_k = 19 mm
	B3	Hk23	0,06	-2,72	0,9998	Huck M20, l_k = 19 mm
R2H-2	B1	Hk24	0,06	-8,60	0,9991	Huck M20, l_k = 19 mm
	B2	Hk25	0,06	1,58	1,0000	Huck M20, l_k = 19 mm
	B3	Hk7	0,06	2,82	1,0000	Huck M20, l_k = 19 mm

Table B-7: Calibration data of long Huck M25,4/1" BobTail lockbolts (chapter 5)

name of the specimen	position of the bolt	name of the bolt	calibration curve			
			a [N/µm/m]	b [kN]	rsq	
RuH-S_4	B1	H40	0,09	1,33	1,0000	Huck M25,4/1", l_k = 56 mm
	B2	H32	0,09	1,45	1,0000	Huck M25,4/1", l_k = 56 mm
	B3	H30	0,09	-1,46	1,0000	Huck M25,4/1", l_k = 56 mm
RuH-S_2	B1	H41	0,10	0,72	1,0000	Huck M25,4/1", l_k = 56 mm
	B2	H33	0,10	1,43	0,9999	Huck M25,4/1", l_k = 56 mm
	B3	H31	0,09	-1,29	1,0000	Huck M25,4/1", l_k = 56 mm
RuH-S_0	B1	H38	0,09	-1,06	1,0000	Huck M25,4/1", l_k = 56 mm
	B2	H37	0,09	-0,27	1,0000	Huck M25,4/1", l_k = 56 mm
	B3	H35	0,09	-0,52	1,0000	Huck M25,4/1", l_k = 56 mm

Table B-8: Calibration data short Huck M25,4/1" BobTail lockbolts (chapter 5)

name of the specimen	position of the bolt	name of the bolt	calibration curve			
			a [N/µm/m]	b [kN]	rsq	
RuH_4	B1	H51	0,09	1,40	1,0000	Huck M25,4/1", l_k = 32 mm
	B2	H47	0,09	1,02	1,0000	Huck M25,4/1", l_k = 32 mm
	B3	H46	0,09	1,03	1,0000	Huck M25,4/1", l_k = 32 mm
RuH_2	B1	H58	0,09	1,04	1,0000	Huck M25,4/1", l_k = 32 mm
	B2	H55	0,09	0,65	1,0000	Huck M25,4/1", l_k = 32 mm
	B3	H57	0,09	1,27	1,0000	Huck M25,4/1", l_k = 32 mm
RuH_0	B1	H62	0,09	1,69	1,0000	Huck M25,4/1", l_k = 32 mm
	B2	H60	0,09	1,48	1,0000	Huck M25,4/1", l_k = 32 mm
	B3	H63	0,09	2,76	0,9999	Huck M25,4/1", l_k = 32 mm

Table B-9: Calibration data on long Huck M25,4/1" BobTail lockbolts used for material testing (ANNEX D)

name of the specimen	position of the bolt	name of the bolt	calibration curve			
			a [N/µm/m]	b [kN]	rsq	
material testing	-	H34	0,09	-0,54	1,0000	Huck M25,4/1", l_k = 56 mm
	-	H39	0,09	0,77	1,0000	Huck M25,4/1", l_k = 56 mm

C BOLT FORCE DIAGRAMS

The following diagrams show the development of the bolt forces from tightening until the end of the test, which is either after one, four or 40 weeks. The black graph illustrates the actual bolt force, whereas the light grey line displays the load requested by Eurocode 3, part 1-8, and the dark grey one implies the clamping load, which the producer guarantees – if such guaranty exists.

The diagrams are always listed in the same way; first the ones showing the pretension force in the specimens with the most coated surfaces, and last the pictures of the bolt forces in the specimens with the least coated surfaces.

In the cases, where two test series are plotted in columns next to each other, the first diagram always shows the development of clamping force of bolt B1, the second of bolt B2 and the lowest of bolt B3.

C.1 Loss of pretension in bolts of tests described in chapter 3

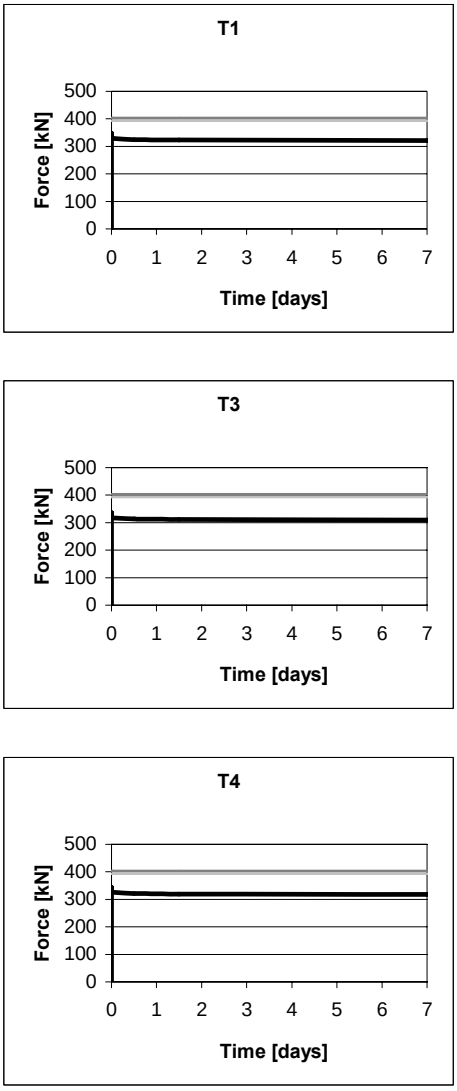

Figure C-1: Bolt forces in R2

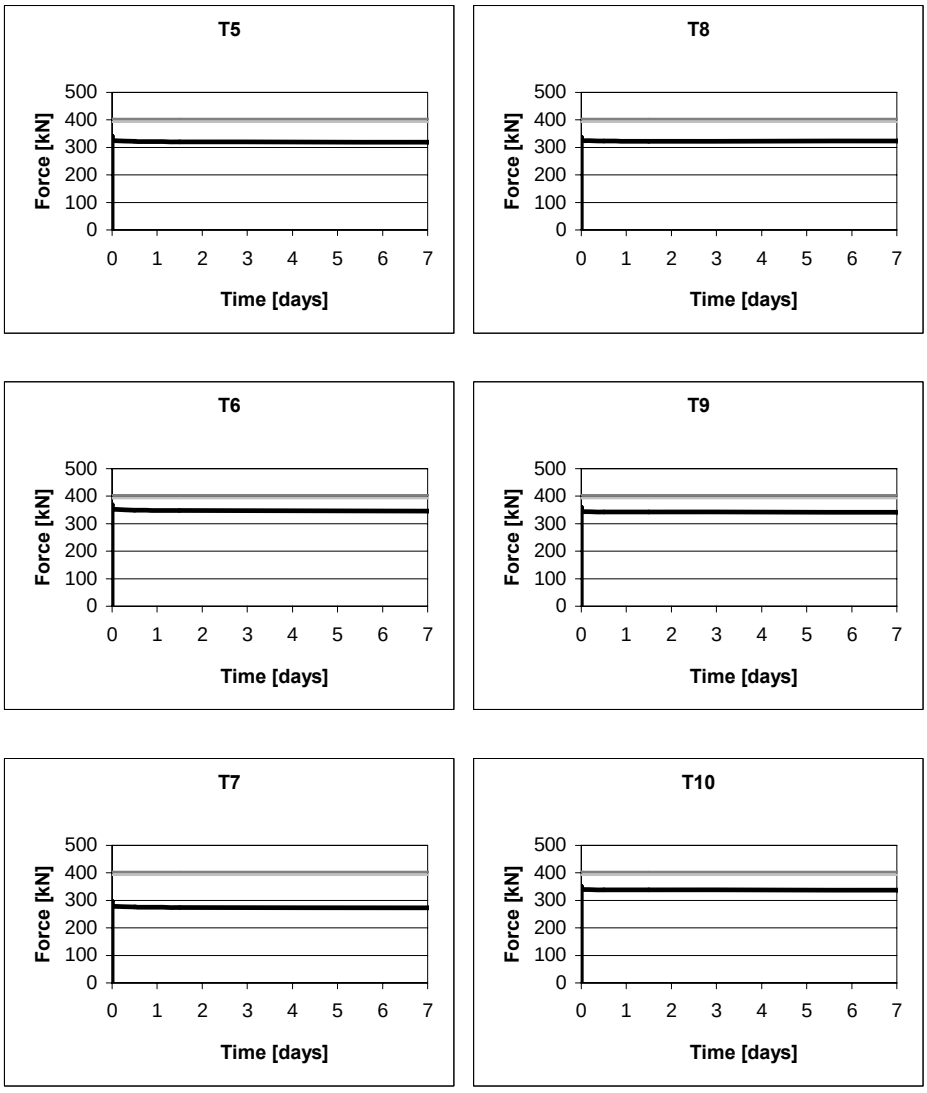

Figure C-2: Bolt forces in R1 (left column) and R0 (right column)

C.2 Loss of pretension in bolts of tests described in chapter 4

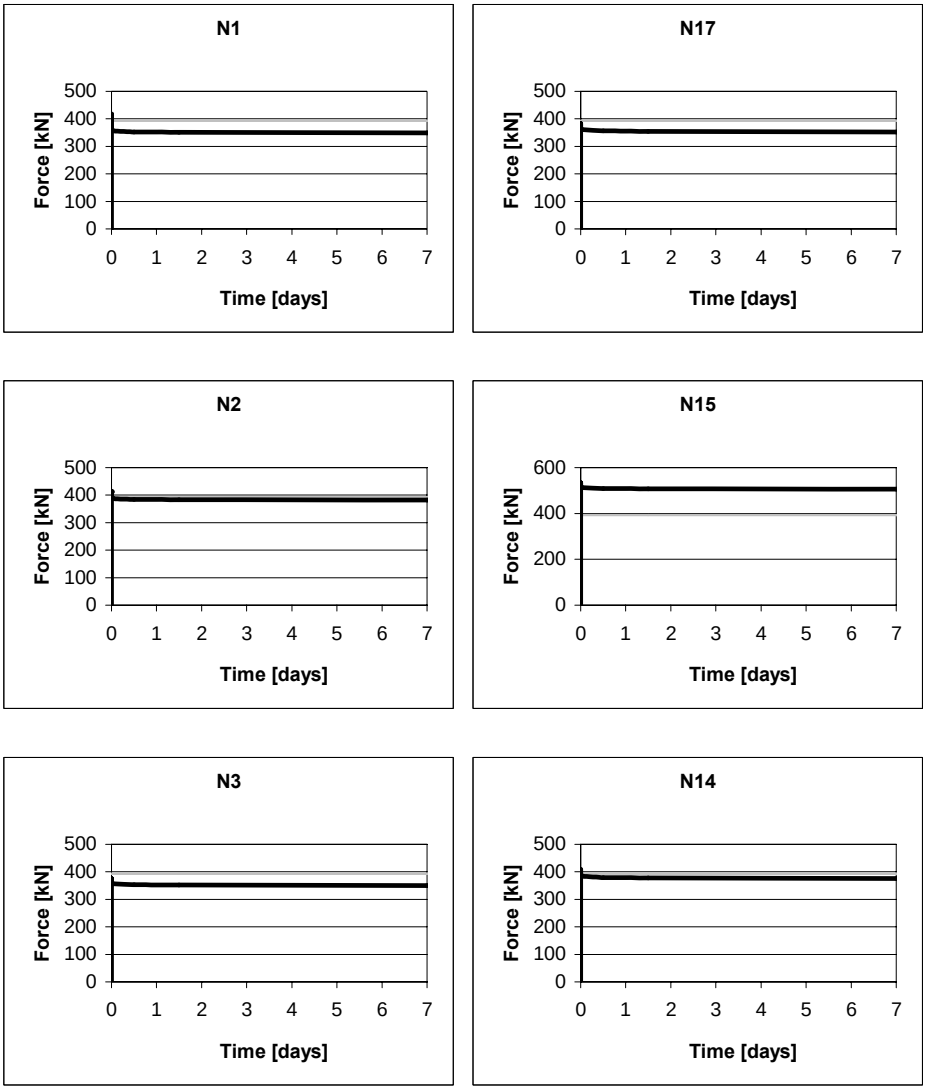

Figure C-3: Bolt forces in R2N-1 (left column) and R2N-2 (right column)

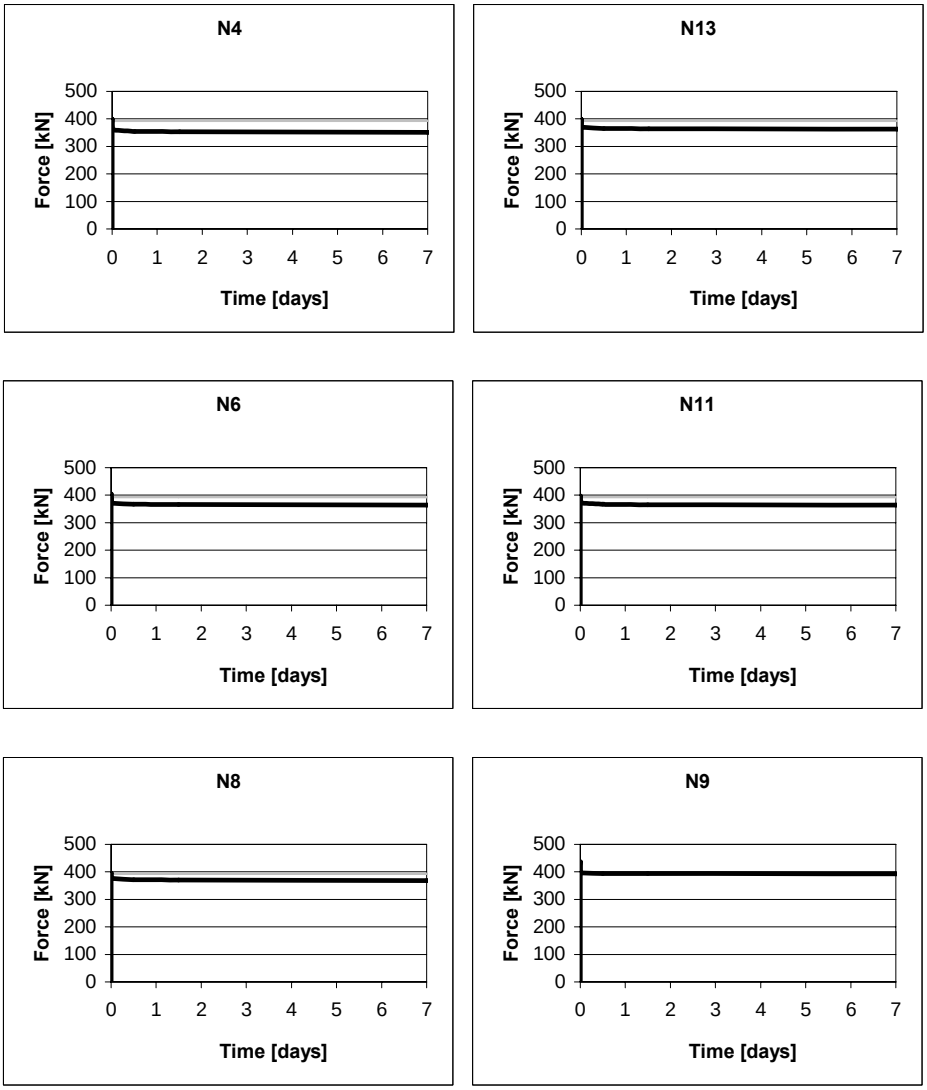

Figure C-4: Bolt forces in R1N-1 (left column) and R0N-1 (right column)

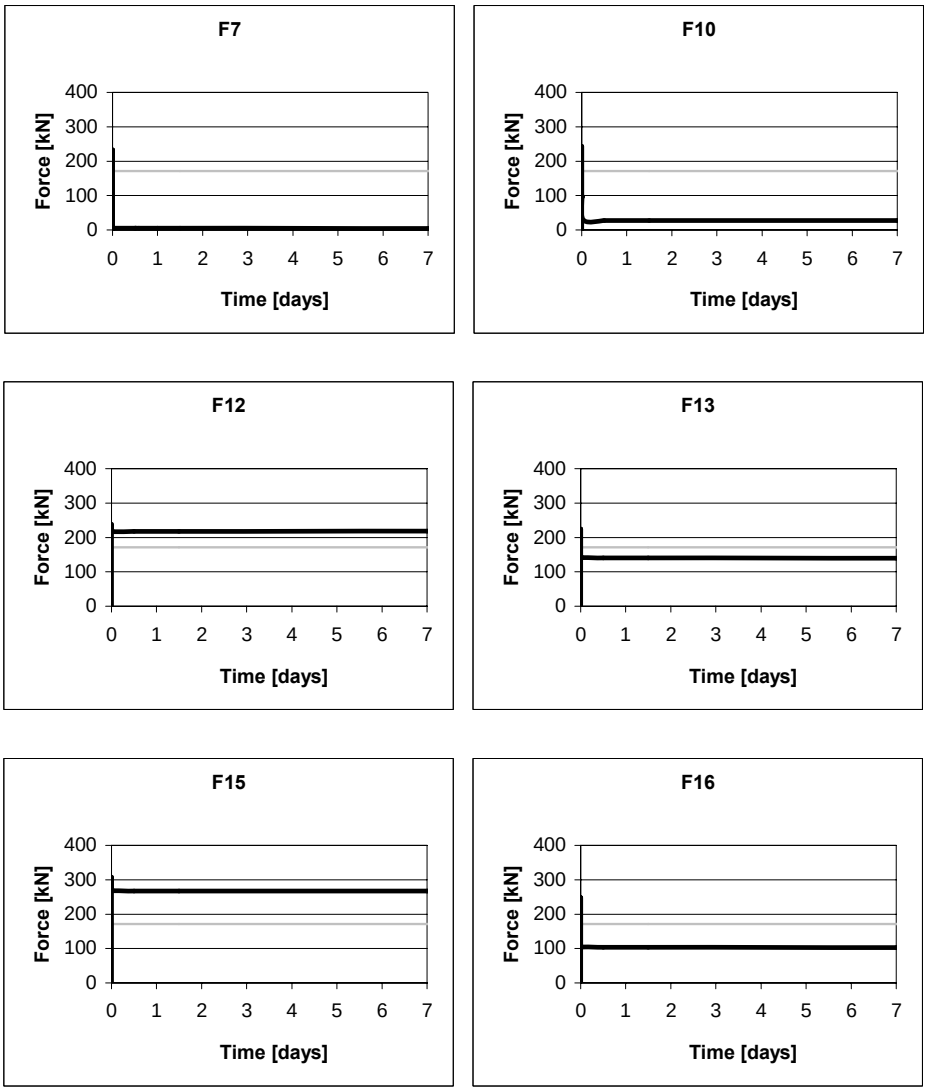

Figure C-5: Bolt forces in R2F-1 (uppermost row), R1F (middle row) and R0F (lowest row)

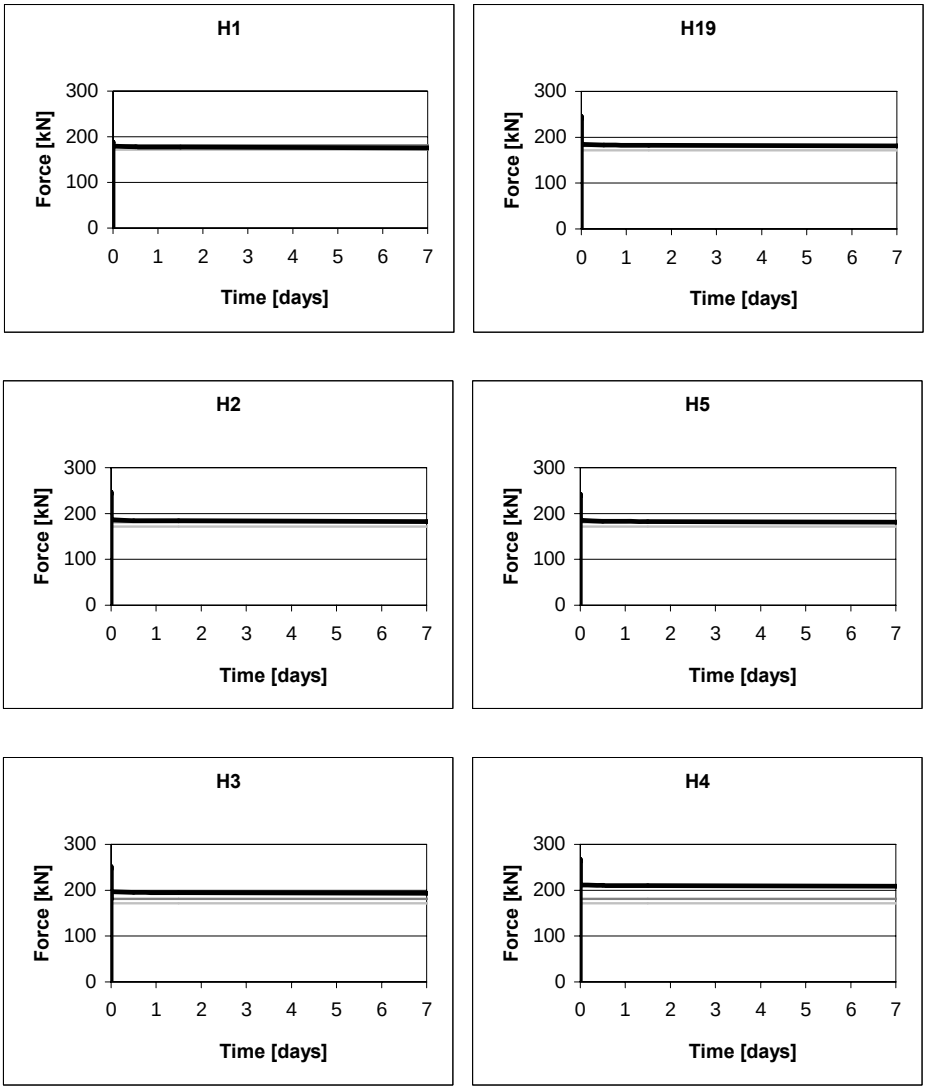

Figure C-6: Bolt forces in RL2H-1 (left column) and RL2H-2 (right column)

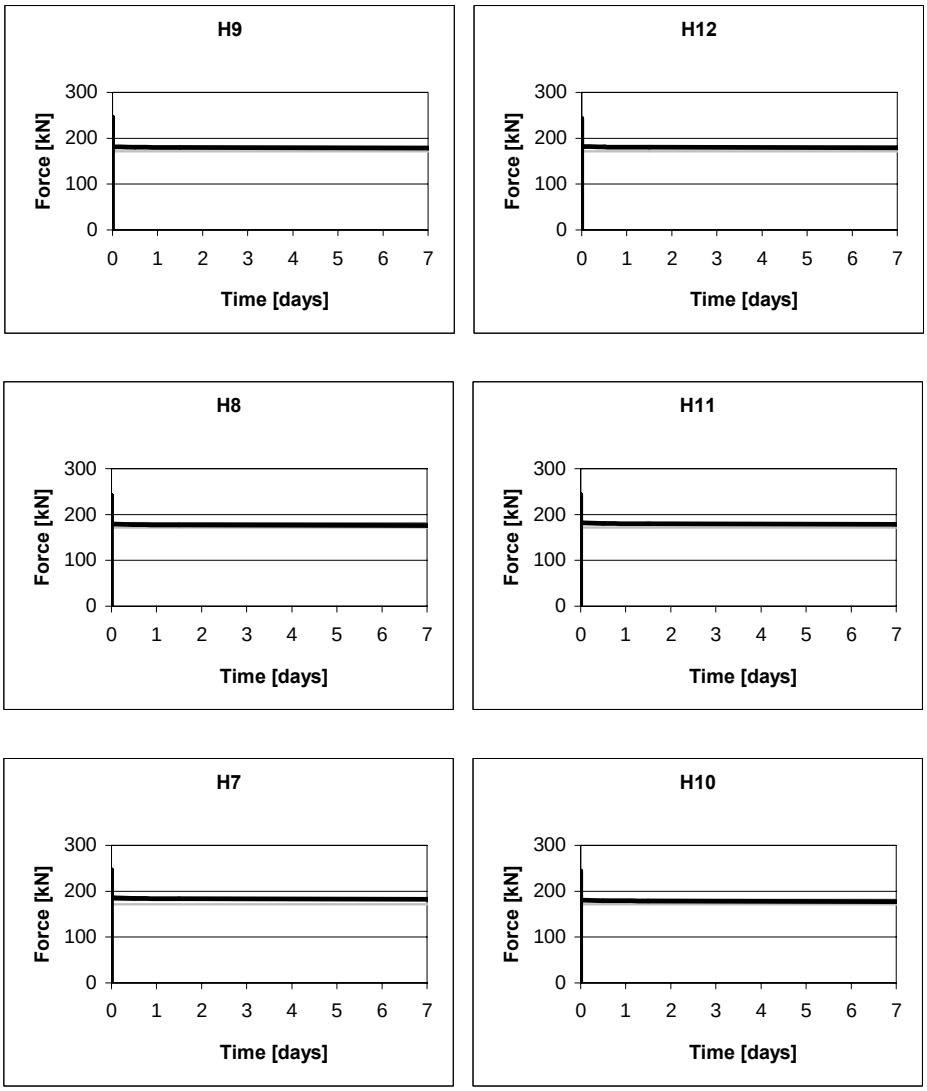

Figure C-7: Bolt forces in RL1H-1 (left column) and RL1H-2 (right column)

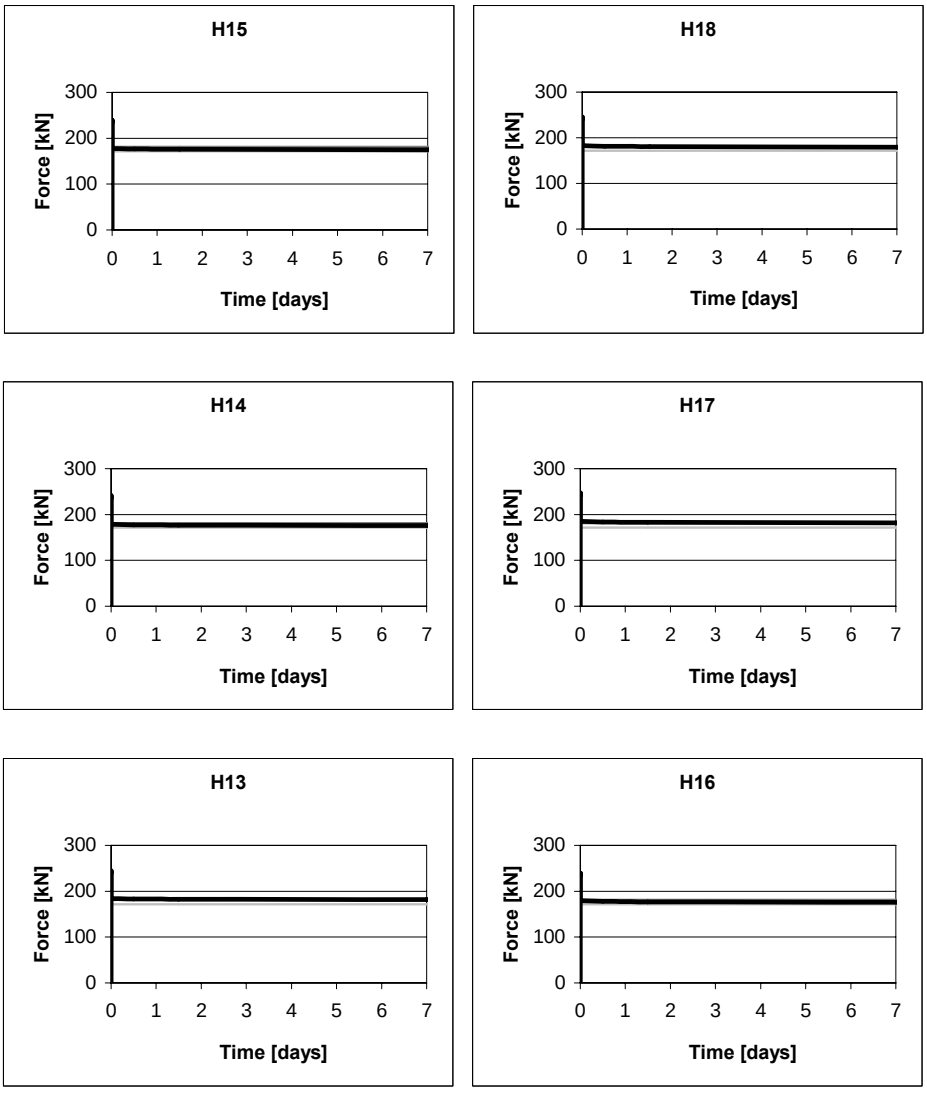

Figure C-8: Bolt forces in RL0H-1 (left column) and RL0H-2 (right column)

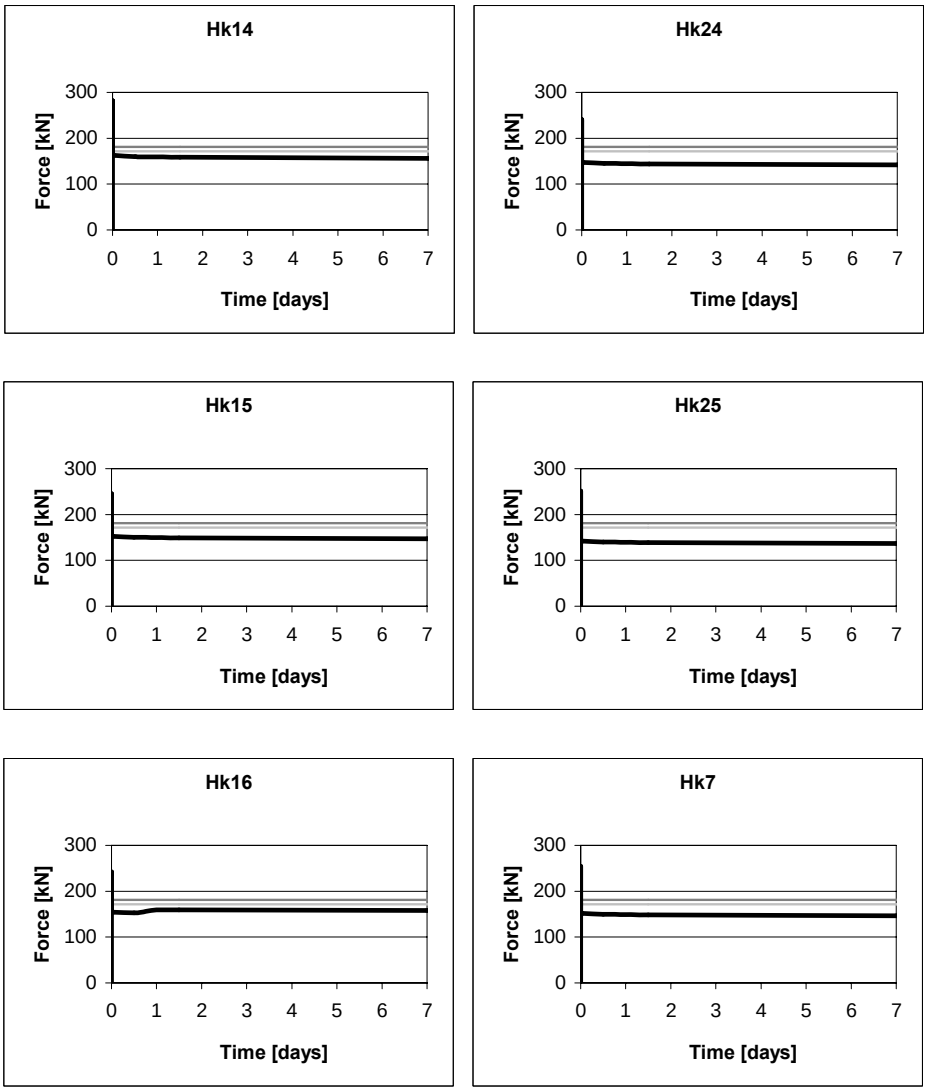

Figure C-9: Bolt forces in R2Hk-1 (left column) and R2Hk-2 (right column)

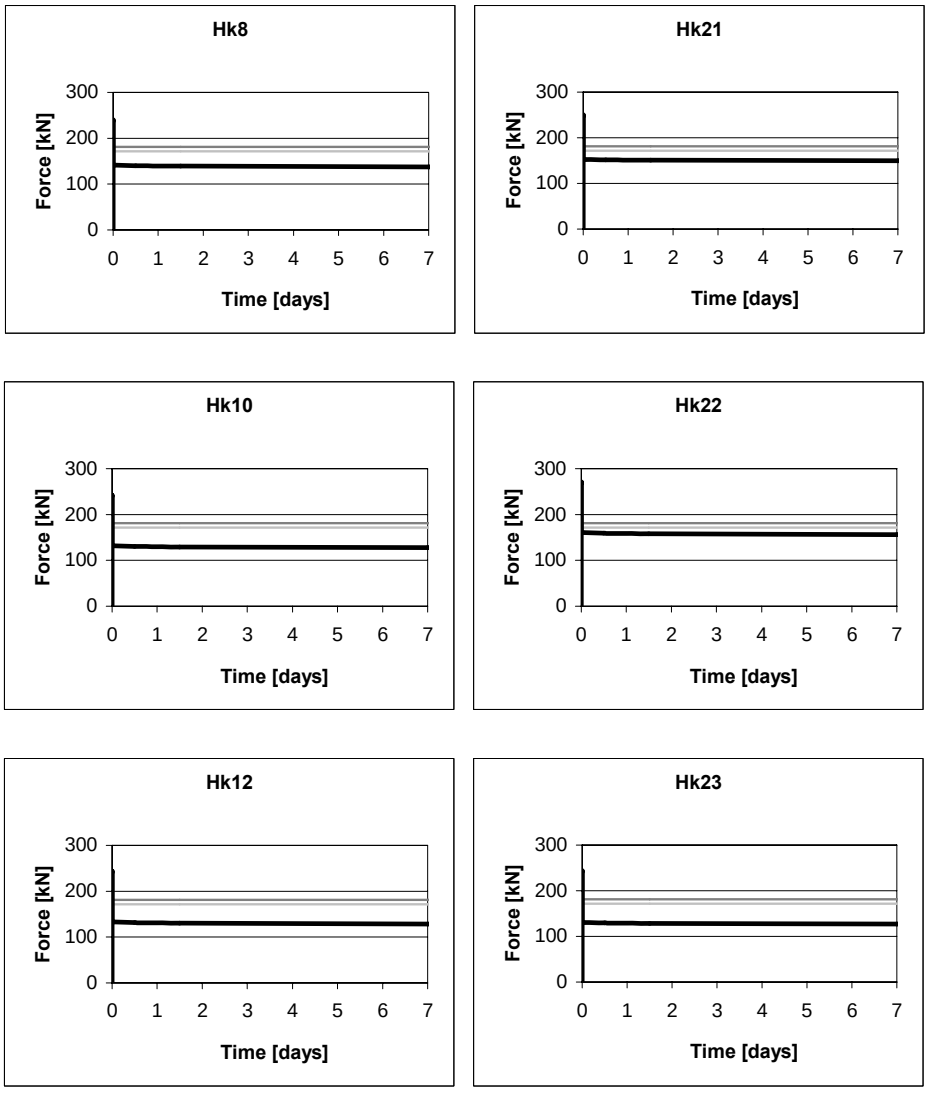

Figure C-10: Bolt forces in R1Hk-1 (left column) and R1Hk-2 (right column)

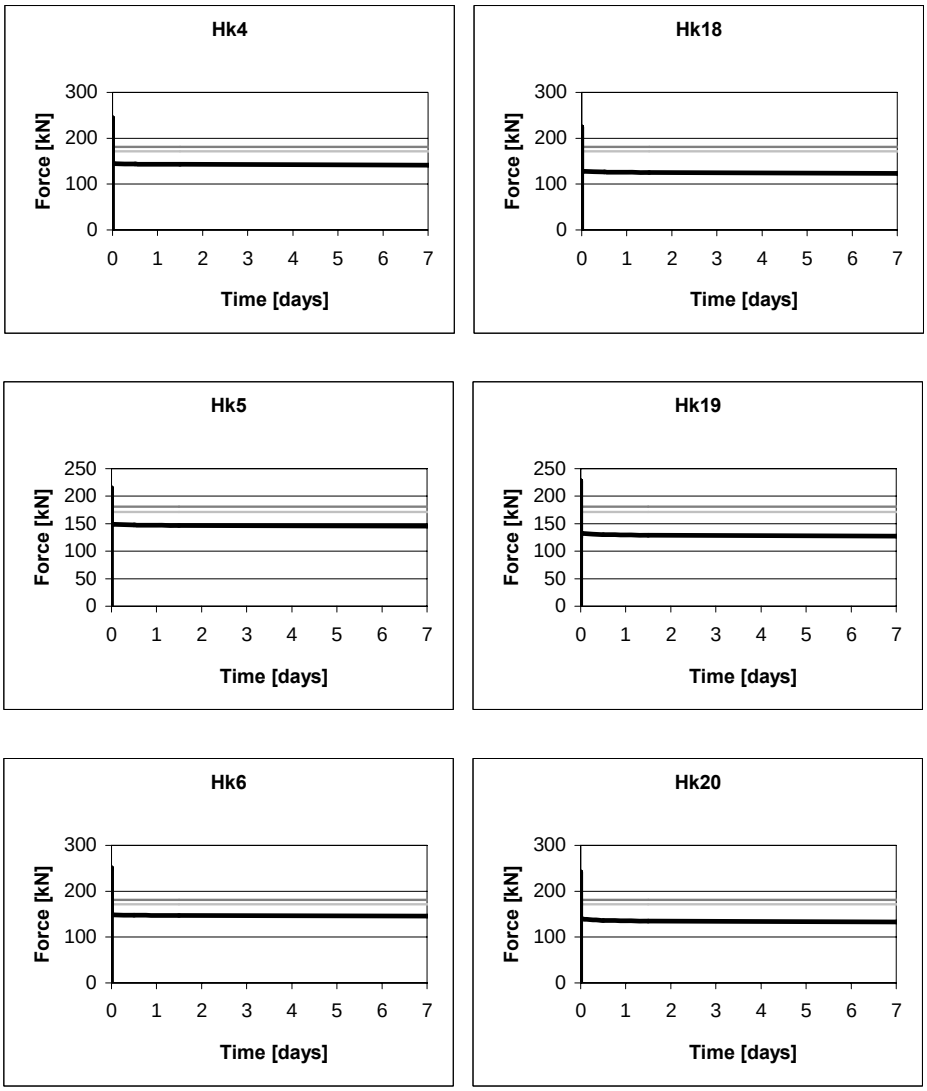

Figure C-11: Bolt forces in R0Hk-1 (left column) and R0Hk-2 (right column)

C.3 Loss of pretension in bolts of tests described in chapter 5

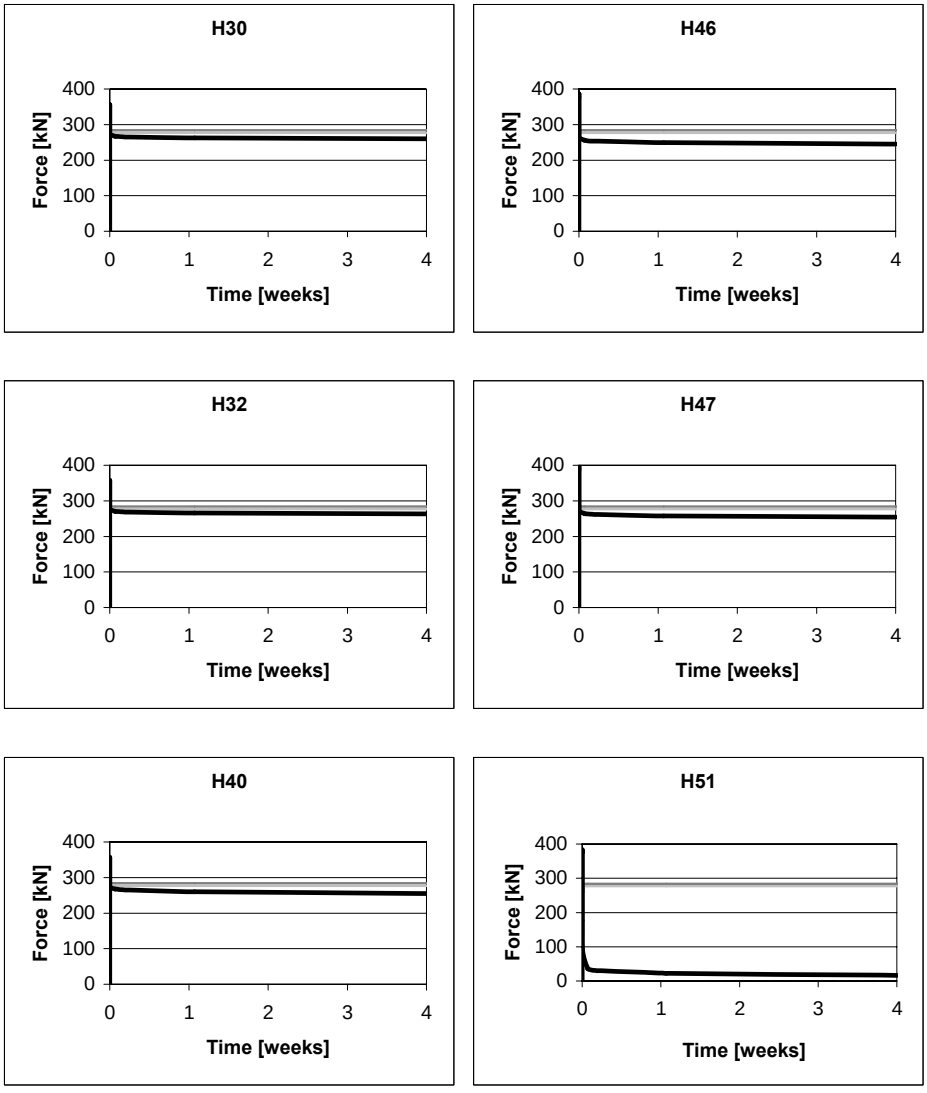

Figure C-12: Bolt forces in RuH-S_4 (left column) and RuH_4 (right column)

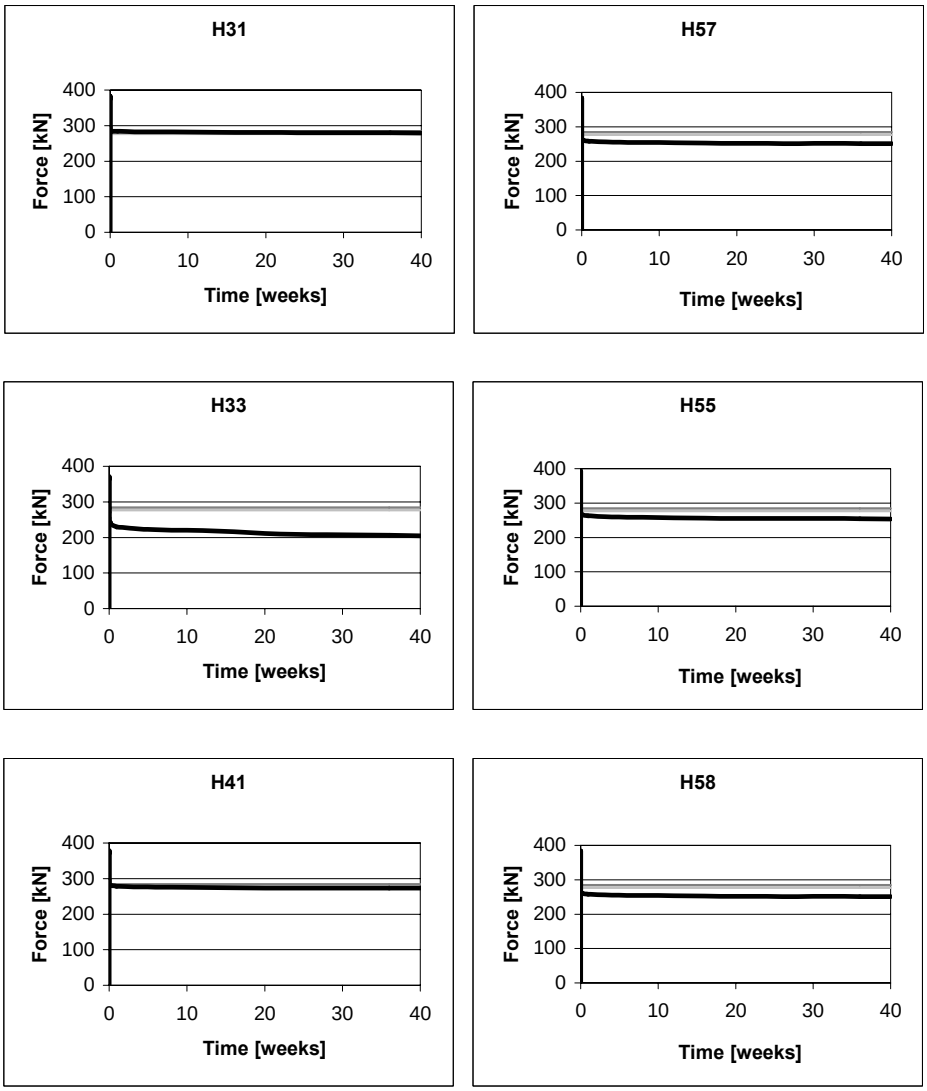

Figure C-13: Bolt forces in RuH-S_2 (left column) and RuH_2 (right column)

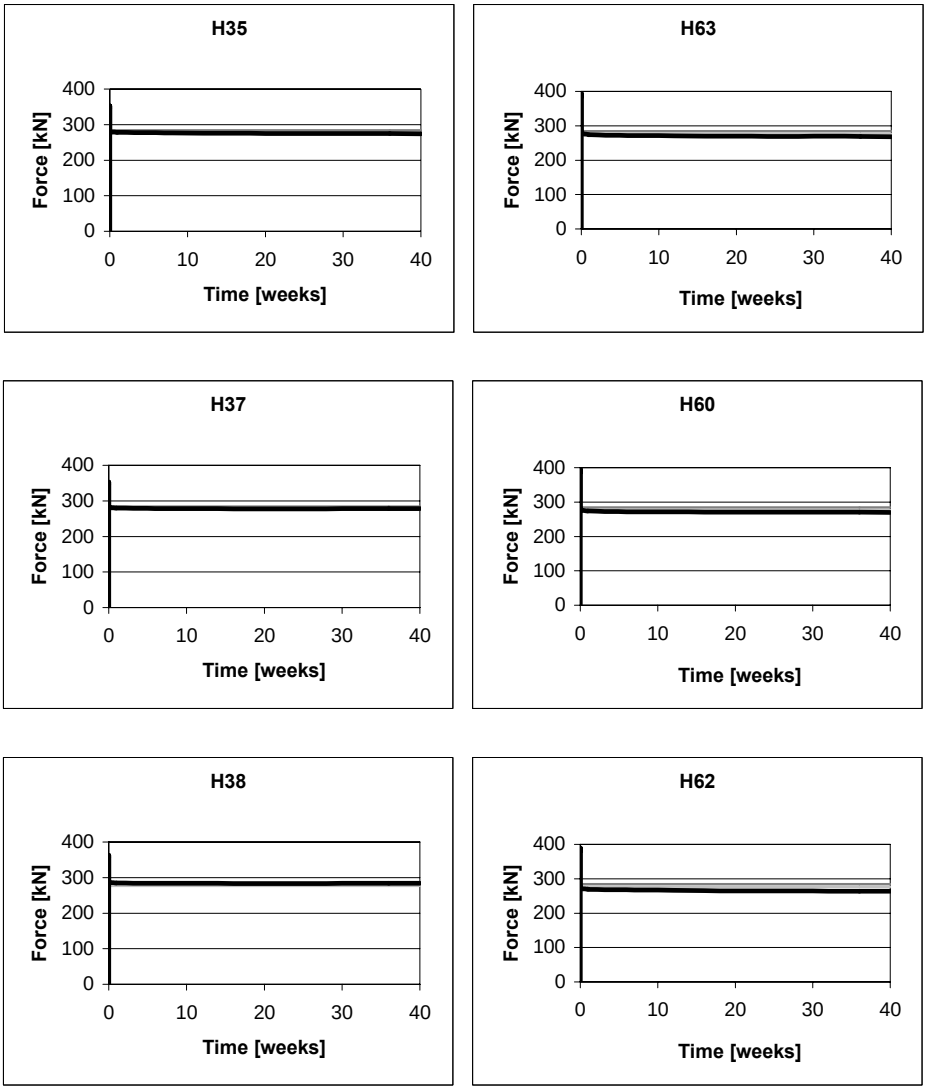

Figure C-14: Bolt forces in RuH-S_0 (left column) and RuH_0 (right column)

D MATERIAL TESTING OF HUCK BOBTAIL LOCKBOLTS M25,4/1”

To achieve a better understanding of the behaviour of Huck BobTail lockbolts in general and the ones used for the tests, which are described in chapter 5 in particular, material tests have been carried out.

The material of four M25,4/1” bolts with a clamping length of 56 mm is checked. Two of them have been used for testing before, namely H30, H34, H39 and H40. While H30 and H40 have been engaged and pretensioned in Test specimen RuH-S_4, which has been used for checking pure relaxation behaviour in the bolts as well as during static loading of the double symmetric lap joint, the other two bolts H34 and H39 have never been in use. However, their shanks have been drilled, strain gauges have been glued inside and the bolts are calibrated. As can be seen in Table B-9 the bolts show reasonable behaviour during their calibration.

To obtain an undamaged round test piece, the material specimens have been cut out of the bolts as can be seen in the drawing in Figure D-1. The ends of the specimens feature a thread of the same size as a standard M12 bolt, so that it can be engaged into the tensile testing machine. Over a length of 8 mm at each end the cross-section narrows down and finally becomes 6 mm in diameter over a length of 50 mm. This is the main area for material testing. The total length of the specimens is 86 mm. All dimensions of the test specimens are listed in Table D-1. A picture of one of the test specimens is shown in Figure D-2. Here, also the locations for the diameter measurements can be seen.

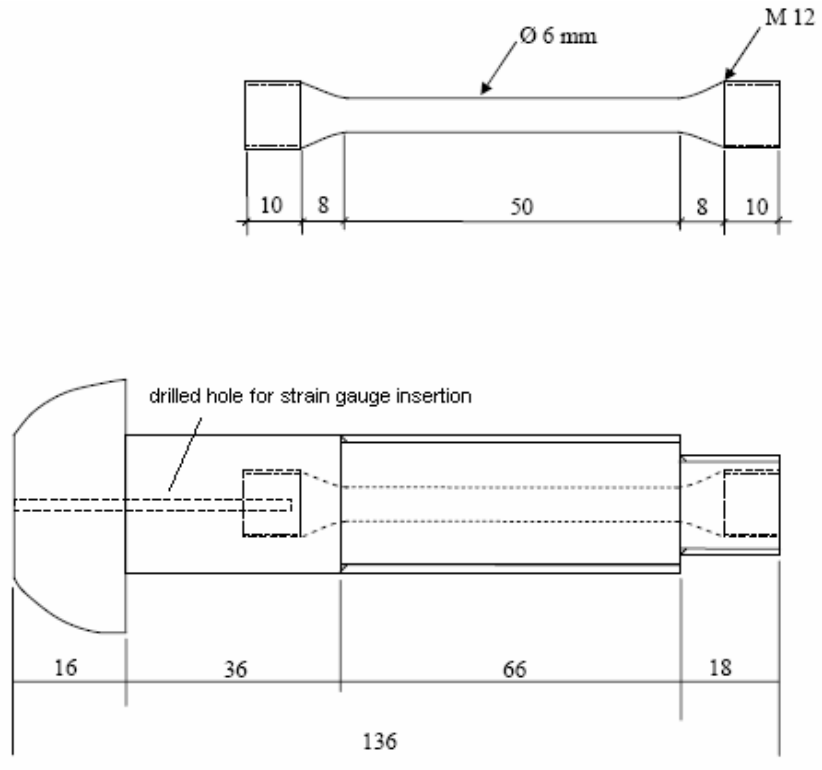

Figure D-1: Test specimen and original location in Huck BobTail lockbolt M25,4/1" of 56 mm grip length, all dimensions given in mm

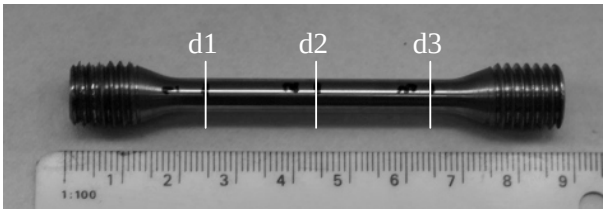

Figure D-2: Test specimen with places of measurements

Table D-1: Dimensions of test specimens cut out from Huck BobTail lockbolts M25,4/1”

Name of specimen		d1 [mm]	d2 [mm]	d3 [mm]	total length [mm]	average cross section [mm²]
H30		6,090	6,085	6,087	86,450	
		6,090	6,087	6,090		
		6,092	6,085	6,095		
	average d	6,091	6,086	6,091		
	area	29,135	29,087	29,135		29,119
H34		6,089	6,070	6,082	86,400	
		6,092	6,071	6,090		
		6,081	6,065	6,095		
	average d	6,087	6,069	6,089		
	area	29,103	28,925	29,119		29,049
H39		6,080	6,062	6,078	86,340	
		6,085	6,065	6,078		
		6,075	6,062	6,080		
	average d	6,080	6,063	6,079		
	area	29,033	28,871	29,021		28,975
H40		6,068	6,048	6,071	86,540	
		6,065	6,045	6,072		
		6,071	6,048	6,075		
	average d	6,068	6,047	6,073		
	area	28,919	28,719	28,963		28,867

Each of the test pieces is set into the machine and loaded in tension until failure.

The achieved test results are shown in Figure D-3, given as a stress-strain-diagram. The graphs clearly show that the bolts, which have been pretensioned previously, fail earlier, whereas the bolts, which never have been employed in a test specimen, bear bigger strains. The “used” specimens can withstand a stress of 1100 N/mm^2 and show strains of 2 %, while the “new” specimens elongate up to 6 % at their maximum stress levels. But whilst the “used” specimens reach about the same maximum stresses, they differ quite much for the “new” ones: H34 reaches a level of 1100 N/mm^2, H39 fails at 1000 N/mm^2 already. The yield stresses, when the material changes from elastic to plastic behaviour, are, of course, reached even earlier: For H34 and H40 the yield stress is 950 N/mm^2. H30 reveals the highest yield strength of 1080 N/mm^2 whereas H39 starts to yield at the lowest level of 880 N/mm^2. The elastic

modulus is more or less the same for specimens H34, H39 and H40; about 210000 N/mm2. For H30 it is with 198000 N/mm^2 a little lower.

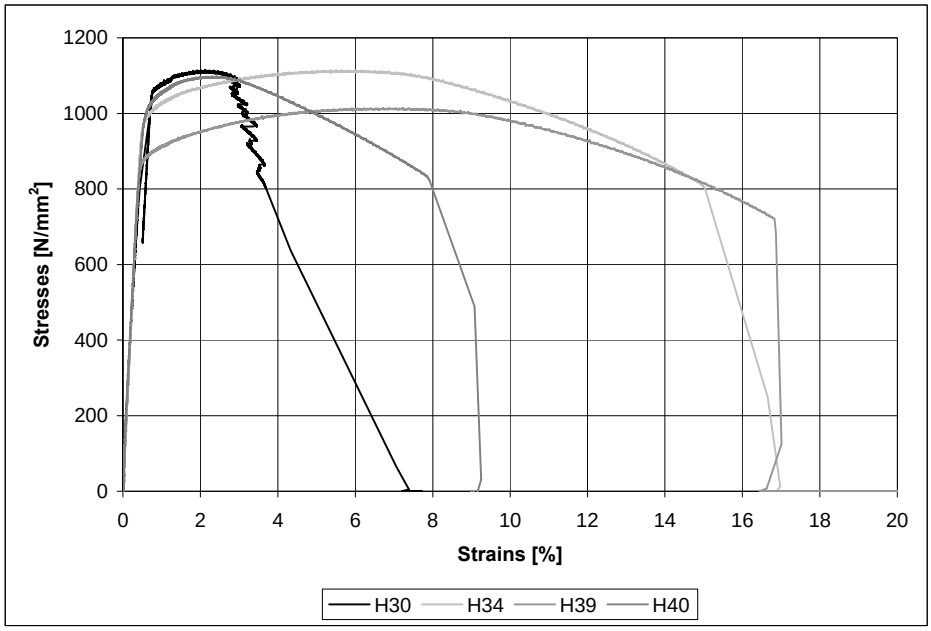

Figure D-3: Stress strain diagram of the tested material specimens

However, the real bolts should anyhow be able to reach the guaranteed clamping load of 284 kN, which corresponds to a stress level of 718,57 N/mm^2, which is lower than the achieved stresses in the material testing.

A picture of one of the specimens after failure shows Figure D-4.

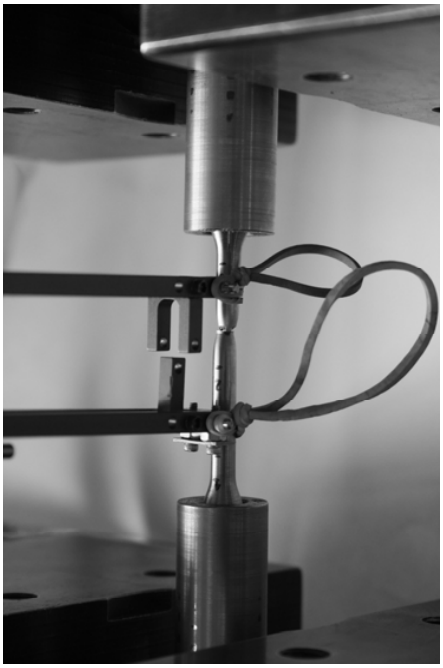

Figure D-4: Picture of a broken test piece

E DATA SHEETS ABOUT HUCK 1”/M25,4, HUCK M20, FRIEDBERG HV RÄNDEL

The following figures give information about the specific details of Huck BobTail lockbolts M20, M25,4/1” and Friedberg HV Rändel M20, which have been used in the performed experiments described in chapters 3 to 5. Information about bolt dimensions, expected forces and material can be found.

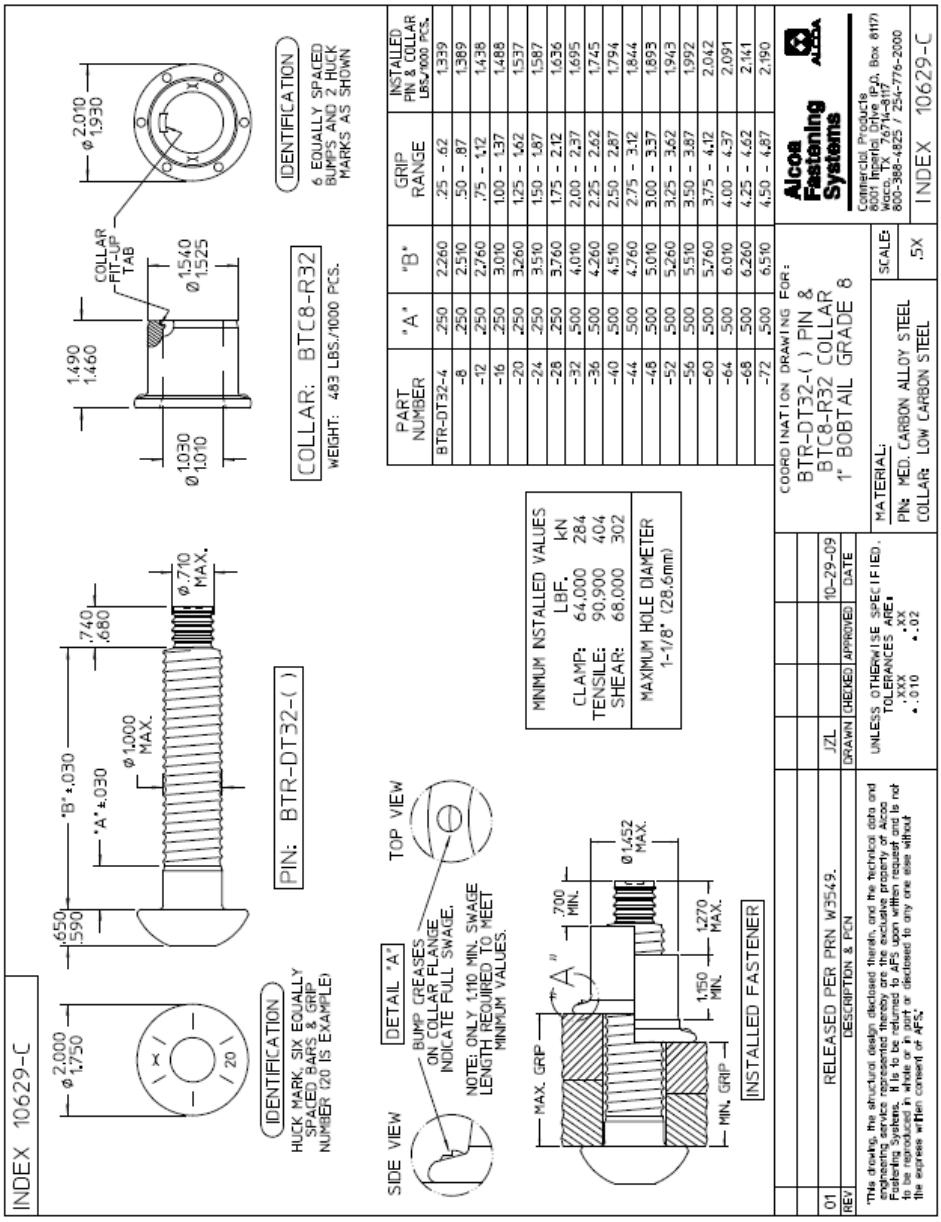

PART NUMBER	"A"	"B"	GRIP RANGE	INSTALLED PIN & COLLAR LBS/1000 PCS.
BTR-DT32-4	.250	2.260	.25 - .62	1,339
-8	.250	2.510	.50 - .87	1,389
-12	.250	2.760	.75 - 1.12	1,438
-16	.250	3.010	1.00 - 1.37	1,488
-20	.250	3.260	1.25 - 1.62	1,537
-24	.250	3.510	1.50 - 1.87	1,587
-28	.250	3.760	1.75 - 2.12	1,636
-32	.500	4.010	2.00 - 2.37	1,695
-36	.500	4.260	2.25 - 2.62	1,745
-40	.500	4.510	2.50 - 2.87	1,794
-44	.500	4.760	2.75 - 3.12	1,844
-48	.500	5.010	3.00 - 3.37	1,893
-52	.500	5.260	3.25 - 3.62	1,943
-56	.500	5.510	3.50 - 3.87	1,992
-60	.500	5.760	3.75 - 4.12	2,042
-64	.500	6.010	4.00 - 4.37	2,091
-68	.500	6.260	4.25 - 4.62	2,141
-72	.500	6.510	4.50 - 4.87	2,190

Figure E-1: Table of dimensions for Huck BobTail lockbolt 1"/M25,4

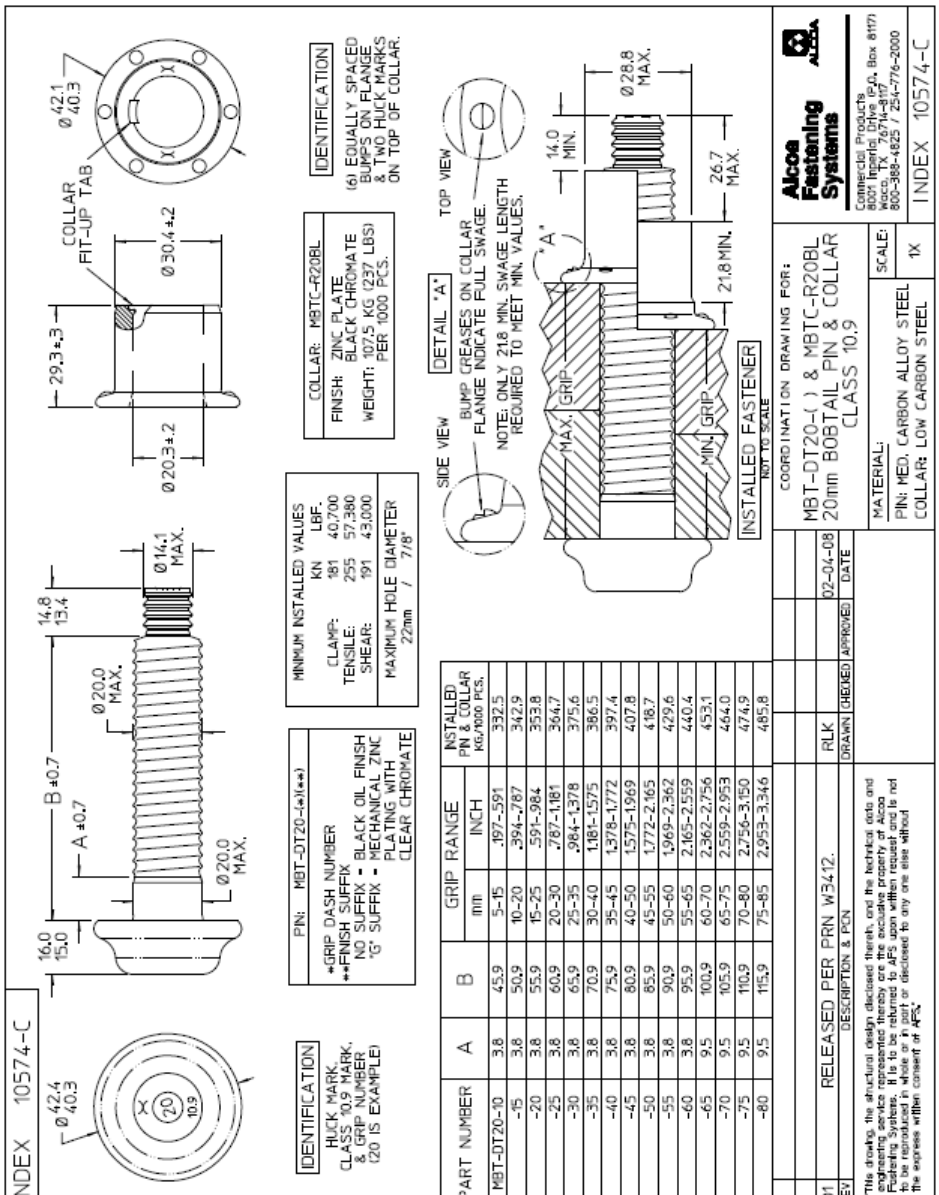

PART NUMBER	A	B	GRIP RANGE min	GRIP RANGE INCH	INSTALLED PIN & COLLAR KG/1000 PCS.
MBT-DT20-10	3.8	45.9	5-15	.197-.591	332.5
-15	3.8	50.9	10-20	.394-.787	342.9
-20	3.8	55.9	15-25	.591-.984	353.8
-25	3.8	60.9	20-30	.787-1.181	364.7
-30	3.8	65.9	25-35	.984-1.378	375.6
-35	3.8	70.9	30-40	1.181-1.575	386.5
-40	3.8	75.9	35-45	1.378-1.772	397.4
-45	3.8	80.9	40-50	1.575-1.969	407.8
-50	3.8	85.9	45-55	1.772-2.165	418.7
-55	3.8	90.9	50-60	1.969-2.362	429.6
-60	3.8	95.9	55-65	2.165-2.559	440.4
-65	9.5	100.9	60-70	2.362-2.756	453.1
-70	9.5	105.9	65-75	2.559-2.953	464.0
-75	9.5	110.9	70-80	2.756-3.150	474.9
-80	9.5	115.9	75-85	2.953-3.346	485.8

Figure E-2: Table of dimensions for Huck BobTail lockbolt M20

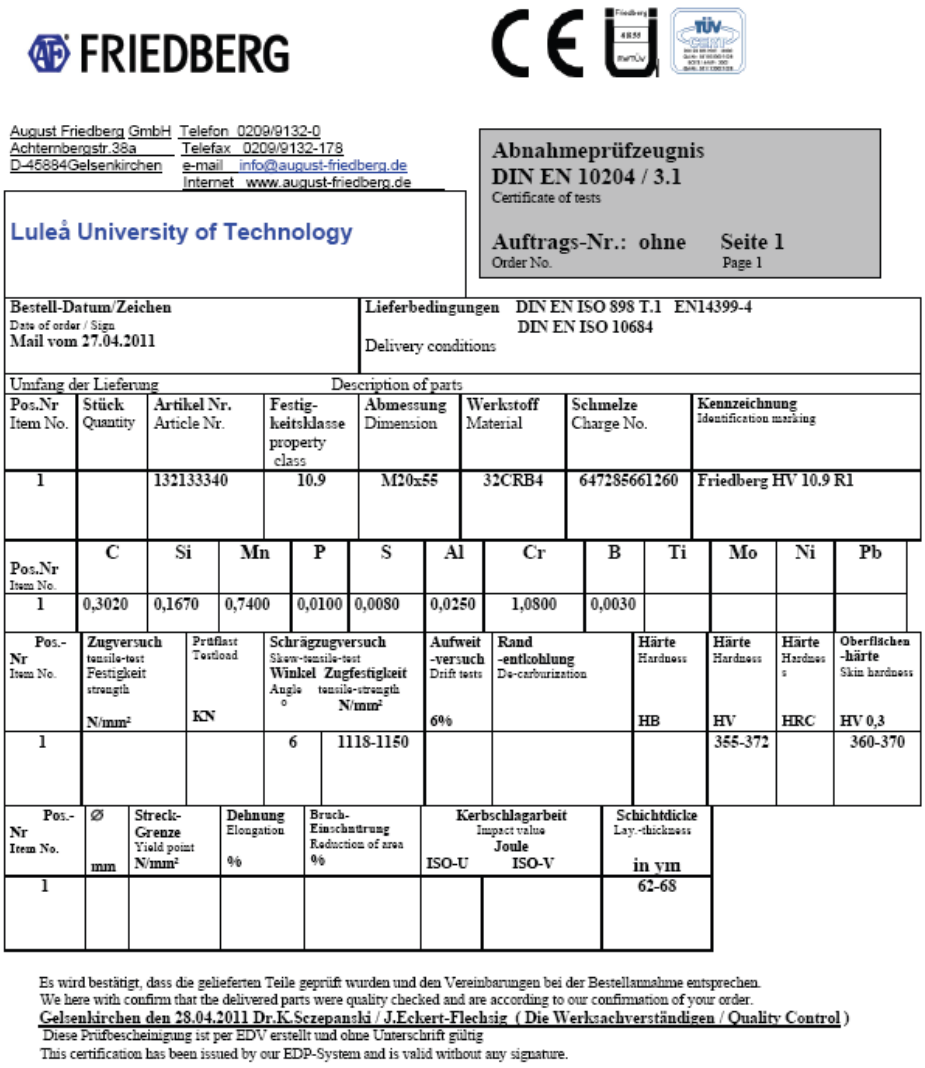

FRIEDBERG

August Friedberg GmbH Telefon 0209/9132-0
Achternbergstr.38a Telefax 0209/9132-178
D-45884Gelsenkirchen e-mail info@august-friedberg.de
Internet www.august-friedberg.de

Abnahmeprüfzeugnis
DIN EN 10204 / 3.1
Certificate of tests

Auftrags-Nr.: ohne **Seite 1**
Order No. Page 1

Luleå University of Technology

Bestell-Datum/Zeichen Date of order / Sign Mail vom 27.04.2011	Lieferbedingungen DIN EN ISO 898 T.1 EN14399-4 DIN EN ISO 10684 Delivery conditions

Umfang der Lieferung — Description of parts

Pos.Nr Item No.	Stück Quantity	Artikel Nr. Article Nr.	Festigkeitsklasse property class	Abmessung Dimension	Werkstoff Material	Schmelze Charge No.	Kennzeichnung Identification marking
1		132133340	10.9	M20x55	32CRB4	647285661260	Friedberg HV 10.9 R1

Pos.Nr Item No.	C	Si	Mn	P	S	Al	Cr	B	Ti	Mo	Ni	Pb
1	0,3020	0,1670	0,7400	0,0100	0,0080	0,0250	1,0800	0,0030				

Pos.-Nr Item No.	Zugversuch tensile-test Festigkeit strength N/mm²	Prüflast Testload KN	Schrägzugversuch Skew-tensile-test Winkel Angle °	Zugfestigkeit tensile-strength N/mm²	Aufweit-versuch Drift tests 6%	Rand-entkohlung De-carburization	Härte Hardness HB	Härte Hardness HV	Härte Hardness HRC	Oberflächen-härte Skin hardness HV 0,3
1			6	1118-1150				355-372		360-370

Pos.-Nr Item No.	Ø mm	Streck-Grenze Yield point N/mm²	Dehnung Elongation %	Bruch-Einschnürung Reduction of area %	Kerbschlagarbeit Impact value Joule ISO-U	ISO-V	Schichtdicke Lay.-thickness in ym
1							62-68

Es wird bestätigt, dass die gelieferten Teile geprüft wurden und den Vereinbarungen bei der Bestellannahme entsprechen.
We here with confirm that the delivered parts were quality checked and are according to our confirmation of your order.
Gelsenkirchen den 28.04.2011 Dr.K.Szczepanski / J.Eckert-Flechsig (Die Werksachverständigen / Quality Control)
Diese Prüfbescheinigung ist per EDV erstellt und ohne Unterschrift gültig
This certification has been issued by our EDP-System and is valid without any signature.

Figure E-3: Inspection certificate of Friedberg HV Rändel press-fitted bolts

F PRODUCT INFORMATION SHEET FOR TEMASIL 90 BY TIKKURILA COATINGS

Tikkurila Oyj is a Finnish company, which produces coatings for steel structures. Their paint Temasil 90 is used as corrosion protection for many wind towers. Its influence on the loss of pretension in preloaded bolts has been checked in the tests described in chapters 3 and 4.

TIKKURILA Coatings

PRODUCT DATA SHEET 03.01.2006
REF. NO TCF 0002
1 (2)

TEMASIL 90

DESCRIPTION

A two component, ethyl silicate zinc rich paint.

PRODUCT FEATURES AND RECOMMENDED USES

- Offers cathodic protection of steel.
- Excellent resistance to abrasion and weathering
- Excellent resistance to high, dry temperatures up to + 480 °C.
- Withstands immersion in oils and various solvents. Separate chemical resistance table available.
- Can be used as a single coat or as a primer in protective coating systems.
- Recommended for bridges, pipework, heat exchangers and chemical tanks etc.

TECHNICAL DATA

Volume solids

55 ± 2 %

Specific gravity

2.0 kg / l (mixed)

Mixing ratio and product codes

Base	1 part by volume	008 7381-2
Hardener	1 part by volume	008 7380

Pot life

5 hours (23 °C)

Recommended film thicknesses and theoretical coverage

Recommended film thicknesses		Theoretical coverage
dry	wet	
60 µm	120 µm	8.5 m^2/l
80 µm	160 µm	6.4 m^2/l

Practical coverage depends on the application method, painting conditions and the shape and roughness of the surface to be coated.

Drying times

DFT 75 µm	+ 10 °C	+ 23 °C	+ 35 °C
Dust dry, after	½ h	15 min	10 min
Touch dry, after	1 h	½ h	15 min
Recoatable, RH 85 % *see overleaf, after	36 h	5 h	2 h
Recoatable, RH 70 %, after	48 h	24 h	7 h
Recoatable, RH 50 %, after	-	48 h	24 h

Drying and recoating times are related to the film thickness, temperature, the relative humidity of the air and ventilation.

Finish

Matt.

Colours

Greenish grey and grey.

Tikkurila Oy | P.O. Box 53 | Kuninkaalantie 1 | FIN-01301 Vantaa | Tel. +358 (0)9 857 71 | Fax +358 (0)9 8577 6911
VAT FI01970674 | Business Identity Code 0197067-4 | Registered OfficeVantaa | www.tikkurila.com

TEMASIL 90

APPLICATION DETAILS

Surface preparation	Oil, grease, salts and dirt are removed by appropriate means. (ISO 12944-4) Steel surfaces: Blast clean to grade Sa2½ - 3. (ISO 8501-1)
Finish	TEMACHLOR 40, TEMACRYL AR, TEMACRYL EA, TEMAL, TEMACOAT GPL-S PRIMER, TEMACOAT GPL-S MIO, TEMACOAT RM 40 and TEMACOAT SPA. **TEMASIL 90 may be overcoated with above mentioned paints when Thinner 1029 does not dissolve the coat.** Before overcoating it is recommended to spray a misty coat with 25 % thinned TEMACOAT GS 50.
Application conditions	All surfaces must be dry. The temperature of the ambient air or surface should not fall below -15 °C during application and drying. Relative humidity should be 50 - 90 %. The surface temperature of the steel should remain at least 3 °C above the dew point.
Mixing components	First stir base and hardener separately. The correct proportions of base and hardener must be mixed thoroughly before use. Use Temaspeed Squirrel Mixer for mixing.
Application	By airless or conventional spray or brush. Agitate during application. Depending on the application method the paint can be thinned 0 - 5 % by volume. Airless spray nozzle tip 0.018" - 0.021" and nozzle pressure 120 - 180 bar. Spray angle shall be chosen according to the shape of the object. When coating interiors of chemical tanks or working in dry conditions, it is recommended to rinse the paint film with fresh water 1 - 24 hours after application. Sharp edges, corners, weld seams and other areas difficult to cover properly by spray application should be coated by a brush before the spray application. Note! There is a risk of mudcracking or peeling with heavier coats than approx. 100 µm dry film thickness. Separate application instructions available.
Thinner	Thinner 1029.
Cleaning of equipment	Thinner 1029.
Storage	Avoid to use more than six months old hardener (packing date on a label).
VOC	The Volatile Organic Compounds amount is 470 g/litre of paint. VOC content of the paint mixture (thinned 5 % by volume) is 480 g/l.
HEALTH AND SAFETY	Containers are provided with safety labels, which should be observed. Further information about hazardous influences and protection are detailed in individual health and safety data sheets. A health and safety data sheet is available on request from Tikkurila Oy.

G INPUT DATA FROM ABAQUS CALCULATION

Table G-1 shows an extract from an input file for the numerical calculations in chapters 6 and 7 with the most important keywords, which are needed to model pretension forces and contact problems in Abaqus.

Table G-1: Extract from an Abaqus input file (static test, S355)

```
** MATERIALS
*Material, name=S355
*Elastic
210000., 0.3
*Plastic
  355.6,     0.
 359.564, 0.0111
 539.021, 0.0528
   612., 0.1794
*Material, name=bolt_10-9
*Elastic
210000., 0.3

** INTERACTION PROPERTIES
*Surface Interaction, name=contact
1.,
*Friction, slip tolerance=0.005
 0.62462,
*Surface Behavior, pressure-
overclosure=HARD

** INTERACTIONS
**Interaction: general_contact
*Contact
*Contact Inclusions, ALL EXTERIOR
*Contact Property Assignment
 ,  , contact

** STEP: pretensioning
*Step, name=pretensioning, nlgeom=YES
*Static
0.001, 1., 1e-05, 1.

** LOADS
** Name: lower_bolt   Type: Bolt load
*Cload
_lower_bolt_blrn_, 1, 236900.
** Name: upper_bolt   Type: Bolt load
*Cload
_upper_bolt_blrn_, 1, 237900.
```

```
** STEP: fix_bolt_length
*Step, name=fix_bolt_length,
nlgeom=YES
*Static
1., 1., 1e-05, 1.

** BOUNDARY CONDITIONS
** Name: lower_bolt Type: Bolt load
*Boundary, op=NEW, fixed
_lower_bolt_blrn_, 1, 1
** Name: upper_bolt Type: Bolt load
*Boundary, op=NEW, fixed
_upper_bolt_blrn_, 1, 1

** STEP: load_step
*Step, name=load_step, nlgeom=YES,
inc=400
*Static, riks
0.01, 1., 1e-05, 0.015, 2.,

** OUTPUT REQUESTS
** HISTORY OUTPUT: lower_bolt
*Output, history
*Node Output,
nset=_lower_bolt_blrn_
TF1,

** HISTORY OUTPUT: upper_bolt
*Node Output,
nset=_upper_bolt_blrn_
TF1,
*End Step
```